UNIVERSITY OF
BIRMINGHAM

Switchable Surfaces for Regulating Biomolecular and Cellular Interactions under Complex Biological Conditions

by

Minhaj B. Lashkor

A thesis submitted to

The University of Birmingham

for the Degree of

DOCTOR OF PHILOSOPHY

School of Chemical Engineering

College of Engineering and Physical Sciences

The University of Birmingham

July 2014

Abstract

Stimuli-responsive surfaces that can regulate specific biomolecular interactions are enabling novel functionalities and new device designs for a variety of biological and medical applications. While substantial attention has been directed to construction and performance of biological switchable surfaces in simple biological systems, less effort has been directed to developing and understanding surfaces capable of switching under more practical biological applications. In this study, a merged approach was taken to produce well-defined self-assembled monolayers (SAMs) that prevent non-specific binding with the ability to electrically switch the SAM to allow control over biomolecular interactions under complex biological matrixes. This SAM system, based on switchable oligopeptides, can be dynamically modulated by an electrical potential under different commonly used biological media, ranging from Dulbecco's Modified Eagle Medium (DMEM) to DMEM supplemented with fetal bovine serum (FBS) and zwitterionic buffering agents such as HEPES.

The electrically switchable mixed SAMs, which are shown to be capable of exposing and concealing the RGD cell adhesion motif, can dynamically regulate the adhesion of immune macrophage cells under complex biological conditions. Macrophage cell adhesion to biomaterial surfaces plays a key role in mediating immune response to foreign materials. Thus, development of such dynamic in vitro model systems that can control macrophage cell adhesion on demand is likely to provide new opportunities to understand adhesion signalling in macrophages and develop effective approaches for prolonging the life-span of implantable medical devices and other biomaterials. This system is one of the first examples of a material surface system that can control macrophage cell adhesion on demand. Hence, this

study will be useful in developing more realistic dynamic extracellular matrix models and is certainly applicable in a wide variety of biological and medical applications.

Acknowledgments

First of all I would like to thank Professor Paula M. Mendes for being such an excellent supervisor and always making time for me whether it be to give me advice or guidance in my research. Her optimism, enthusiasm, passion for research and belief in my work have all contributed in my development within research and other fields. I would also like to thank Professor Jon A. Preece for supporting me in my initial stages of research and pushing me to do my MRes, which is where this journey began.

I would like to thank Dr Paul Yeung for his help throughout my PhD, he has always been there to give me support and advice. I would also like to thank Dr Frankie J. Rawson, who spent a significant amount of time in training me for the second half of my PhD for my work with cells. His work rate and dedication has been an inspiration.

I would like to thank the rest of the Mendes group whom I've had the pleasure to work with both past and present including: Dr Oliver Curnick, Dr Scott Charlesworth, Alex Stevenson-Brown, Zarrar Hussein, Marzena Allen, Dr Cait Costello, Eleonora Cantini, Alice Pranzetti, Dr Parvez Iqbal. Others members of staff whom I'd like to thank include Dr. James Bowen, Dr. Chi Wai Tsang and Professor Liam Grover for allowing me to use the facilities in the cell lab.

I would like to thank all my family especially my parents for their support throughout my PhD. Finally I would like to thank my wife Shelina, for her support and encouragement throughout my PhD and write-up.

Contents

List of illustrations and tables

Chapter 1

Figure 1.13 *Schematic of a dynamic substrate that prevents adsorption of any proteins prior to photoirradiation due to the PEG brushes (Left). However after photoirradiation the PEG brushes are released, the His-tagged proteins (protein A) is immobilised to the NTA group, while keeping adsorption of non-His-tagged proteins (protein B) blocked by the EG_7 underbrushes.*

Figure 1.14 *Schematic of a photoswitchable surface where he azobenzene moiety can be converted photochemically between the E and Z configurations to either present or mask the RGD ligand and hence modulate biospecific cell adhesion.*

Figure 1.15 *Schematic representation of a silane terminated α-CD which forms an inclusion complex via host-guest recognition with an azobenzene-GRGDS molecule. Hela cells adhere to the surface when the azobenzene is in the trans conformation. Upon UV irradiation at 365 nm the trans-azobenzene changes to cis-azobenzene, which results in the detachment of both the azo-GRGDS and cells from the substrate.*

Figure 1.16 *Schematic representation of the DNA lever where a) shows the DNA lying on the surface due to an attractive +0.3 V applied potential, the DNA is repelled when a negative potential of -0.5 V is applied. b) When a protein is attached to a ligand at the top end of the DNA, the upward motion at a negative potential slows and lags behind the DNA lever. The blue circle represents the Cy3 fluorophore when the fluorescence emission quenched by the surface. The yellow circle represents a high fluorescence emission due to the lever being further from the surface.*

Chapter 2

Figure 3.9 *SPR sensorgram traces showing the binding of neutravidin (Nav) to the* ***biotin-4KC****:****C11TEG*** *mixed SAMs. a) The mixed SAMs were exposed to neutravidin under OC conditions and an applied negative potential (− 0.4 V). SPR switching studies were carried out in triplicates to get an average switching efficiency.*

Figure 3.10 *The surface models used in the MD simulations. The purple, blue and dark green parts of the biotin-4KC chain represent the biotin motif, lysine and cysteine residues, respectively. The orange dots, light green balls, yellow balls and short grey chains denote water molecules, chloride ions, gold atoms and TEGT, respectively.*

Figure 3.11 *The conformational changes of* ***biotin-4KC:C11HEG*** *(up) and pure* ***biotin-4KC*** *(down) under different electric fields, along with the MD simulation snapshots. L is defined as the gap distance variation between the biotin and gold surface.*

Figure 3.12 *SPR sensorgram traces showing the interaction of DMEM-FBS-HEPES on the* ***biotin-4KC:C11TEG*** *mixed SAMs under OC conditions and -0.4 V*

Figure 3.13 *Switching efficiency, as determined by SPR analysis under OC conditions and an applied negative potential (− 0.4 V), on* ***biotin-4KC:C11TEG*** *mixed SAMs which were exposed to neutravidin in a) DMEM, DMEM-FBS, DMEM-FBS-HEPES as well in b) FBS and HEPES. Error bars show standard deviations among three different substrates.*

Figure 3.14 *Switching efficiency, as determined by SPR analysis under OC conditions and an applied negative potential (− 0.4 V), on biotin-4KC:C11TEG mixed SAMs which were exposed to neutravidin in a) DMEM, DMEM-FBS, DMEM-FBS-HEPES as well in b) FBS and HEPES. The switching efficiency of the different media was tested at different dilutions in PBS buffer. Error bars show plus or minus one standard deviation of the mean among three different substrates.*

Figure 3.15 *Schematic showing that the characteristics of the media influence the performance of the switching of the electro-switchable oligopeptides. DMEM exhibits similar switching behaviour as PBS, whereas DMEM-FBS-HEPES induces a drop in switching efficiency. However, the switching ability is higher than when only FBS is used. We propose that the presence of HEPES in the DMEM-FBS-HEPES media allows for the formation of hydrogen bonds and electrostatic interactions between HEPES and the serum proteins, leading to a decrease in the interactions between the serum proteins and the switchable surface. High concentrations of HEPES also inhibit to a certain extent the switching of the oligopeptides likely as a result of intermolecular interactions between HEPES and the oligopeptides. Not to scale (see* ***Figure 3.1*** *for the description of the cartoons). The oligo(ethylene glycol) thiols have been removed for clarity.*

Table 3.1. *Advancing and receding water contact angles and ellipsometric thickness for the different SAMs formed for 24 h. The theoretical molecular lengths were derived from ChemBio3D Ultra 12.0 in which the molecules were in fully extended conformations.*

Chapter 4

Chapter 5

Chapter 1: Introduction to Cell Adhesion and Self-Assembled Monolayers

Abstract: *This chapter provides a background to cell adhesion, nonspecific and specific protein binding, followed by a brief introduction to self-assembled monolayers (SAMs) and the recent developments in the field of SAM based stimuli-responsive surfaces also known as switchable surfaces.*

1.1 Introduction to Cell Adhesion

Cell adhesion is facilitated by the extra-cellular matrix (ECM) via cell-surface receptor proteins known commonly as integrins.[1,2] Integrins are proteins that mediate cell adhesion to the ECM via peptide ligands on the surface, which promote signalling between the cell and the ECM.[3,4] Cells adhere via specific proteins such as fibrinogen,[5] vitronectin,[6] collagen,[7] fibronectin[8,9] and the RGD ligand.[2] Adherence to these ligands allows for the regulation of a number of cellular processes including adhesion, migration, growth, secretion and apoptosis all of which can be influenced by the ECM.[10-13] Cells are also able to interact on surfaces in a variety of methods including hydrophobic/hydrophilic, specific and nonspecific interactions however, a lack of adhesion to surfaces can cause apoptosis.[3]

The ECM acts as a structural support and allows the transfer of signals to adhering cells using specific cell recognition proteins which are identified by transmembrane cellular receptors such as integrins. The attachment of cells on a surface is followed by integrin clustering which leads to the formation of focal adhesions where integrins link to intracellular cytoskeletal complexes and bundles of

actin filaments. These complexes in addition to connecting the cytoskeleton to the matrix, also serve as a framework for the association of signalling proteins that regulate transduction pathways leading to integrin-induced changes in cell behaviour.[1,14]

The discovery of a tripeptide motif Arginine-Glycine-Aspartic acid (RGD) in 1984 was shown to be the minimum peptide sequence required for a cell recognition site.[15] The peptide sequence arginine-glycine-aspartate (RGD) found in fibronectin, vitronectin, type I collagen, and other extracellular matrix proteins has been widely studied as an immobilised cell adhesion ligand specific for integrin-mediated cell adhesion.[16-18] These peptides play not only a major role as anchoring molecules but are also important in processes like embryogenesis, cell differentiation, immune response, wound healing and haemostasis.[18] For these reasons, the development of smart interfaces between cells and substrates has been directed towards the RGD peptide and its capacity to undergo on–off switching when tethered to dynamic surfaces using external stimuli.[19,20] Furthermore, the RGD tripeptide unit benefits from the ability to be easily synthesised and handled, although small changes in the conformation or addition or subtraction of amino acids to the RGD motif has profound effects on cell adhesion.[21]

The RGD surface density required for cell adhesion was shown been to be in the region of 10×10^{-15} mol/cm^2.[22] When adhering cells to a RGD functionalised surface it is important to consider RGD ligand to ligand spacing which is essential in fabricating a cell adhesive surface, as the presence of RGD ligand clustering on the surface can be a cause of significant reduction in the ligand density as well as cell adhesion.[23] In recent literature it has been shown that a critical RGD ligand-ligand

inter-distance of approximately 60-70 nm[24] is required for optimal cell adhesion and the formation of focal adhesions (FA). FAs are formed due to the clustering of integrin receptors after the initial attachment of the cells. Ligands with a spacing above 70 nm have been shown to restrict cellular attachment and spreading due to the lack of integrin clustering (**Figure 1.0**).[25]

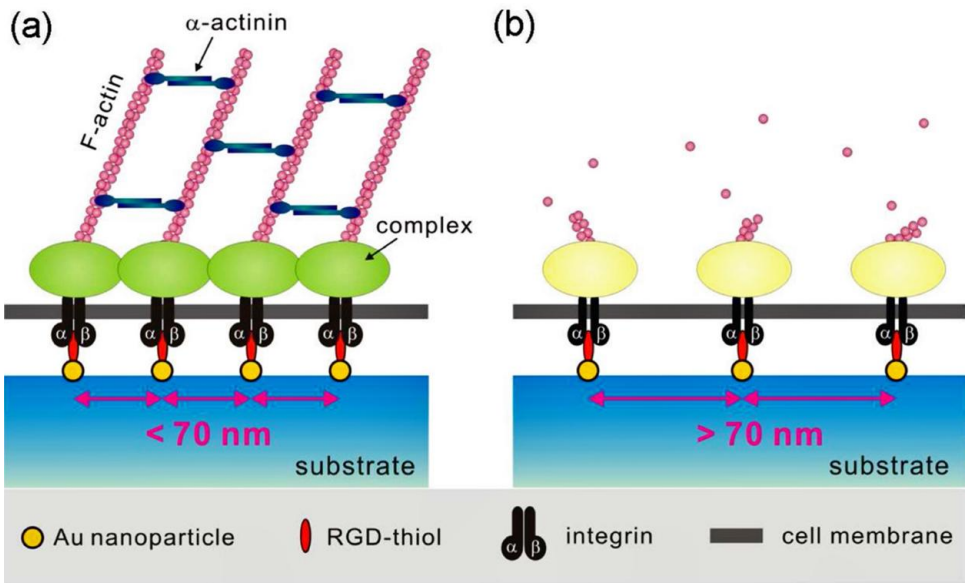

Figure 1.0 *Sketch of integrin clustering and subsequent focal adhesion formation regulated by RGD-thiol ligand nanopatterns. (a) A spacing of < 70 nm between two neighbouring RGD thiol ligands results in effective integrin clustering and focal adhesion complex formation, followed by the formation of the F-actin cytoskeletal network. (b) In contrast, a spacing of > 70 nm results in neither integrin clustering nor FA complex formation.*

1.2 ECM Substratum models based on self-assembled monolayers

Fabricating surfaces that can replicate some of the characteristics of the actual ECM will offer new ways to study how cells sense, integrate and respond to changes in the environment.[16] Surfaces able to reproduce an environment similar to an ECM will provide more systematic research methods than in the past. In addition to being an essential part of cellular studies the new generation of ECM also impacts the field of tissue engineering and medicine regeneration.[26]

Creating novel ECM models using self-assembled monolayers (SAMs) allows for cell attachment and migration via a specific, well-defined and controlled method. Using SAMs in ECM models has a number of advantages for example, the ability to control and fine-tune important parameters of the SAM environment such as thickness and distance between ligands. The high level of precision that SAMs offer enables isolated study of specific biomolecular or cellular interactions. Herein follows a brief description of SAMs and some of the characteristics that make SAMs a feasible option for recreating ECM modelled surfaces.

1.2.1 Self-Assembled Monolayers (SAMs)

SAMs can be defined as highly ordered films that adsorb spontaneously onto solid surfaces from liquids or gases via an active surfactant molecule.[27] One of the earliest reports of monolayer formation was made by Nuzzo and Allara, whom observed that thiol groups form strong non-covalent bonds with gold surfaces resulting in the formation of thiolates on gold-coated surfaces.[28] This important discovery lead the way for extensive study and the characterisation of SAMs on gold

and numerous other surfaces such as glass or silicon, indium tin oxide (ITO) and also 3D nanoparticles.[29-32]

The ability to synthesize a range of functional groups to specifically control surface properties such as hydrophobicity, charge, biomolecular and cellular interactions, have allowed for SAMs to serve as a platform for research in a range of diverse applications.[19,20,33] In addition SAMs offer numerous advantages over other types of scaffolds for the fabrication of dynamic surfaces such as: i) structurally well-defined, ii) characterisable via numerous analytical techniques, iii) chemically flexible for the introduction of organic functionalities on surfaces through simple organic reactions, iv) stable in contact with air and water and suitable for biological studies and v) compatible with diverse external stimuli for induction of dynamicity.[19]

1.2.1.1 Surfactant

The basic molecular structure of SAMs can be divided into three components: the headgroup, the backbone and the endgroup (**Figure 1.1**).[34] The headgroup acts as the anchor and binds the surfactant to the substrate surface via chemisorption. The choice of headgroup will ultimately depend upon the substrate being used, as different headgroups vary in their affinities towards substrates. The most widely studied headgroup-surface interactions include alkanethiolates on gold[32,34,35] and silane derivatives with hydrolysable head groups on silicon oxides.[29]

The backbone, in addition to connecting the headgroup and endgroup, has a number of important characteristics which can affect the molecular orientation,

degree of order within the monolayer and intermolecular distances. For example the length of the backbone has an effect on the molecular ordering of the SAM.

The endgroup is essential in determining the surface properties of the SAMs. A large variety of functional groups can be introduced in the SAMs via the end group that can influence surface properties such as wettability,[36] charge,[37] bio-molecule activity,[38-42] thus allowing for a whole range of potential applications.

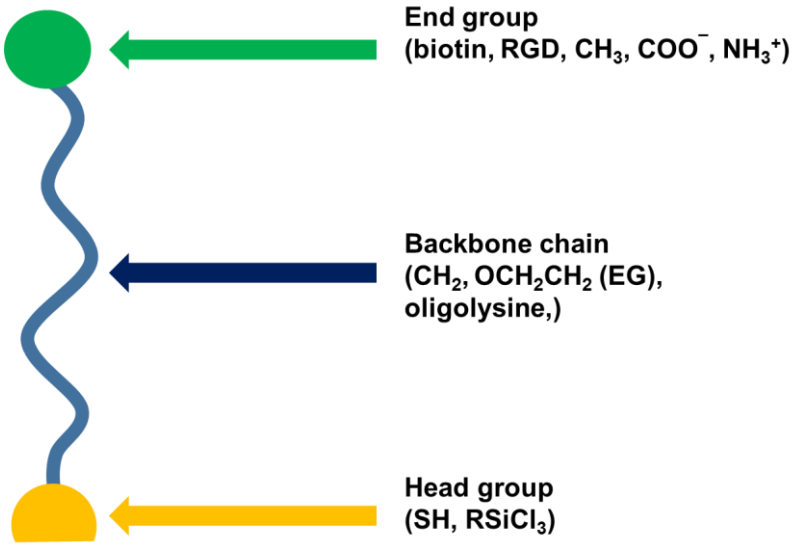

Figure 1.1 *Schematic representation of a surfactant molecule.*

1.2.1.2 Thiol SAMs

SAMs of thiol headgroup derivatives are well known to have a high affinity for a range of metal surfaces including gold surfaces, silver, copper and platinum. However, gold has been the most studied due to its stablity and biocompatibility.[27,31,32] Long-chain alkanethiols with unsaturated and unbranched alkyl chains are known to self-assemble both rapidly and spontaneously to form densely packed, well-ordered monolayers on gold surfaces thus displacing other

materials adsorbed on the surface. (**Figure 1.2**).[27,31,32] The sulphur atoms and alkyl chains promote stability and regular packing of the monolayers via the sulphur-gold bond and van der Waals intermolecular forces.[43-45] The formation of thiols on gold can be carried out either by gas vapour deposition or by immersing in a solution of SAMs. Thus, the ease of preparation of SAMs on gold and their relatively high stability under normal atmospheric conditions make thiol SAMs an excellent option for bio-interface research. Other advantages for using thiols include the ability to characterise the monolayers using numerous surface characterisation techniques such as: ellipsometry, contact angle and x-ray photoelectron spectroscopy. Furthermore the flexibility to synthesise alkanethiols with various functional end groups allows for the presentation of a wide variety of ligands for tailored surface properties.[30-32]

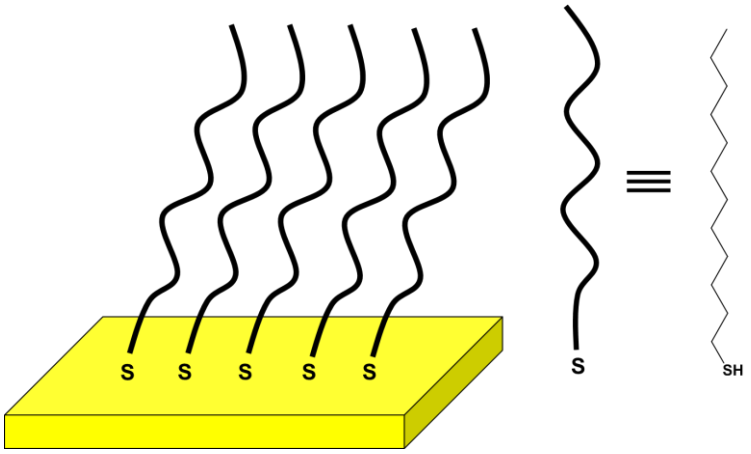

Figure 1.2 *Schematic of a monolayer of dodecanethiol SAMs on a gold substrate.*

1.2.1.3 Silane SAMs

Alkylsilane derivatives such as trichlorosilanes and other hydrolysable silane head groups are used to functionalise substrates bearing hydroxyl groups most commonly silicon oxide (SiO_2).[29] The reactive nature of the silane head groups also allow for the introduction of other groups on the surface, similar to alkanethiols. The formation mechanism of alkylsilanes has been widely disputed, however it is known that water has an important role, in which organosilanes are hydrolysed via condensation reactions with OH groups resulting in the formation of a multilayer of organosilanes via Si-O-Si bonds (**Figure 1.3**).[29]

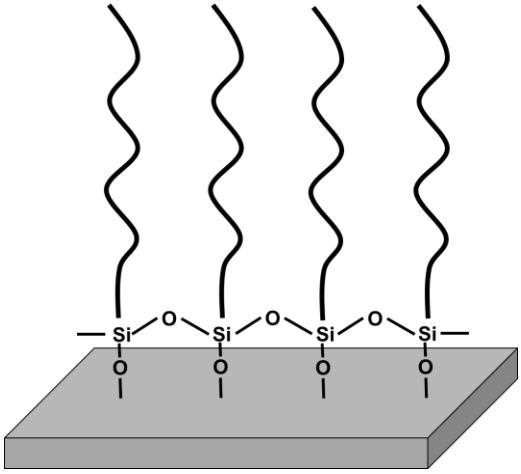

Figure 1.3 *Schematic representation of a monolayer of organosilanes on silicon.*

Silane SAMs also have some limitations for example the choice of functional group is more limited, as the chosen head group should be unreactive to silane head groups. However, silane SAMs are more chemically and thermally stable than thiols on gold, due to the formation of a polymerised network of molecules, which are all covalently bonded to the surface.[46] Despite the greater stability of silane SAMs, the process of

producing high-quality silane SAMs has proven difficult due to the need to control the amount of water in solution and temperature.[47] On the other hand the absence of water results in incomplete formation of monolayers.[48] For the purpose of this thesis, only thiol SAMs on gold will be further discussed.

1.2.1.4 SAM Formation

The adsorption of thiol on gold is a two-step kinetic adsorption process, which begins with the initial physisorption, followed by a stronger chemisorption step leading to complete monolayer formation.[46,47] The initial physisorption step occurs rapidly, requiring a few minutes to reach almost 90% of the final thickness and surface coverage.[44] In this first step small monolayer islands of disoriented thiols begin to form in the laying position on the surface of gold substrates (**Figure 1.4a**).[48,49] The chemisorption step (**Figure 1.4b**) occurs after the physisorption step and takes from a few hours to a few days to reach completion, after which the SAMs reach their final thickness (**Figure 1.4c**).[44,50] In the final process alkyl chains rearrange, undergoing inter-chain van der Waals interactions to form closely packed monolayers (**Figure 1.4c**). The alkyl chains are found to be tilted from the perpendicular on the gold surface, resulting in an angle between 26 and 28°. The rate at which the initial SAMs form and the order of the SAMs varies according to the length of the alkanethiol.[27,44]

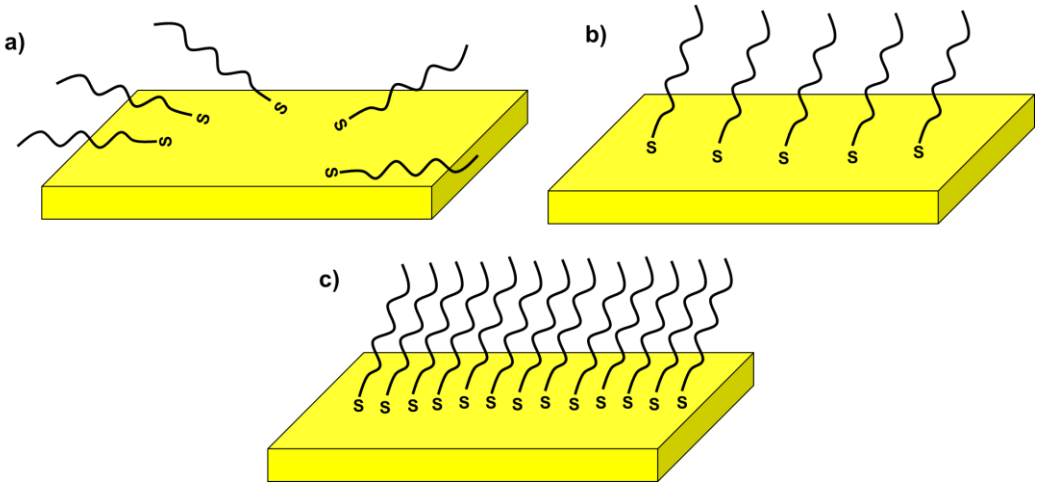

Figure 1.4 *Schematic of SAM formation on gold where a) shows the initial physisorption step followed by b) the chemisorption step which leads to more ordered monolayers and finally c) fully formed SAMs*

1.2.1.5 Mixed thiol SAMs

The formation of mixed SAMs is a more complex process than forming a single SAM, which involves the combination of two or more different surfactants.[51] One of the uses for mixed monolayers is in creating a greater spatial distribution between SAM molecules, hence they are being used increasingly for purposes such as the immobilisation of biomolecules. For example specific molecular bio-recognition systems have been successfully produced using mixed biotin-functionalised monolayers to immobilise proteins such as neutravidin and streptavidin onto biotin binding sites.[52,53] These systems have been pivotal in the development of protein immobilisation on surfaces and as immunosensors.[53,54]

Mixed SAMs can be achieved by selectively changing the endgroup functionality subsequent to SAM formation or by co-adsorbing two or more species

onto the substrate during SAM formation. Co-adsorption is more widely used as it is still possible to control the final molecular composition and order of the SAM.[44] It is important to note that the ratio of two components in a solution of mixed SAMs is usually not identical to the SAM on the surface, due to preferential adsorption of one component over the other.[55] Other factors that can influence the composition and surface coverage of the monolayer include intermolecular interactions, the solvent and the surface during SAM formation.[52,56]

1.2.2 Nonspecific protein adsorption and protein inert surfaces

SAM surfaces with biomolecular recognition units can be immensely useful for carrying out measurements for specific binding interactions. However, a significant challenge for these biological systems is the problem of nonspecific adsorption, which is the unwanted adsorption of molecules on to the substrate surface other than the specific binding sites. This form of adsorption can dramatically decrease the functionality of interfaces potentially considered for biorecognition purposes, by producing either a high degree of background noise or "false positives."[57] Thus, in order to produce materials that can be used for biotechnological applications, a requirement for the design of these bio-interfaces is that they must provide high specific binding with reduced nonspecific binding.

Significant research effort has gone into finding molecules that prevent non-specific binding of proteins, which has led to the usage of oligoethylene glycol (OEG)-terminated SAMs. OEGs have been used for numerous biological applications due to their ability to resist protein adsorption.[54] It has been shown that OEG SAMs have high surface coverage and are able to prevent nonspecific protein

adsorption.[57] Thus, OEG terminated SAMs are used commonly in diluting protein immobilisation surfactants, i.e. by the formation of mixed monolayers of OEG and a surfactant that has a reactive site that interacts with a specific moiety of the proteinto be immobilised. By diluting the surface it is possible to control the overall spatial distribution of proteins on the surface. Thus, a sufficiently spatially distributed surface will mean that the immobilisation of proteins is specific and not affected by any neighbouring protein molecules. A primarily protein-inert surface will allow for proteins to be immobilised in an accurate manner and thus, it is possible to study the desired cell protein interactions.[16] Furthermore OEG alkanethiol assemblies of HS-$(CH_2)_{11}$-$(OCH_2CH_2)_n$-OH (EG_n), where n= 3 or 6 have been studied extensively and shown to suppress protein adsorption. However shorter EG_n chains were found to be ineffective.[54,58] In the case of mixed SAMs, in order to prevent protein adsorption, a surface should be composed of a high proportion of EG_n (>50%) and where $n \geq 3$. The protein resistant characteristics of OEGs are generally attributed to hydrogen bonding between the EG_n units and water, thus forming a hydrophilic monolayer that prevents protein adsorption.[59,60]

The usefulness of OEG surfaces partly depends on their protein inert properties, but in order for these surfaces to have practical application, it is essential that specific protein binding can still take place.

1.2.2.1 Specific protein adsorption on surfaces

The ability to specifically detect the binding of proteins on surfaces modified with receptor ligands which act as specific binding sites is essential to better understand protein affinity on surfaces. One of the systems that has been widely

studied is the biotin-bound protein complexes, which have been used in a wide variety of bioanalytical applications, such as biochip sensor fabrication,[61-66] immunoassays,[67,68] and targeted drug delivery and screening.[69] In many of these applications proteins are often used to bind to a biotin tethered to the surface by taking advantage of the high affinity and specificity of biotin-bound proteins such as avidin,[65,66,68,70] streptavidin[69,71-73] and neutravidin.[62,63] The avidin protein is a tetramer with four identical subunits, each of which consists of one binding site for biotin (**Figure 1.5**). Furthermore, avidin has an extremely high binding affinity to biotin ($K_a \approx 10^{15}$ M^{-1}) and forms a stable complex over a range of temperature and pH values.[74] Although avidin is an excellent candidate for the study of specific adsorption, it has a major drawback; high nonspecific adsorption.[74] The positively charged avidin protein can bind to negatively charged surfaces such as cell membranes[74] or silica based substrates.[75] The cause of avidin's high nonspecific binding can be attributed to its basic isoelectric point (pI ~10)[74] and its carbohydrate groups, which are made up of four mannose residues and three *N*-acetylglucosamine residues per subunit.[76]

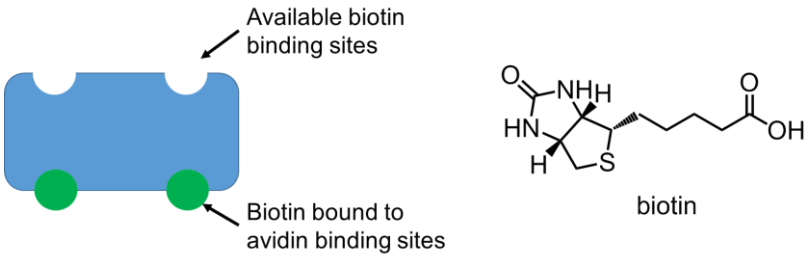

Figure 1.5 *Schematic of avidin tetramer with four biotin binding sites and biotin molecule.*

In order to counter the high nonspecific binding of avidin, alternative biotin-bound protein complexes such as streptavidin and neutravidin have been used and shown to have high affinity and specificity for biotin.[62,63,70,73,77] Streptavidin is a nonglycosylated protein with a slightly acidic pI of ~5-6.[74] Neutravidin is a deglycosylated form of avidin with a more neutral pI of 6.3. Both streptavidin and neutravidin are commonly used in biosensing applications due to their nonspecific binding and high specific adsorption onto biotin functionalised SAM surfaces.[70]

1.2.3 Dynamic switchable surfaces

In the past, studies for cell adhesion were commonly carried out on glass or polystyrene substrates coated with an adsorbed protein layer.[16] Although this method is very simple, it has a number of shortcomings, the most problematic being the lack of control of the orientation and conformation of the adsorbed protein layer on the surface.[16] This can reduce reproducibility of experiments due to the differences in available binding sites, in addition to numerous other variables within the system such as protein-surface interactions.[78]

The fabrication of tailored substrates capable of dynamically controlling biomolecular and cellular interactions has many advantages in improving the understanding of cell mechanisms for adhesion and migration. SAM based surfaces offer an effective approach to producing dynamic control over cell adhesion. More recently there has been an emphasis on dynamically controlled substrates which include an “on/off” mechanism via a range of external stimuli (**Figure 1.6**).

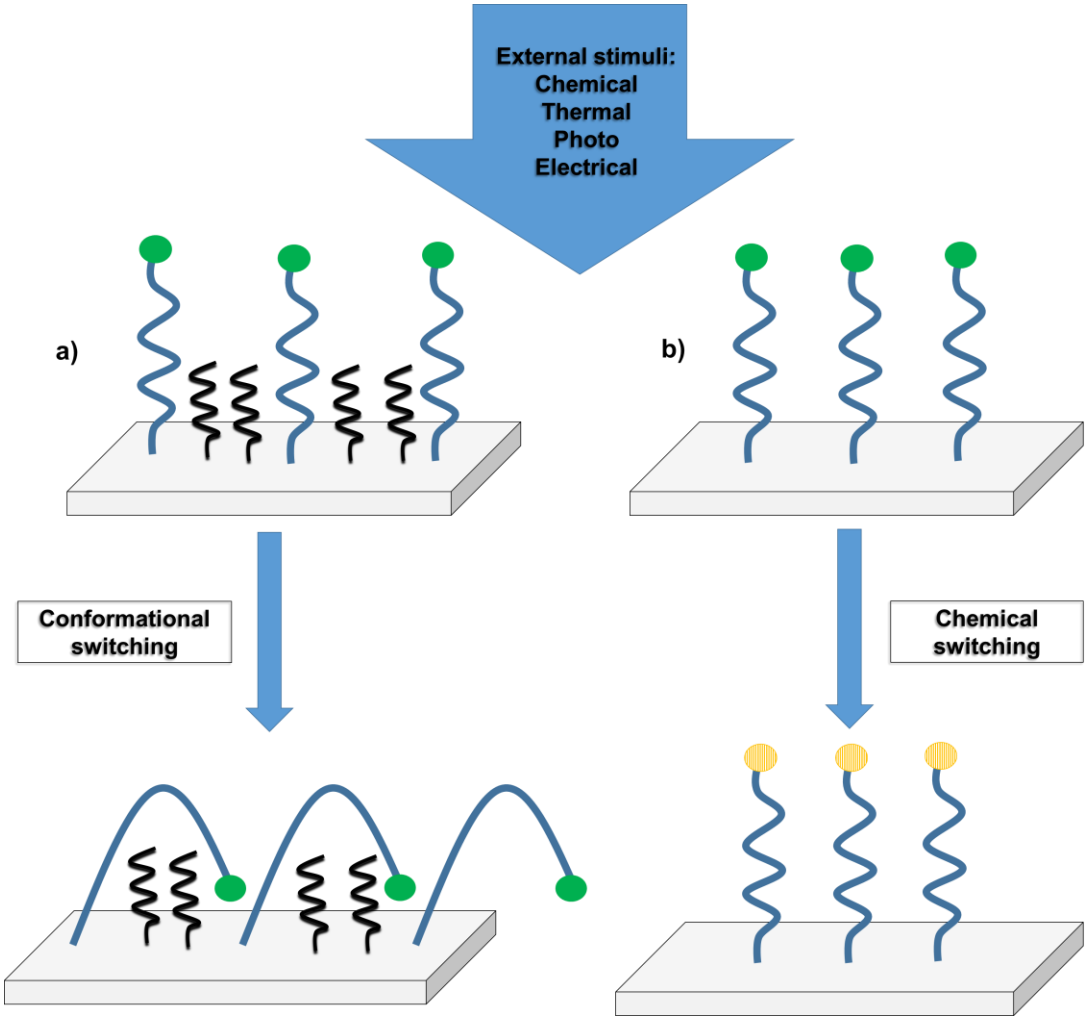

Figure 1.6 *Schematic showing different external stimuli that can be applied to a surface resulting in a) conformational switching and b) chemical switching.*

By applying an external stimulus in the form of chemical, thermal, photo and electrical it has been shown that the conformation of molecules or chemical composition on the surface can be manipulated.[33] Thus, concealing or exposing the binding ligands allowing for some degree of control over cell adhesion on surfaces.

1.2.3.1 Chemical and biological stimuli responsive surfaces

Surfaces showing smart responsive behaviour towards both chemical and biological stimuli have been fabricated with high sensitivity and shown to be re-usable biosensors. One example is the development of electrochemical DNA (E-DNA) sensors.[79,80] These sensors work via chemical interactions by becoming fluorescent upon hybridisation with target DNA molecules. The E-DNA sensor consists of a surface-bound DNA stem-loop labelled with an electroactive sensing element in this case ferrocene (Fc), which is in close proximity to the electrode and produces large Faradaic currents. After hybridisation with target DNA, the DNA stem-loop becomes upright, significantly increasing the distance between the electroactive moiety and the electrode surface, thus resulting in a measurable reduction in current. This was known as a signal-off E-DNA sensor, due to the signal being generated when an "off signal" was recorded (**Figure 1.7**).

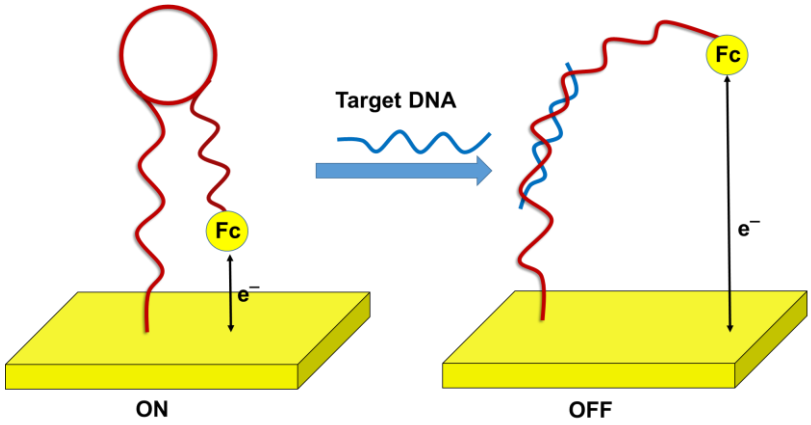

Figure 1.7 *Signal OFF E-DNA sensor based on a surface-confined stem-loop oligonucleotide that holds the Fc group into close proximity with the gold electrode, which allows for electron transfer from the redox group to the electrode. Upon hybridisation with the target DNA sequence, the distance between the Fc group and the electrode is altered, thus decreasing the electron transfer efficiency.*[80]

The disadvantage of this E-DNA system is that the sensitivity is very limited (~10 pM) due to the mechanism of the sensor, as the signal can be no more than 100% of the original signal. The original E-DNA sensor was further developed and improved to enable “signal on” sensors using a similar ferrocene moiety[81] and a methylene blue electroactive probe with a significantly improved detection limit of 400 fM[82] upon hybridisation of the target DNA. More recently Chen and co-workers used the ferrocene attached to the DNA system as an electrochemical cell sensor to check the electron transfer efficiency before and after entering cells via cell transfection.[83] These findings were then used as a basis to carry out quantitative studies to differentiate between tumour cells and normal cells.[84]

Iqbal and co-workers reported an effective method of controlling spatial distribution of functional groups on surfaces using pH-switchable SAMs with surface-appended pseudorotaxanes.[85] The multi-step formation of the SAMs, involved the self-assembly in solution of a dendron containing crown and a dibenzylammonium (DBA) recognition site with fluorine end group and a thiol for surface tethering to gold. The dendron provides the SAM space for each pseudorotaxane occupied on the SAM. In the second step following SAM formation, the dendron was released from the surface by switching off the noncovalent interactions upon raising the pH. The vacant space was backfilled with a second SAM. Thus, producing a surface that can tailor both density and spatial distribution of functional groups on the surface (**Figure 1.8**).

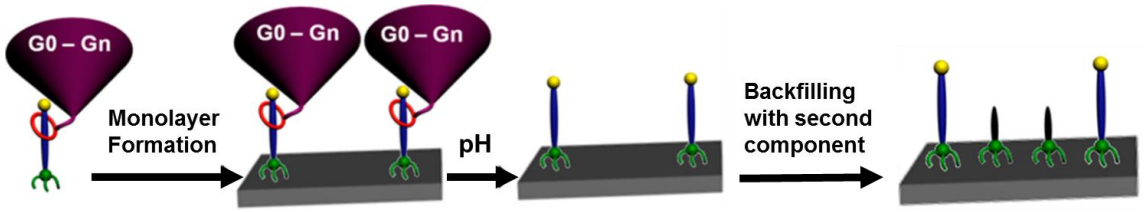

Figure 1.8 *Schematic representation of strategy for controlling density and spatial distribution of functional groups on surfaces using a pH-switchable supramolecular system.*[85]

1.2.3.1.1 Electrochemical stimuli responsive surfaces

Surfaces functionalised with electroactive groups such as the hydroquinone (HQ) and benzoquinone (BQ) redox couple have been studied extensively and provide real-time molecular-level control between surfaces and biomolecular or cellular interactions.[39,86-94] Mrksich and co-workers have pioneered a number of cell-based sensors, demonstrating methods of molecular communication between cells via electroactive functionalised surfaces.[39,40,91,95,96] An early example of electrochemical release was reported with SAMs formed on gold using ligands such as biotin and RGD peptide tethered to quinone ester groups.[40,95] An electrical potential was then used to reduce the BQ to a HQ resulting in an intramolecular cyclisation reaction to give lactone, thus releasing the ligand and allowing for electrochemical control of specific binding of streptavidin and selectively releasing cells from substrates on demand (**Figure 1.9a**).[40,95]

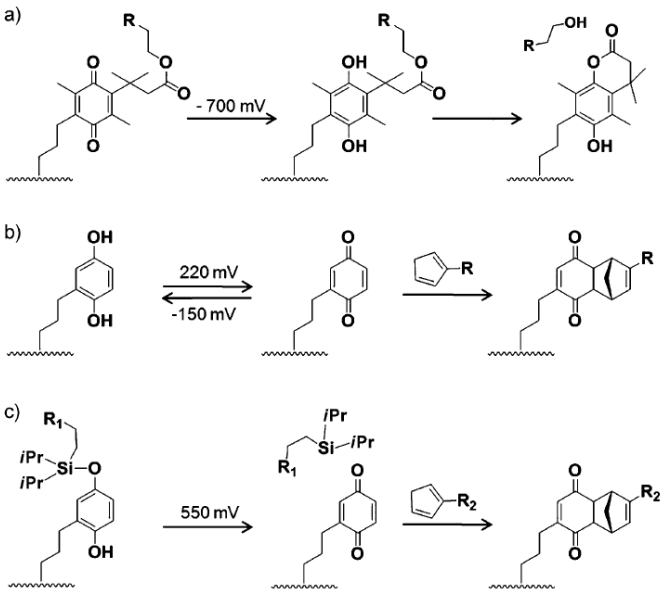

Figure 1.9 *Three examples of hydroquinone (HQ)/benzoquinone (BQ) presenting SAMs on gold surfaces, activated by electrical potential. a) Reduction of BQ to give HQ, which undergoes intramolecular cyclisation and the release of ligands.*[40,95] *b) HQ is reduced to BQ, which is linked with a diene-tagged ligand via Diels-Alder reaction.*[39] *c) An O-silyl-protected HQ is oxidised resulting in the cleavage of the O-Si bond and conversion of HQ to BQ which is then used to immobilise diene-tagged molecules.*[96]

Another method for electrochemically controlling ligand immobilisation was introduced using SAMs presenting HQ, which were electrochemically oxidised to form BQ, upon which diene-modified molecules were immobilised via Diels-Alder cycloaddition (**Figure 1.9b)**.[39] The electrochemical oxidation method of converting the HQ to BQ was further developed to allow for two dynamic properties including: the release of one ligand and the immobilisation of another ligand (**Figure 1.9c**).[96] Yousaf *et al.* recently extended this work to demonstrate an electrochemical

switchable surface for controlling peptide structures to modulate between cell-adhesive and a non-cell-adhesive state by grafting RGD peptide.[97] Many of the HQ and BQ based systems require very specific potentials in order to trigger the electroactive group of interest, hence in most of the systems described PBS was used as the electrolyte of choice, whereas more complex culture media was avoided.

Ciampi and co-workers developed the use of quinone chemistry further and reported a unique reversible method for an electrochemical switch using a H-terminated silicon surface (Si(100)) and hydrosilylation of alkynes followed by the attachment of other moieties via modular assemblies to control cell adhesion (**Figure 1.10**).[98] The Si(100) surfaces were shown to change from being resistant to cell adsorption to promoting cell adhesion. The SAM could be chemically switched to attach an oligo(ethylene oxide) (OEO), which was the cell resistant molecule. However, application of a reducing potential of -1800 mV caused the cleavage of the OEO molecule via a redox-sensitive quinone moiety making the surface amenable to cell adhesion. Once again PBS was opted over culture media for the electrolyte in this system probably in order to reduce any potential inference with the electrochemical switching mechanism.

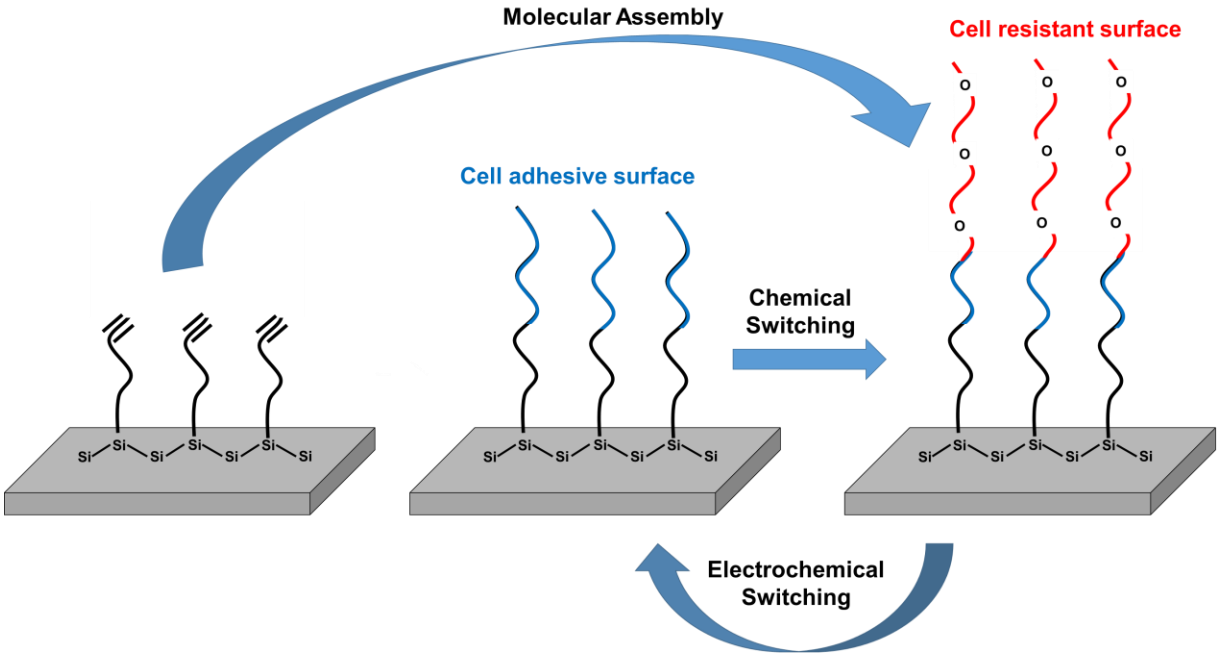

Figure 1.10 *Schematic for electrochemical switching of Si(100) modular assemblies.*

Another recent example of electrochemically controlled release of cells was demonstrated by An and co-workers using a supramolecular system, by using a RGDS functionalised with an N-terminal tryptophan-glycine-glycine (WGG) motif and cucurbit[8]uril (CB[8]), a macrocyclic host molecule capable of binding two aromatic guest molecules simultaneously (**Figure 1.11**).[99] The WGG tripeptide was bound as a ternary complex in the cavity of a viologen CB[8] inclusion complex. The electroactive viologen was modified with an alkyl thiol group in order to bind to a gold surface.

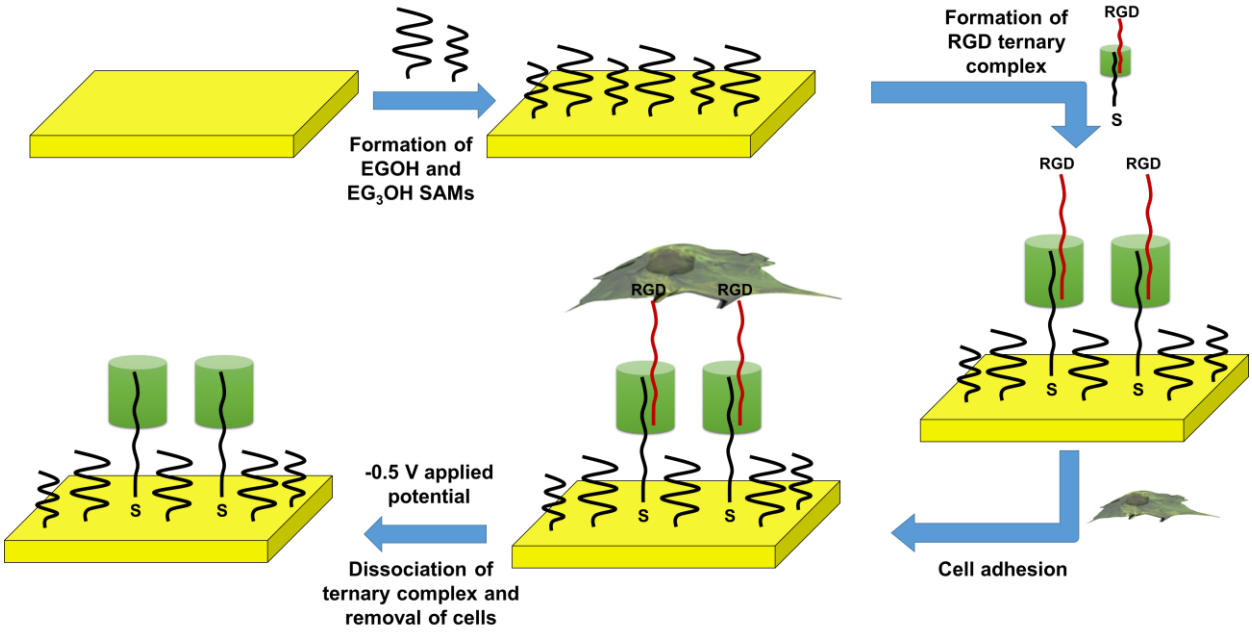

Figure 1.11 *Schematic showing a supramolecular system for the controlled electrochemical release of cells.*

Two ethylene glycol groups (EGOH and EG_3OH) were initially formed on the gold surface followed by the formation of the ternary complex. Cells were then adhered to the surface in DMEM without serum. By applying a -0.5 V electrical potential to the surface the viologen could be reduced thus releasing the RGD ternary complex to dissociate. The dissociation mechanism of the ternary complex was then used to electrochemically control cell adhesion. Mouse myoblast cells were seeded for 1 h, after which an electrical potential of -0.5 V was applied for 200s and the surface was successfully shown to remove over 90% of the original adherent cells form the surface after washing with saline.

1.2.3.2 Thermo-responsive surfaces

The use of temperature as a stimulus is another well-known method to control biological properties on the surface. Reports of thermo-responsive surfaces have been primarily based on polymers designed for biomedical applications.[100-102] However, it has been shown by Balamurugan *et al*. that compositions of mixed SAMs of oligo(ethylene glycol) (OEG)- and methyl- terminated alkanethiols exhibit changes in their resistance to protein adsorption, bacterial cells used for attachment and wettability at room temperature and at 37 ^{o}C.[103] Proteins were dissolved in PBS prior to exposure to surfaces whereas bacterial attachement took place using a chemostat culture in modified basal medium.

Zareie and co-workers also reported temperature-responsive OEG SAMs which were shown to reversibly switch the wettability of the surface and more importantly control the binding of streptavidinto a biotinylated surface.[104] In order to demonstrate the protein-resistant nature of the OEG, streptavidin dissolved in nanopure water was immobilised onto a mixed SAM of the OEG along with a shorter biotinylated disulphide. It was shown that at 23^{o}C the biotin molecules were embedded in the OEG layer due to the difference in length. However, when the temperature was raised from 23 ^{o}C to 45 ^{o}C there was an increase in the adsorption of streptavidin by ~29 fold, which was attributed to the increased availability of the biotin molecules due to the collapse of the neighbouring OEG chains (**Figure 1.12**).

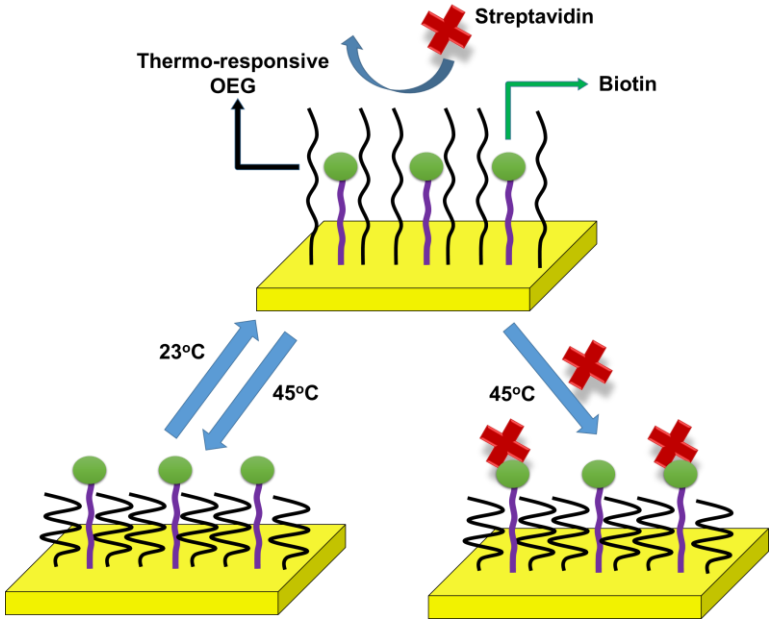

Figure 1.12 *Schematic representations of the mixed SAM (OEG and biotinylated disulfide) and streptavidin binding onto the mixed SAM at 45°C, however at 23°C streptavidin is unable to bind due to the OEG chains masking the biotin.*

1.2.3.3 Photo-responsive surfaces

Numerous studies have successfully reported cell-material surfaces which are responsive to light. Nakanishi and co-workers reported a method to capture genetically tagged extracellular matrix protein in response to light on gold functionalised surfaces.[105] The substrate was composed of mixed SAMs of three disulfide compounds including (i) a photocleavable poly(ethylene glycol) (PEG) (ii) nitrilotriacetic acid (NTA) and (iii) hepta(ethylene glycol) (EG_7). The NTA group has a high affinity for oligohistidine tag (His-tag) sequences, however this interaction was suppressed due to the steric hindrance of the PEG brushes which prevented the His-tag from binding to the NTA. Photoirradiation of the substrate in water released the PEG brushes thus, allowing for the capture of the His-tag proteins, while preventing

non-specific adsorption of non-His-tagged proteins via the the EG_7. (**Figure 1.13**) Furthermore the same method was used to immobilise a His-tagged fibronectin fragment to irradiate patterned regions in order to selectively attach cells to the irradiated regions. These results provided a useful method for studying cellular behavior on specific extracellular matrix proteins in cell-culturing environments.

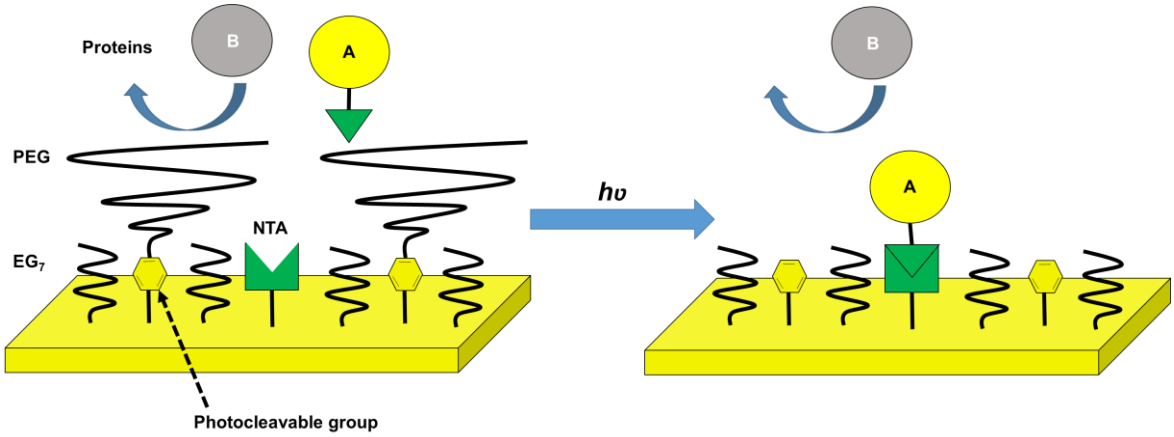

Figure 1.13 *Schematic of a dynamic substrate that prevents adsorption of any proteins prior to photoirradiation due to the PEG brushes (Left). However after photoirradiation the PEG brushes are released, the His-tagged proteins (protein A) is immobilised to the NTA group, while keeping adsorption of non-His-tagged proteins (protein B) blocked by the EG_7 underbrushes.*

Liu and co-workers fabricated a photo-switchable RGD peptide SAM based on azobenzene, which displayed reversible control of cell adhesion (**Figure 1.14**).[106] This approach to controlling cell adhesion using an RGD containing switching moiety

was based on previous work carried out by Kessler and co-workers.[107] The azobenzene unit acts as the switching mechanism through reversible *cis-trans* isomerisation. In the *E* isomer the RGD peptide is presented for the adhesion of cells in DMEM containing 10% FBS and can be switched by irradiation of UV light (λ = 340-380 nm) to the *Z* isomer, which masks the RGD peptide in PEG-terminated SAMs to prevent cell adhesion. Reverse isomerisation occurs by the irradiation of visible light (λ = 450-490 nm). This study demonstrates clearly that small changes in conformation of the RGD peptide can offer effective dynamic control of cell adhesion.

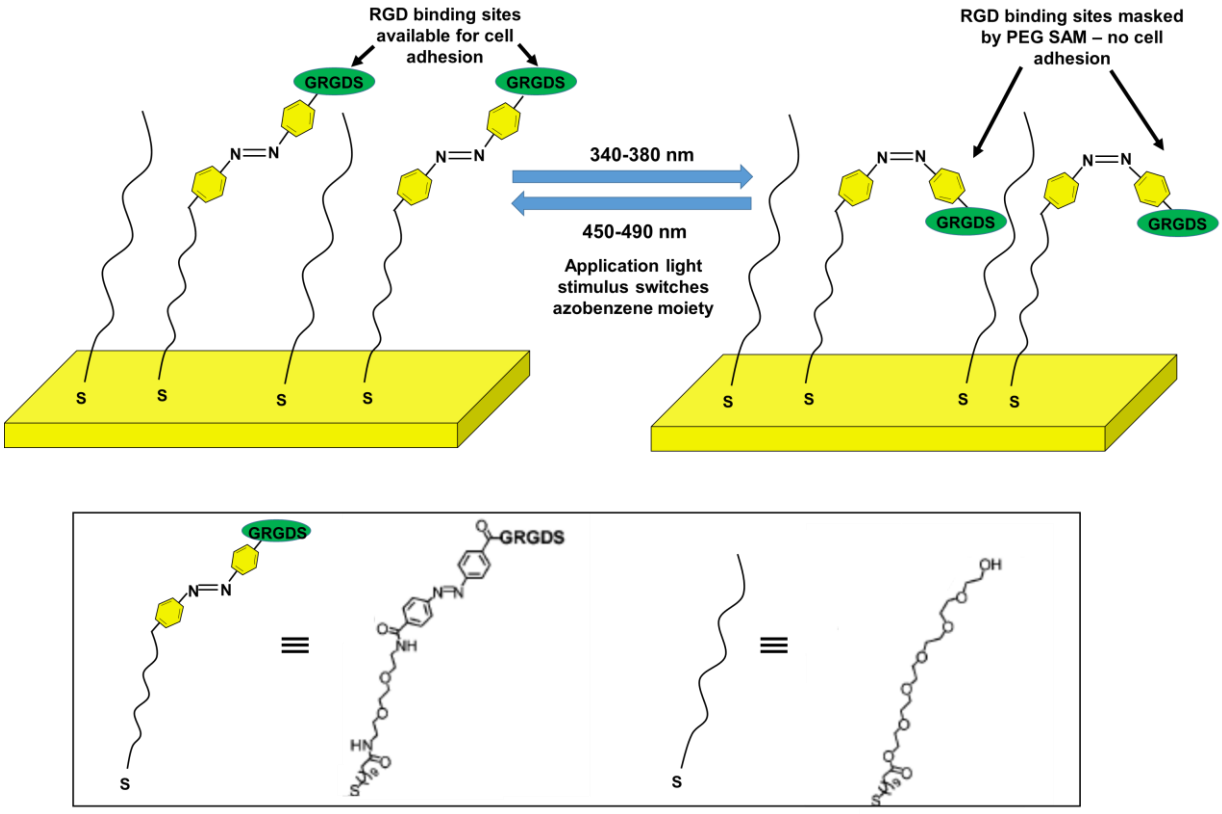

Figure 1.14 *Schematic of a photoswitchable surface where he azobenzene moiety can be converted photochemically between the E and Z configurations to either present or mask the RGD ligand and hence modulate biospecific cell adhesion.*

Another method of using azobenzene SAMs to control cell adhesion was reported via host-guest complexation. The host-guest interactions between a GRGDS terminated azobenzene (azo-GRGDS) and *α*-cyclodextrin (*α*-CD) terminated silane SAM were utilised by Gong and co-workers[108] to reversibly control cell adhesion (**Figure 1.15**). After the assembly of the azo-GRDGS to the *α*-CD, the azo-GRGDS could be released upon UV irradiation along with adherent cells (**Figure 1.15**)

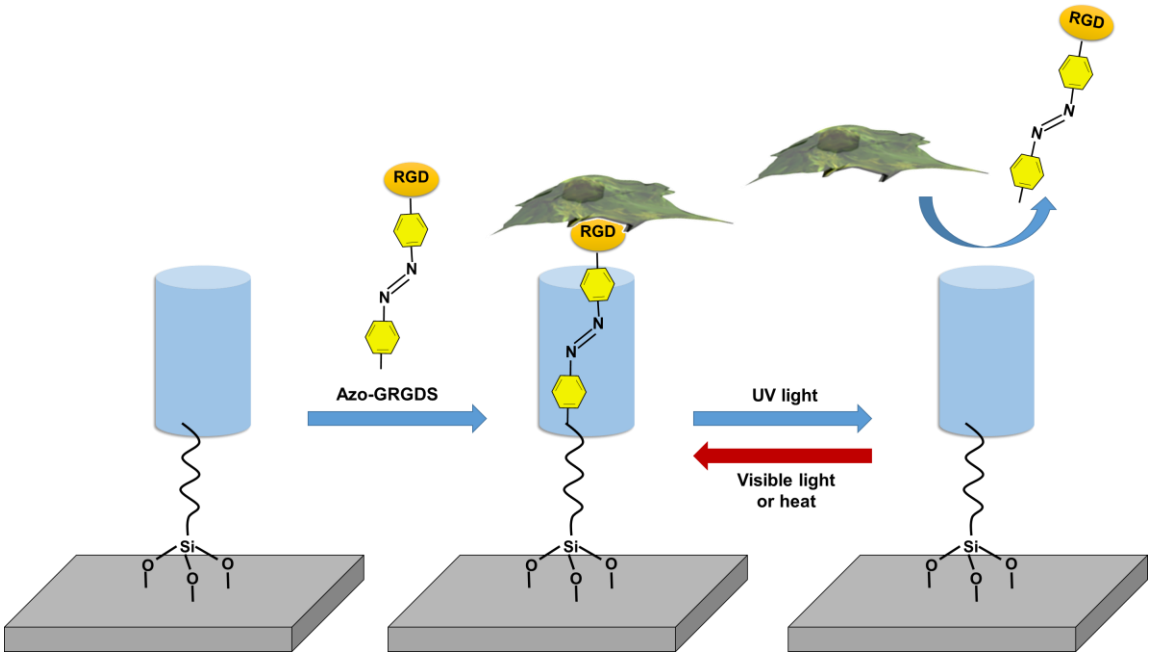

Figure 1.15 *Schematic representation of a silane terminated α-CD which forms an inclusion complex via host-guest recognition with an azobenzene-GRGDS molecule. Hela cells adhere to the surface when the azobenzene is in the trans conformation. Upon UV irradiation at 365 nm the trans-azobenzene changes to cis-azobenzene, which results in the detachment of both the azo-GRGDS and cells from the substrate.*[108]

1.2.3.4 Electrically responsive surfaces

Electrically responsive surfaces have been among the most studied in the field of switchable surfaces. Numerous electroactive groups have been successfully employed to switch functionalities in *situ*, thus offering the ability to manipulate the interactions of peptides,[39,40,88,91,96,109] DNA,[110-112] proteins[41] and cells[39,40,91,96] with surfaces. Recently a label-free method for analysing interactions of proteins with surface-tethered ligands was developed in which an electrical field was used to control the conformational switching of surface-bound negatively charged DNA levers tethered to Cy3 dyes (**Figure 1.16**).[113]

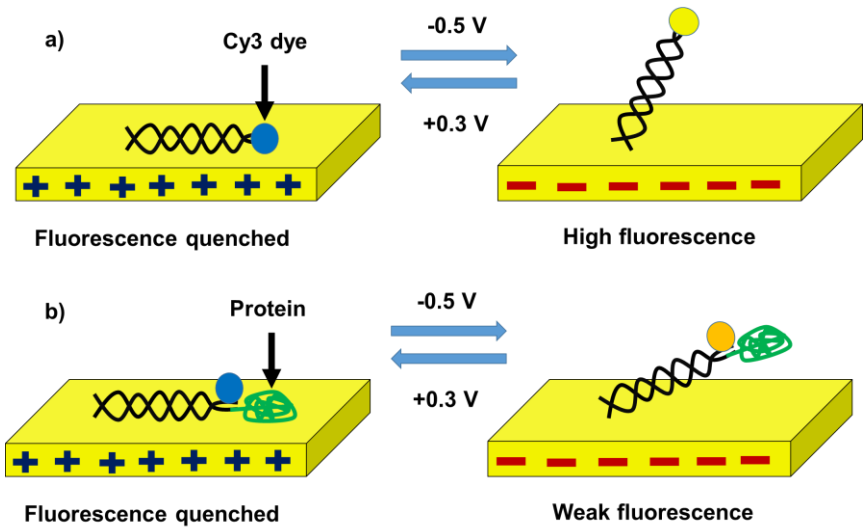

Figure 1.16 *Schematic representation of the DNA lever where a) shows the DNA lying on the surface due to an attractive +0.3 V applied potential, the DNA is repelled when a negative potential of -0.5 V is applied. b) When a protein is attached to a ligand at the top end of the DNA, the upward motion at a negative potential slows and lags behind the DNA lever. The blue circle represents the Cy3 fluorophore when the fluorescence emission quenched by the surface. The yellow circle represents a high fluorescence emission due to the lever being further from the surface.*

Application of an attractive +0.3 V applied potential caused the DNA to lie on the surface. Thus, in the lying down conformation the fluorescence emission from the Cy3 dyes attached at the distal end of the DNA was low, due to the proximity quenching effect of the metal substrate.[114] However, when the electrical potential was switched from +0.3 V to -0.5 V, the DNA was repelled from the surface and pushed into a more vertical position, hence increasing the fluorescence emission due to the Cy3 dyes moving further away from the quenching surface. The fluorescence emission was an effective method to report the distance of the DNA's top end to the gold surface. Thus, when a protein was bound to the DNA lever (**Figure 1.16b**), there was a lag behind the dynamics of the bare lever, attributed to the hydrodynamic drag that occurs when protein bind to the DNA's top end. It was possible to measure the diameter of the protein with angstrom resolution by using time-resolved upward dynamics. In addition, this method revealed avidity effects and differentiation between analytes with one or more binding sites.

Conventionally SAMs have been shown to be densely packed and so regulating conformational changes on surface-tethered molecules has not been possible. The development of low density SAMs[115,116] has allowed for the design and fabrication of numerous novel SAMs for the dynamic control of protein adsorption and release under electrical stimuli.[42,117] These surfaces display reversible switching via conformational changes of surface bound molecules in response to an applied potential. Changes in molecular orientation have been proven using different techniques such as sum-frequency generation (SFG)[115,118] and atomic force microscopy (AFM).[119] Lahann and co-workers demonstrated the possibility of using a low density SAM with reversible switchable properties by using a hydrophobic

mercaptohexadecanoic acid (MHA) chain capped by a hydrophilic carboxylate group (**Figure 1.17**).

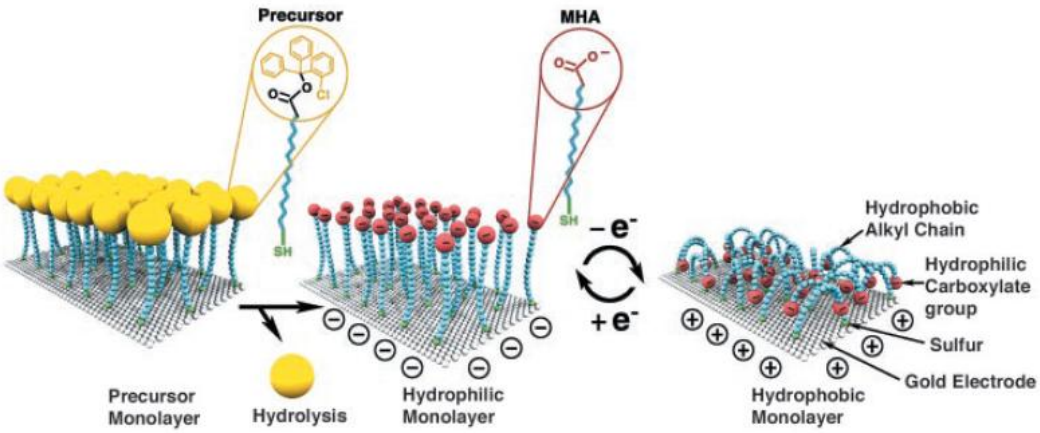

Figure 1.17 *Schematic showing the formation of LD-SAMs by utilising a bulky head-group, thus creating a monolayer that switches between hydrophilic and hydrophobic states upon the application of an electrical potential.*[37]

A space-filling end group was used to provide sufficient spatial distribution for each molecule in order to undergo a conformational change between “straight” and “bent”. After SAM formation cleavage of the space-filling end group presented the low density SAM. Furthermore conformational change was confirmed due to the change in wettability of the surface from hydrophobic to hydrophilic upon the application of an electrical potential. Thus, clearly demonstrating reversible control of a low density SAM using an electrical stimulus.

Liu and co-workers further developed the low density 16-mercaptohexadecanoic acid (MHA) SAMs to produce carboxylic-termintated and amino-terminated SAMs that could undergo conformational changes in response to

an electrical stimulus.[120] A similar system was developed with carboxylic functionalised microfluidic chips and shown to control the adsorption and release of streptavidin and avidin proteins in PBS buffer due to conformational changes (**Figure 1.18**).[42]

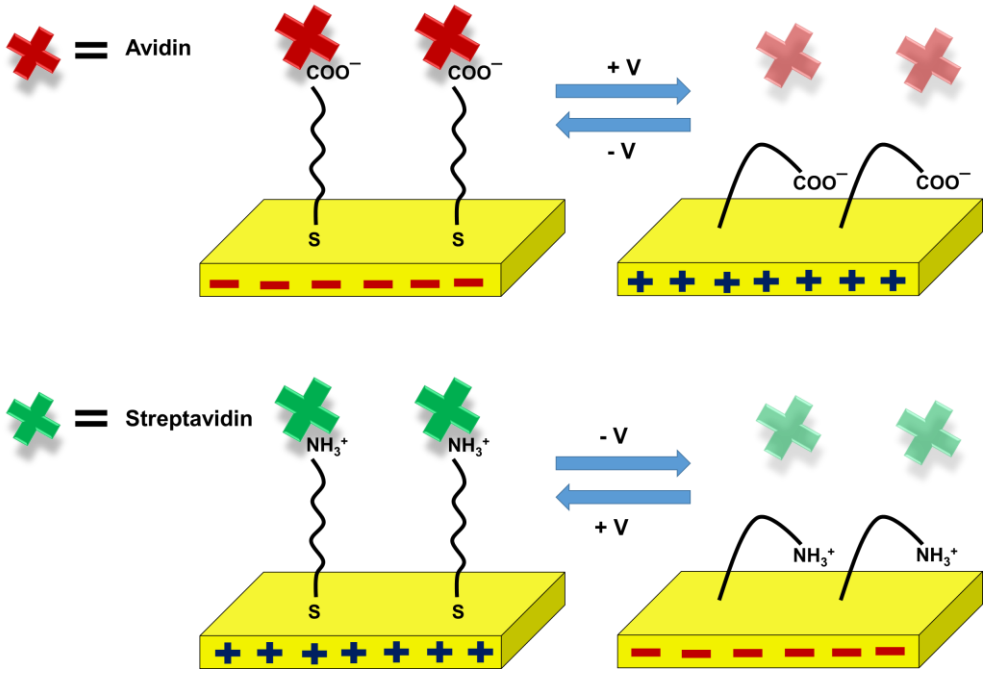

Figure 1.18 *Schematic representation of electrically controlled adsorption and release of avidin and streptavidin proteins.*

The positively charged avidin adsorbed to the surface under a negative potential, whereas the avidin was released when a positive potential was applied. Streptavidin, a negatively charge protein, was also used to show a similar adsorption and release with an amine-functionalised microchip under alternate potentials.

The concept of electrically switchable surfaces was developed further recently in our group[121] in which an electrically switchable oligopeptide surface was fabricated. The surface consisted of a positively charged oligolysine backbone which has at one extremity a cysteine group able to anchor to a substrate and a bioactive molecular moiety at the other extremity, which act as functional components on switchable surfaces for controlling specific biomolecular interactions. The surface also had a neutral triethylene(glycol) thiol (**TEGT**) to provide sufficient space for the switching of the peptide.

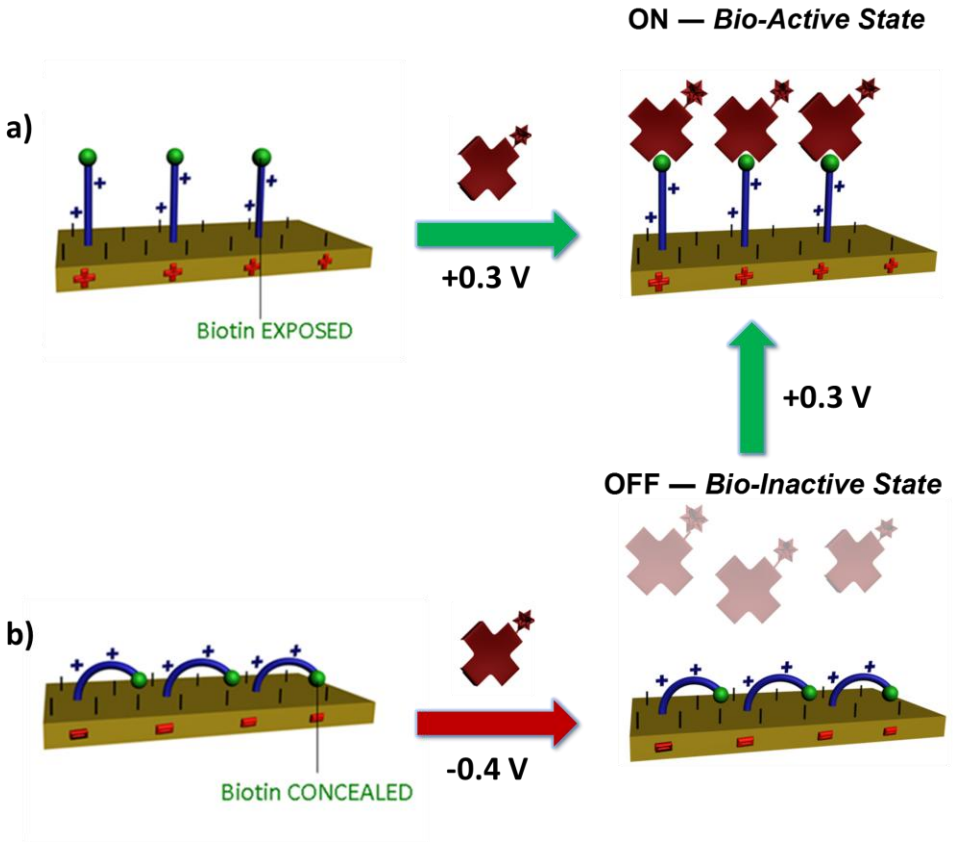

Figure 1.19 *Schematic representations showing the biotin-4KC:TEGT electro-switchable biological surfaces. Upon the application of a) +0.3 V applied potential the biotin group is exposed allowing for neutravidin binding and b) -0.4 V applied potential the biotin group is concealed preventing neutravidin binding.*

The electro-switchable system is based upon the conformational switching of positively charged oligolysine peptides that are tethered to a gold surface, such that bioactive molecular moieties incorporated on the oligolysines can be reversibly exposed (bio-active state) or concealed (bio-inactive state) on demand, as a function of surface potential (**Figure 1.19**). Switching of the surfaces was determined by observing the binding events during two applied potentials of either +0.3 V and -0.4 V. Fluorescence images were taken of the labelled neutravidin-biotin binding and were observed under fluorescence microscope, where higher fluorescence intensities were observed for +0.3 V whereas, minimal fluorescence was observed for -0.4 V. SPR experiments further confirmed the switching of the surface by showing a 90% reduction in neutravidin binding under PBS buffer conditions with a negatively applied potential. Further work carried on the biotin-4KC:TEGT mixed SAMs demonstrated the reversible conformational changes of the biotinylated peptide by using SFG[118] and molecular dynamic simulations,[122] which indicated that a negative applied potential caused a collapse of the oligopeptide backbone thus, masking the biotin binding sites.

Gooding and co-workers[123] further developed the concept of regulating conformational change of molecules attached to the surface using electrical potential and designed two-component SAMs with the aim of controlling control cell adhesion using a 0.1% serum containing media. The two-component SAMs consisted of a protein-resistant backbone chain of hexa(ethylene glycol) (EG_6), with a charged moiety at the distal end and the second component was RGD terminated to allow for cellular adhesion receptors to bind via integrins (**Figure 1.20**). Two SAM surfaces were prepared using different EG_6 molecules, one with a sulfonate (anionic) distal moiety and the other with an ammonium (cationic) distal moiety. These components

could be switched depending on the potential applied to the surface. Thus, if the potential applied was the same polarity as the charged distal moiety, the EG_6 component would stretch out (**Figure 1.20a** and **Figure 1.20c**) to conceal the RGD moiety, producing a cell resistant surface. Whereas if the polarity of the applied potential was opposite (**Figure 1.20b** and **1.20d**), the distal moiety would flip towards the surface, hence exposing the RGD peptide resulting in cell-adhesive properties.

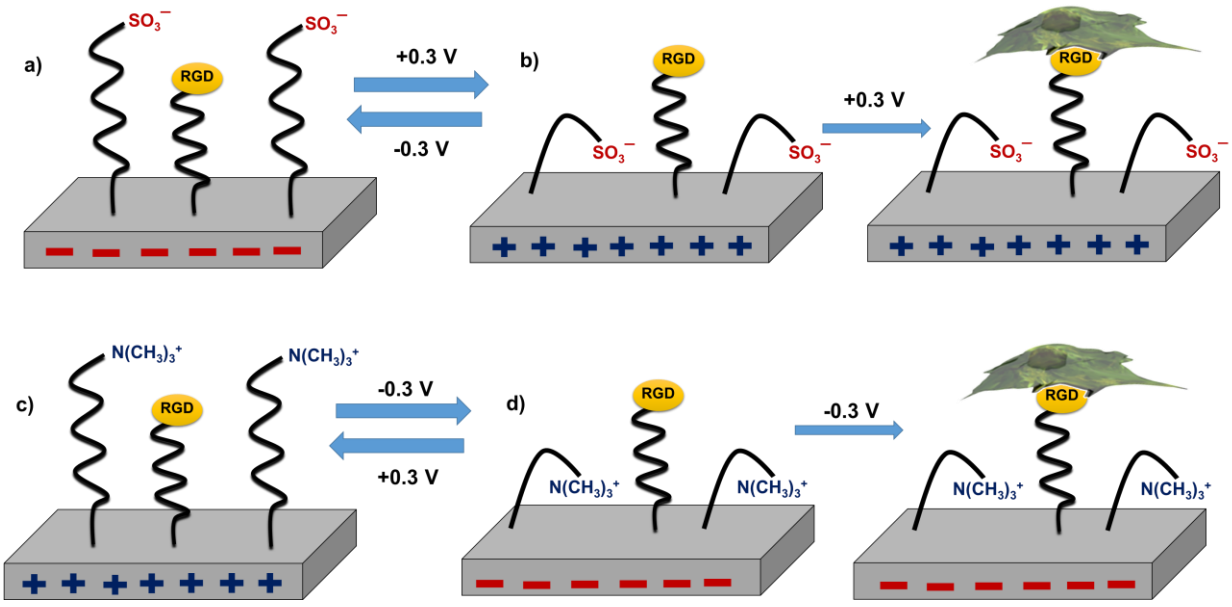

Figure 1.20 *a) EG_6-sulfonate mixed SAMs where the RGD is masked due to a negative potential repelling the negatively charged sulfonate group resulting in a cell resistant surface. b) Upon the application of a positive potential, the sulfonate group is attracted to the surface exposing the RGD group for cell adhesion. c) and d) display a positively charged ammonium terminated group that can also control cell adhesion by alternating potentials.*

1.3 Concluding remarks

The literature mentioned thus far has shown a number of successful switchable systems that can modulate surface properties via conformational or chemical switches. These stimuli-responsive surfaces can regulate specific biomolecular interactions enabling novel functionalities and new device designs for a variety of biological and medical applications. However, in order to realise the full potential of these surface-bearing responsive architectures, it is imperative to understand their operation under complex and realistic biological environments. A key challenge yet to be fully fulfilled by switchable surfaces is to regulate, and understand, specific biomolecular interactions that are driven by external stimuli in complex biological conditions. This will ensure that biological information and control generated through such tools mimic the natural biological environment. Biological systems are typically a complex mixture of inorganic salts, inorganic complexes, amino acids, peptides, and proteins.[124] The majority of studies on stimuli-responsive surfaces reported thus far either rely on controlling non-specific interactions (i.e., hydrophobic/hydrophilic and electrostatic) of the biomolecules with the active surface,[101,125-128] or have focused on demonstrating modulation of specific biomolecular interactions under simple biological conditions, typically water or buffer solutions.[104,105,129]

To date, few studies have considered switching using more complex biological systems.[99,107,123] As an example, very recently, Ng and co-workers[123] reported a route to control adhesion of bovine aortic endothelial cells on electrically switchable arginine–glycine–aspartate (RGD)-functionalised surfaces using 0.1% serum containing media. Although development of surfaces with switching functions

under complex biological conditions is highly desirable from the standpoint of biomedical applications, studies to such effect are scarce and more investigations are clearly needed to understand and develop molecular–based platforms to address solutions within the biomedical field.

1.4 PhD Overview

The aim of this PhD is to design and fabricate novel biological surfaces which are able to selectively control i) biomolecular interactions and ii) cellular interactions under more realistic complex biological conditions thus, could potentially lead to uses in medical and biological applications. The focus of this project will be on:

i) Fabricating mixed SAMs to control biomolecular interactions under complex biological conditions, using an electrical stimulus. This study will aim to enhance the **biotin-4KC:C3TEG (TEGT)** switchable surface for switching under culture media. This will be a significant step in providing a better understanding of the relationship between different components within the culture media and switching efficiency.

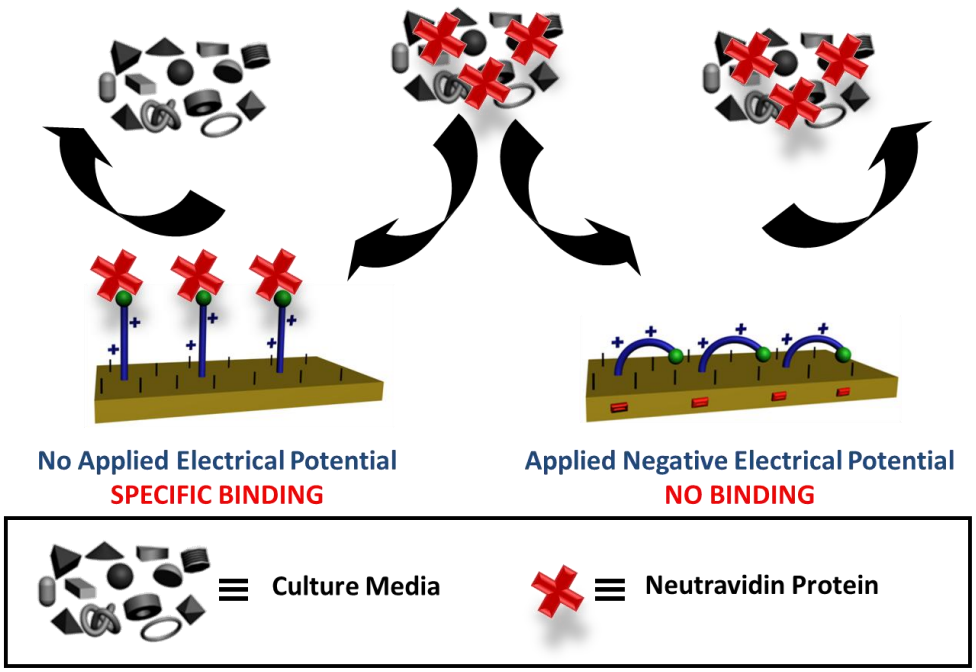

Figure 1.21 *Schematic showing the electro-switchable surface for control of biomolecular interactions under complex biological conditions.*

ii) Fabricating mixed SAMs to dynamically regulate immune cell interactions on the surface under complex biological conditions, using an electrical stimulus. This study will aim to selectively adhere immune cells to an electro-switchable RGD-terminated mixed SAM with an OEG group to prevent nonspecific binding from the culture media. It is expected that under open circuit conditions cells will adhere to the surface due to the RGD group being exposed for cell attachment. However, under an applied potential of -0.4 V cells are expected to be prevented from adhering to the surface due to the concealment of the RGD group and the protrusion of the OEGs.

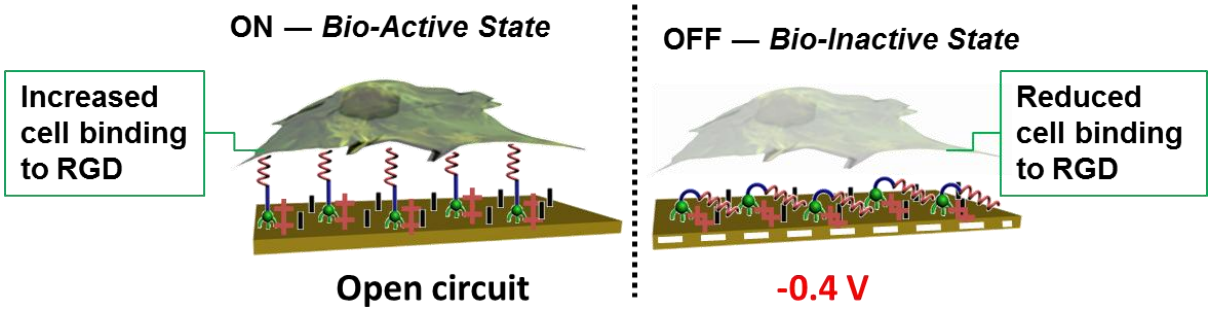

Figure 1.22 *Schematic showing the electro-switchable surface for controlling cellular interactions under complex biological conditions.*

Chapter 2: Surface Characterisation Techniques

Abstract: *This chapter gives a brief summary and description of the various surface characterisation techniques available for the analysis of SAMs. In order to understand the chemical and physical properties of a SAM surface it is essential to piece together the characteristics of the surface via as many techniques as possible in order to ensure accurate analysis of the surface can be achieved. Thus, some of the most well known techniques are reviewed such as contact angle measurements, ellipsometry, X-ray photoelectron spectroscopy (XPS) and surface plasmon resonance (SPR).*

2.1 Contact Angle

Contact angle is a simple but effective technique at measuring the static and dynamic angle of a surface. A typical contact angle consists of a syringe filled with a solvent, a fibre optic cable, which allows for the illumination of the surface of interest and a camera which is connected to a computer for analysis. To begin the contact angle measurement, the solvent is added dropwise onto the surface which is then recorded by the camera and analysed.

The contact angle is determined using the Young's equation[130] (**Equation 2.1**) where γ_{SV} is the free energy between the solid and the vapour, γ_{SL} is the free energy between the solid surface in contact with liquid and γ_{LV} is the free energy of the liquid-vapour interface.

$$\gamma_{SV} - \gamma_{SL} = \gamma_{LV}$$

Equation 2.1

When a water droplet is deposited on a hydrophobic surface there is lower surface energy and the droplet does not spread on the surface hence producing a higher contact angle (>90^0) (**Figure 2.1a**). However a water droplet on a hydrophilic surface results in the water spreading in order to minimise the free surface energy, which leads to a lower contact angle (**Figure 2.1b**).

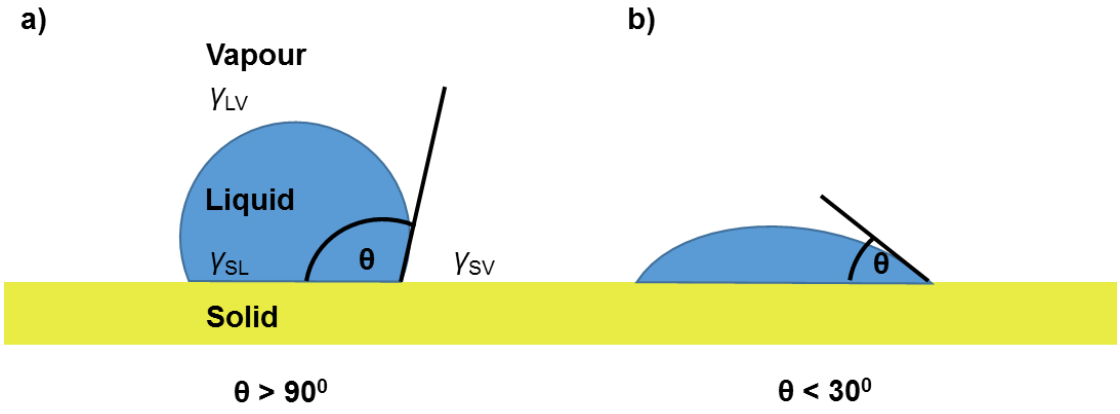

Figure 2.1 Illustration representing a sessile *liquid drop on a solid surface which forms a contact angle (θ). a) hydrophilic surface with a high contact angle (θ >90^0) and b) hydrophilic surface (θ < 30^0).*

There are two primary methods of measuring the contact angle; static contact angle and dynamic contact angle. Static contact angle is measured by a droplet of a measured volume on the surface which remains constant. Dynamic contact angle is

measured by the addition and withdrawal of the droplet through a needle, where the addition produces the advancing contact angle (θ_a) and withdrawal of the droplet produces the receding contact angle (θ_r).

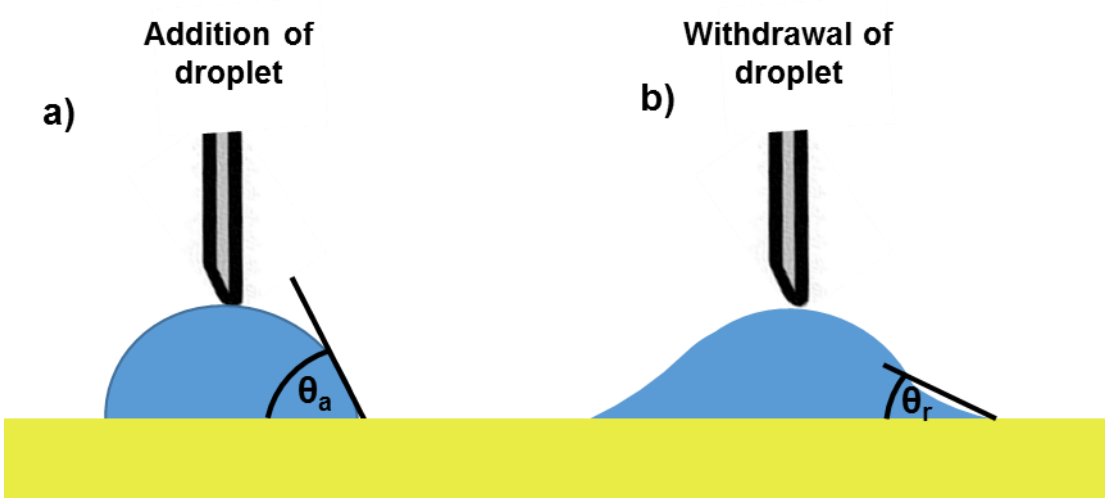

Figure 2.2 *Illustration representing a) advancing and b) receding contact angle when a droplet is added or withdrawn from the surface.*

The differences between the advancing and receding contact angles is called the contact angle hysteresis ($\Delta\theta = \theta_a - \theta_r$). A small hysteresis ($<5^0$) indicates a homogenous and well ordered surface, whereas a large hysteresis suggests the surface is contaminated, non-homogenous and/or relatively rough.[131]

2.2 Ellipsometry

Ellipsometry is a non-destructive optical technique that can calculate the change in polarisation of light upon reflection in order to give valuable information about the formation of SAMs via thickness measurements up to 1000 Å.[132]

Ellipsometry works by the use of a plane-polarised light, which interacts with a surface at an angle. The light can be considered to comprise two components denoted s- and p-polarised.[27] The two components are then reflected from the surface with a different phase and amplitude. Finally when the s-and p- polarised light are combined once again they result in elliptically polarised light. This process allows ellipsometry to measure the thickness between the surface of a substrate and air due to the ratio r between r_p and r_s, which are the reflection coefficients of the p- and s- polarised light respectively (**Figure 2.3**).

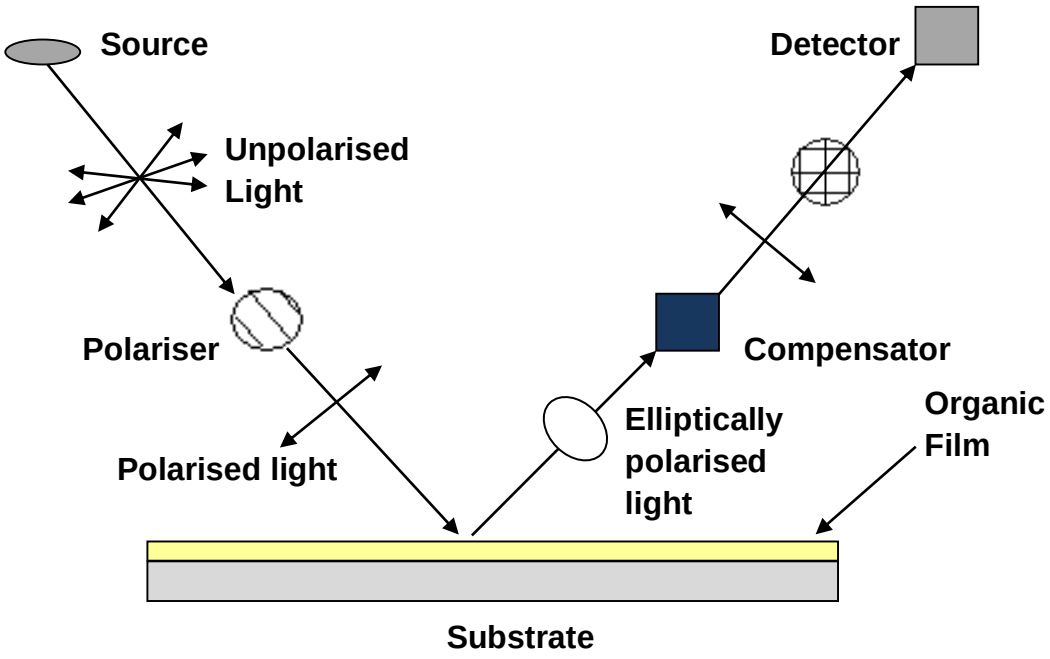

Figure 2.3 *Schematic of the mechanism of an ellipsometer. Polarised light interacts with the target surface at an angle. The light is then split into s- and p-polarised light. The s- and p- polarised light beams are then combined resulting in the elliptically polarised light, which is the then reflected off the surface at different times due to the refraction through the organic thin film. Thus, the amplitude and phases of both components are changed.*[133]

The thickness value of SAMs is based on the model of the air/SAM/solid in which the SAMs are assumed to be free of defect (homogeneous) and with a refractive index of 1.50.[133] This model is based on the Cauchy equation, which consider the SAMs as a transparent layer, where the thickness is obtained using multi guess iterations and provides a thickness result with the lowest χ^2 (chi-square distribution).

2.3 Surface Plasmon Resonance

The earliest documented observation of surface plasmons was made by Wood in 1902.[134] Wood reported the appearance of dark and light bands in reflected light in the diffracted spectrum of metallic gratings illuminated with polychromatic light. This phenomenon, which Wood referred to as an anomaly, was later explained in terms of surface plasmon resonance (SPR) in 1968 by several researchers[135-137] whom observed the optical excitation of surface plasmons.

The method of detection of SPR consists of a monochromatic and polarised light source, a glass prism, a thin metal film (usually 50 nm of gold) in contact with the glass prism and a photodetector.[137] SPR works by the interaction of polarised light with a surface interface, when the angle of incidence is above the critical angle as shown in **Figure 2.4**. The critical angle is the angle of incidence beyond which total internal reflection of the incident light occurs, below this angle there is both reflection and refraction. Total internal reflection results in an evanescent field[138] which extends from the prism into the metal film. This evanescent field couples to an electromagnetic surface wave, known as a surface plasmon, at the metal/liquid interface. Coupling is achieved at a specific angle of incidence, known as the SPR angle.[139] At this angle, the reflected light intensity goes through a minimum due to

the surface plasmon resonance. The position of the SPR angle depends on the optical properties of the prism, the metal, the medium in contact with the metal (usually a liquid), the metal film thickness, and the wavelength of the light source used.

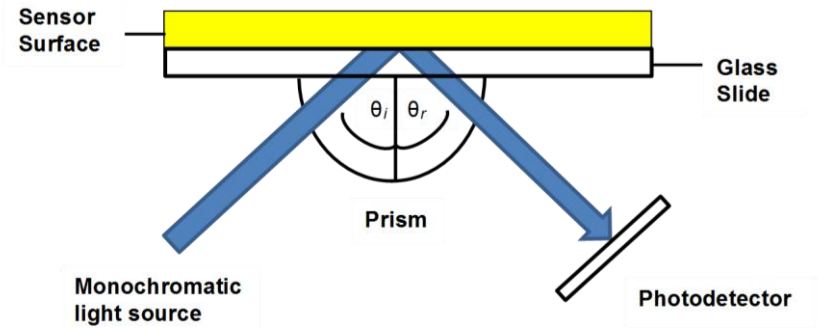

Figure 2.4 *Schematic of the mechanism of surface plasmon resonance. Polarised light shines onto the back of the sensor chip and the reflected light intensity is measured in the photodetector.* θ_i *is the angle of incidence, where the excitation of surface plasmon occurs inducing a reduction of the intensity of the reflected light.* θ_r *is the angle of refractive light, a change in the refractive index at the gold surface causes a shift of the intensity of the reflected light thus an analyte is detected.*

The SPR angle is highly sensitive to changes in the refractive index of a thin layer adjacent to the metal surface which is sensed by the evanescent wave. Thus, changes in refractive index to the surface can be measured within ~200 nm from the surface of the sensor immersed in solution in order to monitor the kinetics of adsorption of target molecules (**Figure 2.5a**).[140] For example when a protein layer is adsorbed on the metal surface, the SPR angle shifts to larger values (**Figure 2.5b**). The binding kinetics of target molecules on the surface is presented in the form of a SPR sensogram (**Figure 2.5c**), which can be split into three different phases:

baseline, association and dissociation. The baseline phase occurs prior to the injection of the analyte and usually a buffer solution such as phosphate buffer saline. Association is the phase where the analyte is injected, then flows over the surface of the sensor chip and binding occurs between the ligand and analyte. Depending on the binding kinetics and experimental condition the interactions may or may not reach a plateau, which is an indication that the interactions have reached equilibrium. Finally, dissociation is the phase after the injection is completed and the initial buffer is used againto rinse off any unbound molecules from the surface.

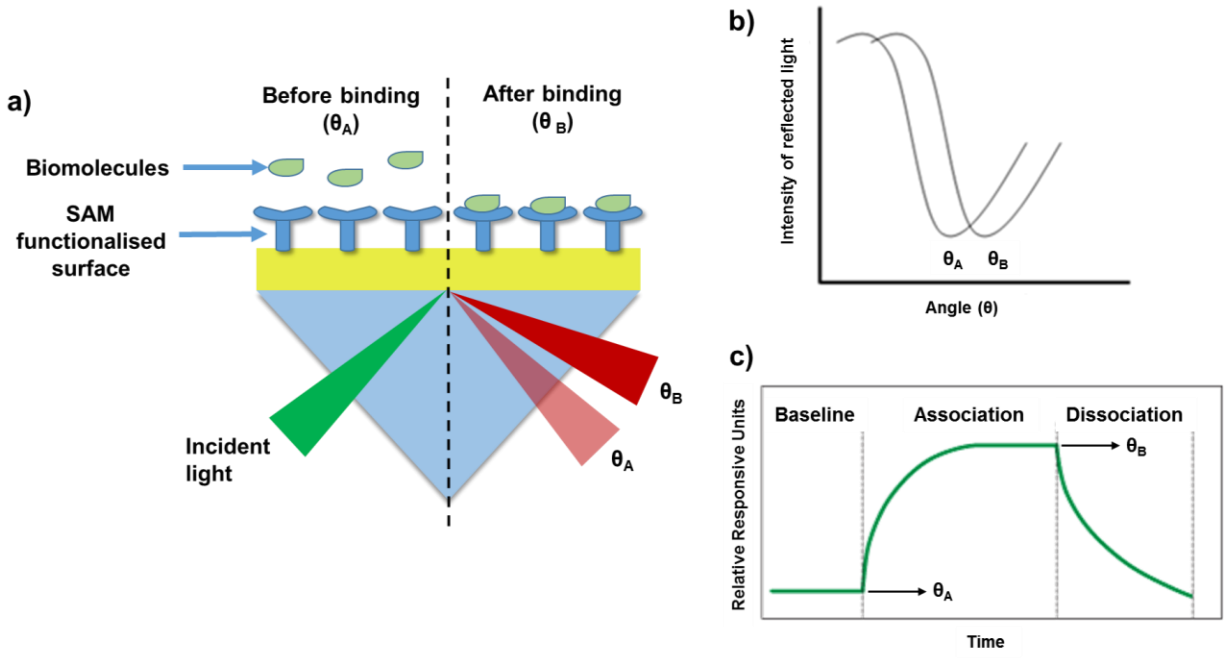

Figure 2.5 a) *Schematic representation of an SPR sensor equipped with suitable surface functionalised biorecognition element which can be used as an SPR biosensor. Biological analytes labelled biomolecules are shown to interact with the biorecognition elements labelled as the SAM. b) A change in the refracted light intensity is observed from* θ_A *to* θ_B *after the biomolecules are bound to the surface. c) A typical sensogram displaying the three sensogram phases.*

2.4 X-ray photoelectron spectroscopy (XPS)

XPS is a technique that can analyse the elemental composition on a surface by irradiating the sample with a photon of energy (hv), which penetrates the surface and excites a core level electron. Upon excitation the core level electron exceeds the binding energy (E_B), the atom then emits an electron, which is detected by the electron spectrometer. The conducting sample is in electrical contact with the spectrometer such that both the sample and spectrometer have a common reference for measuring electron energy, called the Fermi level. By analysis of the kinetic energy (E_K) involved in the emission of an electron the following equation can be derived[141]:

$$\boldsymbol{E_K + \emptyset = hv - E_B}$$

Equation 2.2

Where ø is the work function of the spectrometer and remains constant, hv refers to the photon energy usually in the form of monochromatic x-rays, E_K is the kinetic energy of the electron and E_B is the binding energy of the electron. The binding energy provides an elemental identification of the surface, thus the number of ejected electrons is proportional to the number of atoms that are on any given surface. Photoelectrons are generated via ejection from the solid surface upon excitation of core level orbitals by a photo source:

$$\boldsymbol{A + hv \rightarrow A^{+*} + e^{-}}\ (\text{photoelectron})$$

Equation 2.3

Where A is a neutral atom or molecule, A^{+*} is the excited ion and e^- is the ejected photoelectron. The photoionisation process is illustrated in **Figure 2.6**. The relatively non-destructive nature of XPS can be attributed to the fact that only the ejection of electrons is required for analysis. The atomic nuclei that are examined during electron spectroscopic measurements remain unchanged. However, it is important to note that this does not include samples which may be sensitive to decomposition from exposure to an X-ray source.[142]

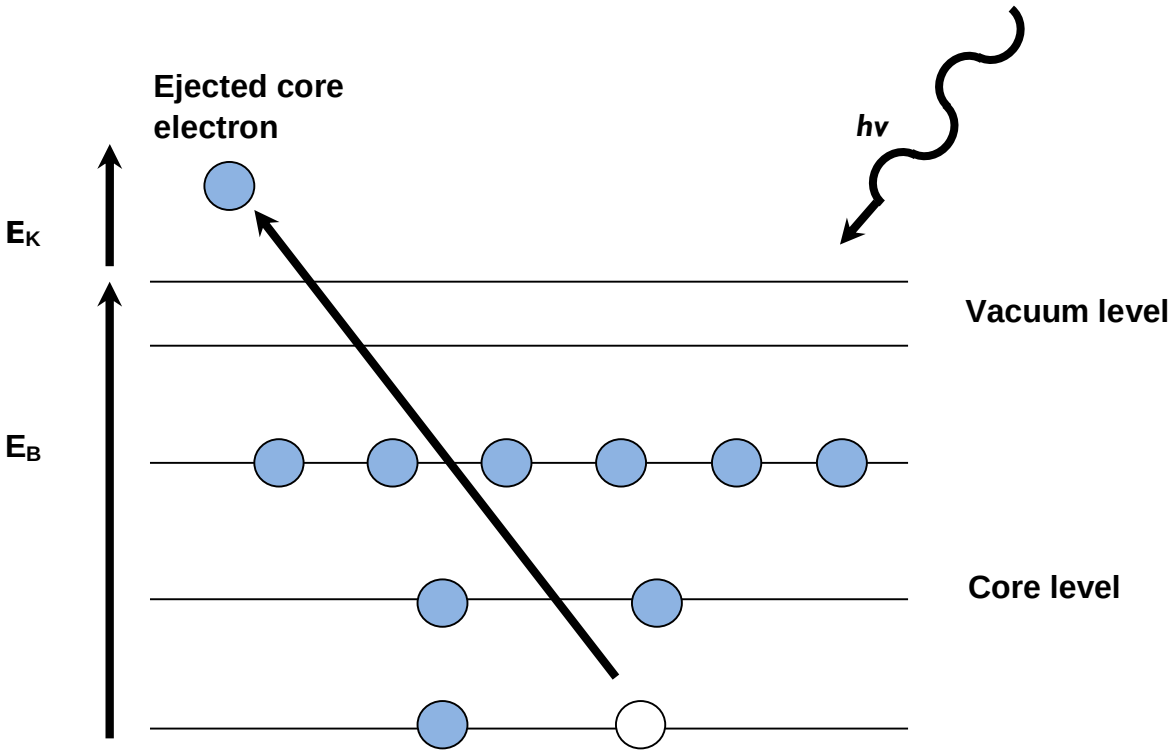

Figure 2.6 *Schematic of the XPS process, showing the photoionisation of an atom by the ejection of a core electron.*

XPS is sensitive up to a detection limit of 0.1% of a monolayer and can detect most elements except H and He. In well-calibrated XPS systems, the precision of the

quantitation measurements are typically within ±5%; thus, XPS is suited for both quantitative and qualitative elemental analysis.[142] An XPS spectrum consists a plot of the number of electrons detected versus the binding energy. Each element has a set of characteristic peaks with certain binding energy values, which aids in the identification of the element after a sample is analysed. The binding energy differs from atom to atom and hence it determines the positions of the XPS peaks. **Figure 2.7** shows an example of a typical XPS S 2p spectrum for an alkanethiol designated C_nSH where n = 16. The S 2p spectra for this SAM has a doublet structure due to the presence of the S $2p_{3/2}$ and S $2p_{1/2}$ peaks. The binding energy of the S $2p_{3/2}$ peak is at 161.9 eV which is in agreement with previous reports of sulphur atoms bound to a gold surface as a thiolate species.[143] The spectrum was fitted using a 2:1 peak area ratio and a 1.2 eV splitting.

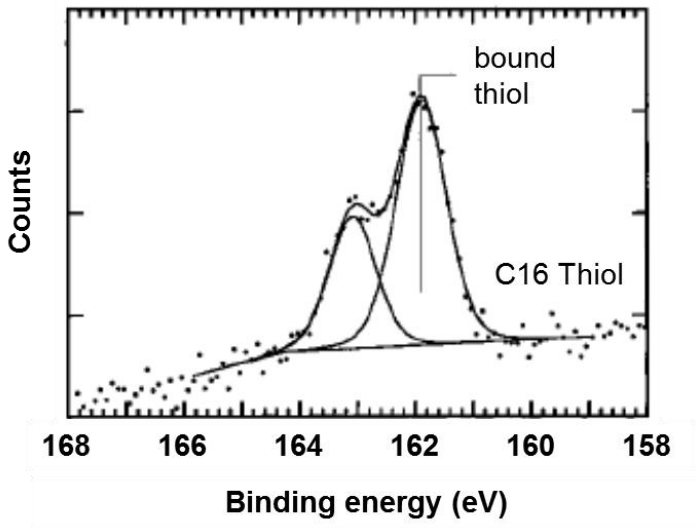

Figure 2.7 *XPS spectrum of an alkanethiol C_nSH where n = 16. C16SH thiol peaks were fitted using one Sp_2 doublet with a 2:1 are ratio and a splitting of 1.2 eV.*

Chapter 3: Switching Specific Biomolecular Interactions on Surfaces under Complex Biological Conditions

This chapter is based on two manuscripts, “Switching Specific Biomolecular Interactions on Surfaces under Complex Biological Conditions” by *M. Lashkor, F. J. Rawson, J. A. Preece, P. M. Mendes, Analyst,* ***2014****, 139, 5400* and partially on “Modulation of Biointeractions by Electrically Switchable Oligopeptide Surfaces: Structural Requirements and Mechanism” by *C. L. Yeung, X. Wang, M. Lashkor, E. Cantini, F. J. Rawson, P. Iqbal, J. A. Preece, J. Ma, P. M. Mendes, Advanced Materials Interface,* ***2014****, 1*, *1300085*.

Abstract: *This chapter discusses the development and characterisation of an electrically switchable mixed self-assembled monolayer system based on oligopeptides, followed by an in-depth study for their suitability in achieving control over biomolecular interactions in the presence of complex biological conditions. This model system, a biotinylated oligopeptide tethered to gold within a background of tri(ethylene glycol) thiol, excels in both switching specific protein interactions in highly fouling media while still offering the non-specific protein-resistance to the surface. Furthermore, the work demonstrated that the performance of the switching on the electro-switchable oligopeptide is sensitive to the characteristics of the media, and in particular, its protein concentration and buffer composition, and thus such aspects should be considered and addressed to assure maximum switching performance. This study lays the foundation for developing more realistic dynamic extracellular matrix models and is certainly applicable in a wide variety of biological and medical applications.*

3.1 Introduction

Stimuli-responsive surfaces that are capable of modulating their biological properties in response to an external stimuli, including temperature,[144,145] light,[146] magnetic field[147] and electrical potential,[41,121,148] are of growing interest for a variety of biological and medical applications.[33] Switchable surfaces that can be controlled on-demand are playing an increasingly important part in the development of highly sensitive biosensors,[79,81,149-152] novel drug delivery systems[153-156] and highly functional microfluidic, bioanalysis, and bioseparation systems.[157-160] Additionally, dynamic, synthetic surfaces that can control the presentation of regulatory signals to a cell are expected to have a significant impact in the field of tissue engineering and regenerative medicine. This will provide unprecedented opportunities in fundamental studies of cell biology.[26,161] The availability of sophisticated and functional switchable surfaces is expected to emulate more complex, *in vivo* like extracellular environments and provide a powerful means to probe and control the dynamic interactions between the cell and its external environments.

Previously,[121] the operation of switchable oligopeptides on mixed SAMs on gold surfaces was tested, in order to control biomolecular interactions under only very limited biological conditions (i.e. phosphate buffer saline – PBS) using an electrical potential as an actuator. These SAMs have been shown to regulate the binding between the biotin ligand on the surface and neutravidin from solution. Switchable SAMs used to control biomolecular interactions via an electrical stimulus are particularly appealing because of their fast response times, ease of creating multiple individually addressable switchable regions on the same surface, as well as low-driven voltage and electric fields that are compatible with biological systems.[123]

These inherent properties, along with the diversity of bioactive molecular entities which can be chemically attached to the oligopeptide, make these oligopeptide SAMs excellent candidates to realize high performance electrical switchable surfaces for complex biological conditions.

To address the challenge of developing and understanding new switchable surfaces a detailed study was conducted, using electrochemical surface plasmon resonance (SPR) spectroscopy, on the influence of the characteristics of complex biological medium (both its chemical and protein composition and its inherent physicochemical properties) on the switchable properties of an oligopeptide SAM model system (**Figure 3.1**). The switchable oligopeptide SAM model system was composed of two molecular components: (i) a positively charged 4-mer of lysine (K) that is functionalized at one end with biotin, which recognises the neutravidin protein, and at the other end with a cysteine (C) for binding to gold substrates via the thiol group (**biotin-4KC**), and (ii) an ethylene glycol-terminated thiol (**C3TEG**, **C11TEG** and **C11HEG**). The ethylene glycol molecules to be used in the formation of the mixed SAM are known to have protein resistant properties, however as mentioned in **Section 1.2.2**, the EG_n chain has an effect on the protein resistant properties of a surface. Hence it is hoped that by testing three ethylene glycol molecules, the optimal monolayer for specific binding of protein and the effective prevention of nonspecific adsorption from complex media can be achieved.

The interaction of the neutravidin proteinto the surface appended biotin ligand was chosen for these studies because it can be easily monitored and quantified by SPR, allowing for facile evaluation of the switching performance under various biological conditions.

3.1.1 Objectives

1) To optimise the composition of the oligopeptide mixed SAM to resist nonspecific protein adsorption, by comparing the nonspecific binding on three different ethylene glycol groups: **C3TEG**, **C11TEG** and **C11HEG**.

2) To fully characterise the mixed SAMs via XPS, contact angle and ellipsometry.

3) To use computer modelling to better understand how the switchable oligopeptide SAM controls the neutravidin-biotin interactions.

4) To evaluate the switching properties of the electrically switchable oligopeptide mixed SAMs in three commonly used biological media, namely Dulbecco's Modified Eagle Medium (DMEM), DMEM with 10% fetal bovine serum (DMEM-FBS) and DMEM-FBS with 24 mM HEPES buffer (DMEM-FBS-HEPES).

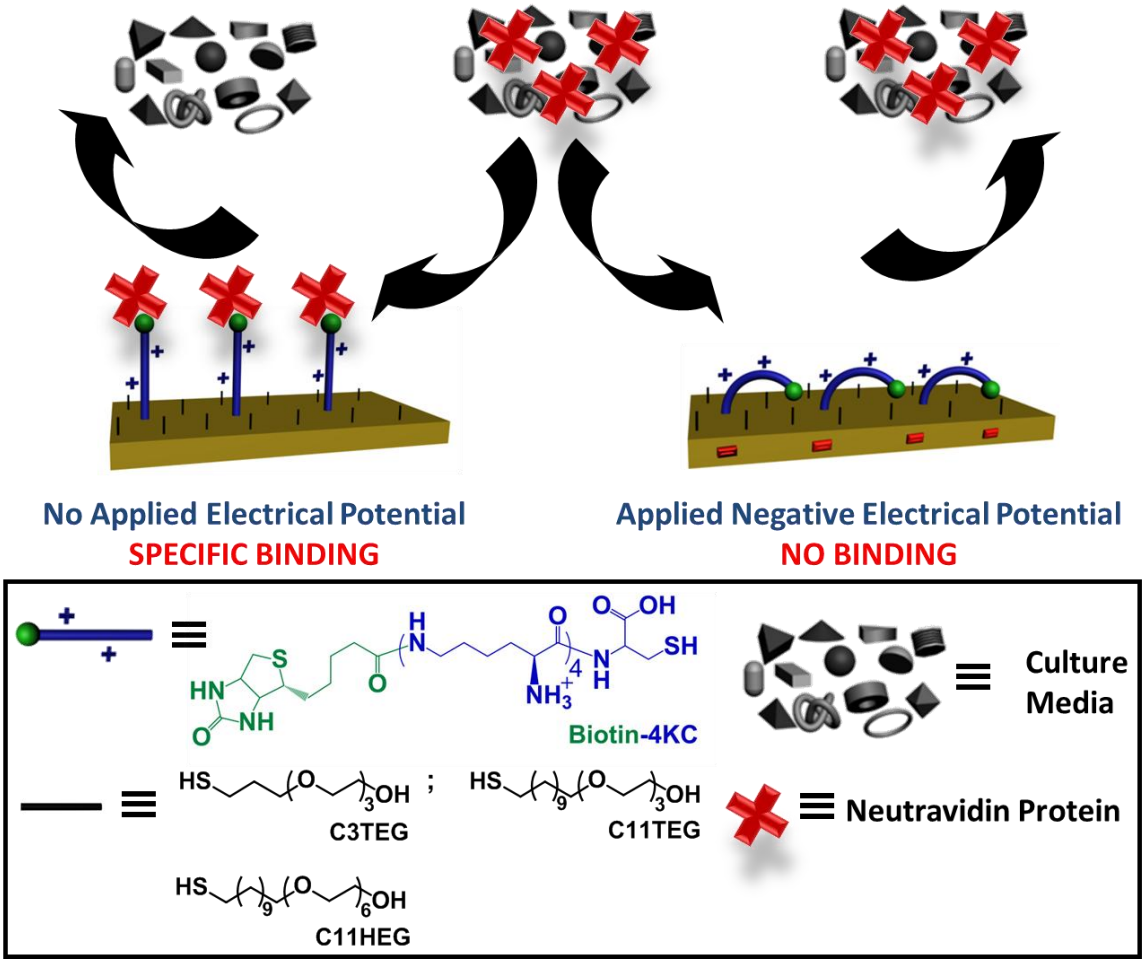

Figure 3.1 *Schematic showing proposed mechanism for switching a biotinylated peptide in complex biological conditions. Under no applied electrical potential, neutravidin binds specifically to the biotin headgroup while non-specific binding from complex media is prevented. Under an applied negative potential no binding is observed from neutravidin and the complex media.*

3.2 Results and Discussion

3.3 Formation and characterisation of mixed SAMs on gold substrates

3.3.1 Formation of mixed biotin-4KC:OEG SAMs

Cleaned gold surfaces were functionalized with a two-component mixed SAM of **biotin-4KC** peptide with either **C3TEG, C11TEG or C11HEG** as shown in **Figure 3.2**. The **biotin-4KC** peptide consists of a cysteine group, four lysines and a biotin functional group. The oligopeptide will be immobilised to the gold surface via the cysteine group, which contains a thiol moiety that binds to gold. The four lysine groups provide a flexible backbone, which provides ample manoeuvrability to switch conformations between the on and off states as shown previously.[121] The main role of the **OEG** groups**,** in addition to providing spatial distribution for the **biotin-4KC** peptide to switch, is to prevent non-specific binding from complex media.

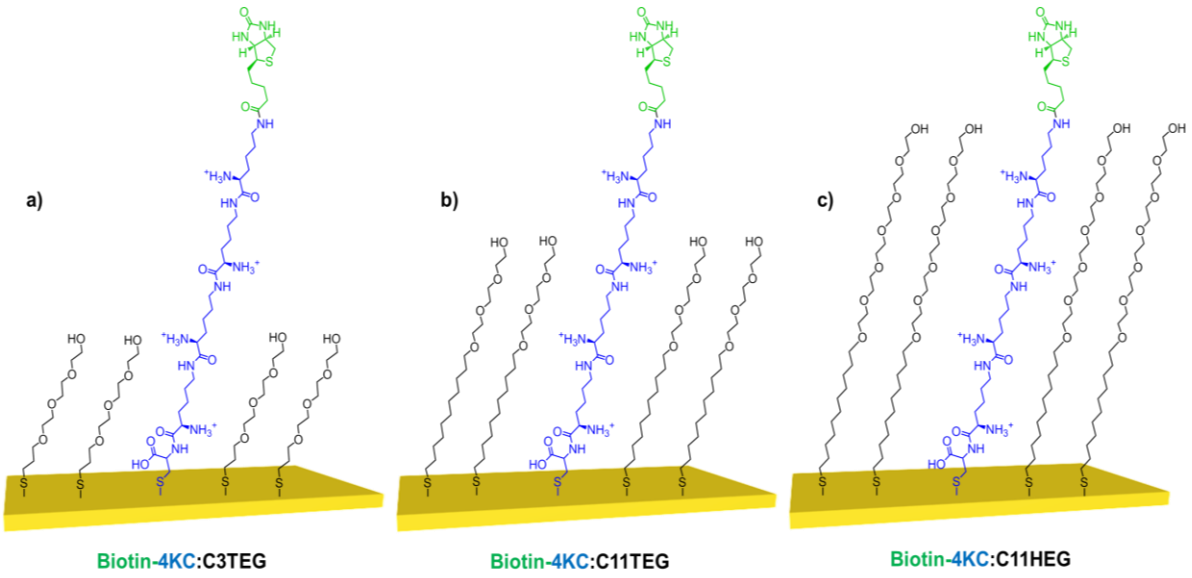

Figure 3.2 *Schematic of the formation of a)* ***biotin-4KC:C3TEG*** *b)* ***biotin-4KC:C11TEG*** *and c)* ***biotin-4KC:C11HEG*** *mixed SAMs.*

3.3.2 XPS Characterization of the oligopeptide mixed SAMs with different OEGs

The next critical issue was to choose oligopeptide mixed SAMs with a surface ratio that offers switching properties while providing high specific binding to neutravidin without interference from non-specific interactions. The **biotin-4KC:C3TEG** mixed SAM was previously characterised by XPS[121] and it was demonstrated that the **biotin-4KC:C3TEG** had a surface ratio of 1:16 ± 4 from a solution ratio of 1:40, which allows for excellent switching properties while offering optimum binding capabilities. Thus, a similar surface ratio was sought for the other mixed SAM systems consisting of the **biotin-4KC** with either the **C11TEG** or **C11HEG** components. By using the same 1:40 solution ratio as previously shown,[121] **biotin-4KC:C11TEG** and **biotin-4KC:C11HEG** mixed SAMs were formed over 24 hours for XPS analysis.

XPS analysis revealed the presence of the elemental species S, N, C and O on the **biotin-4KC**:**C11TEG** SAM (**Figure 3.3**), confirming thus the formation of the mixed SAM. The S 2p spectrum (**Figure 3.3a**) consists of two doublet peaks, with one doublet peak at 163.2 eV (S $2p_{1/2}$) and 162.0 eV (S $2p_{3/2}$), indicating that the sulphur is chemisorbed on the gold surface.[162] The second doublet peak can be observed at 163.8 eV and 165.0 eV, which is assignable to the S-C bond in the biotin moiety.[163,164] The N 1s spectrum (**Figure 3.3b**) can be deconvoluted into two peaks, which support the presence of the peptide on the surface. The first peak centred at 400.5 eV is attributed to amino (NH_2) and amide (CONH) moieties. The second peak centred at 402.3 eV is ascribed to protonated amino groups.[165] The C 1s spectrum (**Figure 3.3c**) can be deconvoluted into three peaks, which are attributed to five

different binding environments. The peak at 285.1 eV is attributed to C-C bonds,[166] while the peak at 286.4 eV corresponds to C 1s of the three binding environments of C-S, C-N and C-O.[166] The third and smaller peak (288.7 eV) is assigned to the C 1s photoelectron of the carbonyl moiety, C=O.[166] The O 1s spectrum (**Figure 3.3d**) is de-convoluted into two different peaks, corresponding to two different binding environments, arising from the C-O (533.2 eV) and C=O (532.0 eV) bonds.[166]

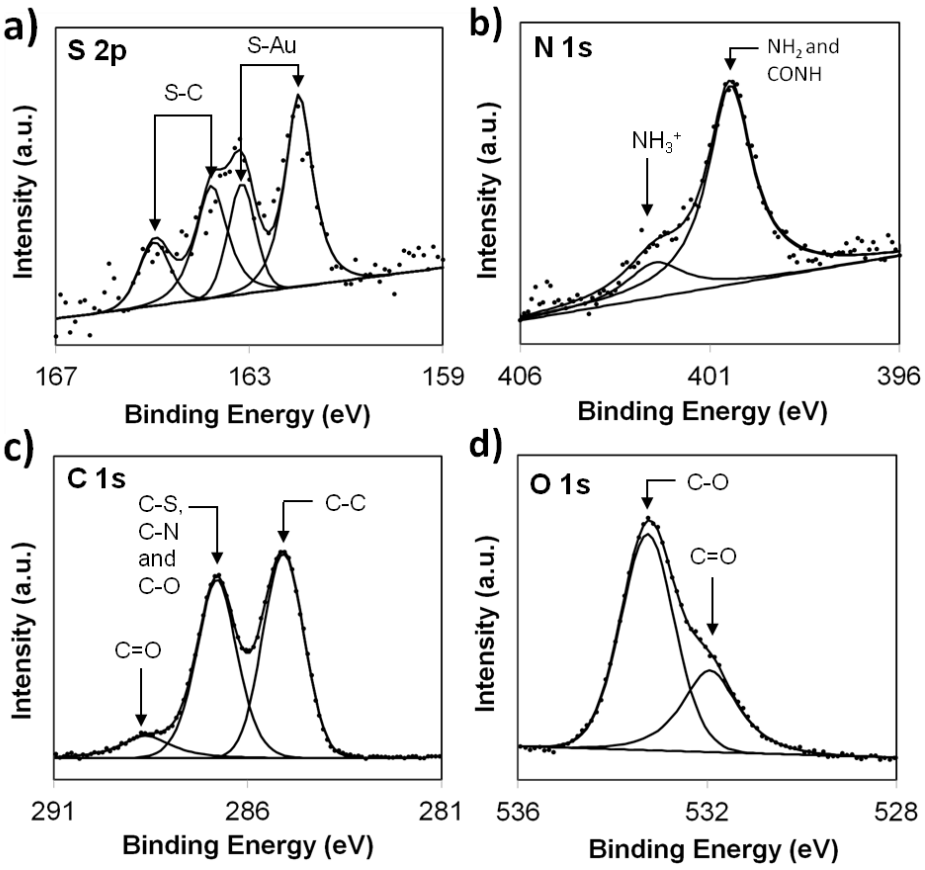

Figure 3.3 *XPS spectra of the a) S 2p, b) N 1s, c) C 1s and d) O 1s peak regions of* ***biotin-4KC*****:*****C11TEG*** *mixed SAMs at a 1:40 solution ratio.*

XPS analysis was also carried out for the **biotin-4KC:C11HEG** revealing the presence of the elemental species S, N, C and O (**Figure 3.4**), confirming the formation of the mixed SAM. The S 2p spectrum (**Figure 3.4a**) consists of two doublet peaks, with one doublet peak at 163.8 eV (S $2p_{1/2}$) and 162.6 eV (S $2p_{3/2}$), indicating that the sulphur is chemisorbed on the gold surface.[162] The second doublet peak can be observed at 164.3 eV and 165.5 eV, which is assignable to the S-C bond in the biotin moiety.[163,164] The N 1s spectrum (**Figure 3.4b**) can be deconvoluted into two peaks, which support the presence of the peptide on the surface. The first peak centred at 400.9 eV is attributed to amino (NH_2) and amide (CONH) moieties. The second peak centred at 402.4 eV is ascribed to protonated amino groups.[165] The C 1s spectrum (**Figure 3.4c**) can be deconvoluted into three peaks, which are attributed to five different binding environments. The peak at 285.6 eV is attributed to C-C bonds,[166] while the peak at 287.4 eV corresponds to C 1s of the three binding environments of C-S, C-N and C-O.[166] The third and smaller peak (288.6 eV) is assigned to the C 1s photoelectron of the carbonyl moiety, C=O.[166] The O 1s spectrum (**Figure 3.4d**) is de-convoluted into two different peaks, corresponding to two different binding environments, arising from the C-O (533.7 eV) and C=O (532.0 eV) bonds [166]

Furthermore, from integrating the area of the S 2p and N 1s peaks and taking into consideration that the **biotin-4KC** oligopeptide consists of 11 N atoms and 2 S atoms and both OEGs (**C11TEG** and **C11HEG)** have no N and 1 S atom only. The E**quation 3.1** was formulated to calculate the number of **C11TEG** and **C11HEG** molecules per peptide on the surface.

$$\boldsymbol{Number\ of\ C11TEG = \left(No.of\ N\ per\ peptide \times \frac{S\ area}{N\ area}\right) - No.of\ S\ per\ peptide}$$

Equation 3.1

From this equation it was possible to infer that the ratio of **biotin-4KC**:**C11TEG** on the surface was 1:8 ± 4 and the ratio of **biotin-4KC**:**C11HEG** on the surface was 1:11 ± 6.These ratios are lower but still within the error margins of that obtained for the previous **biotin-4KC**:**C3TEG** (1:16 ± 4),[121] and hence suitable to carry out the switching studies.

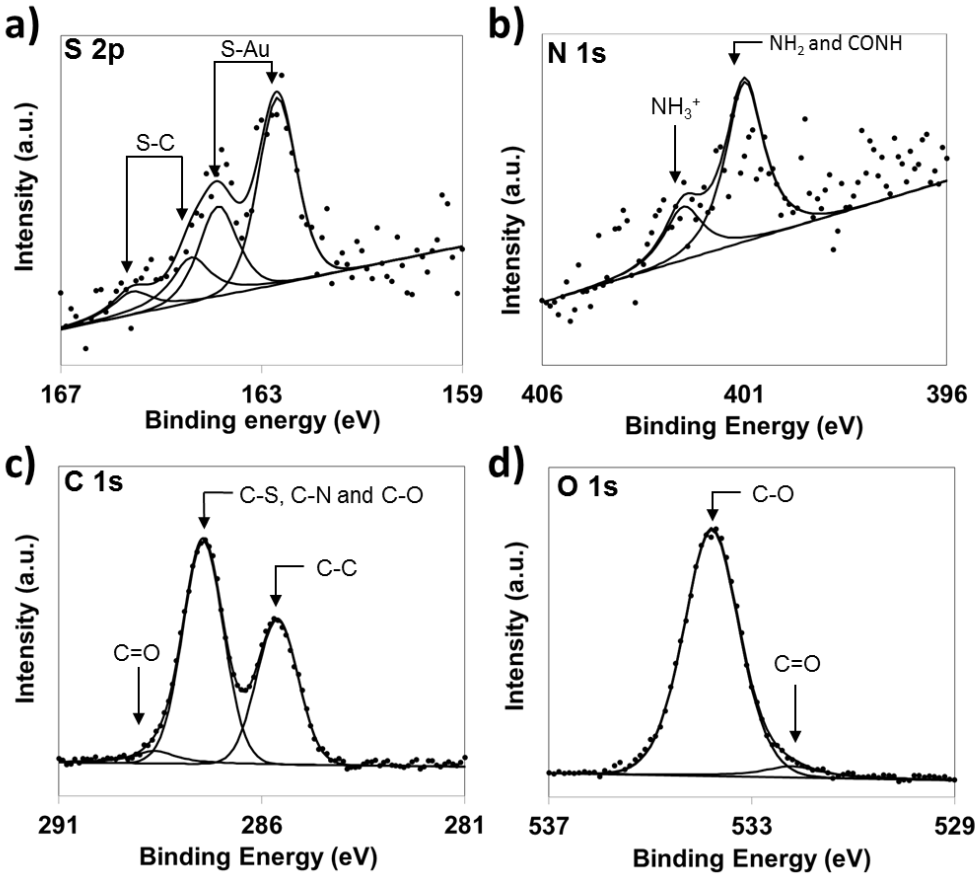

Figure 3.4 *XPS spectra of the a) S 2p, b) N 1s, c) C 1s and d) O 1s peak regions of* ***biotin-4KC*****:*****C11HEG*** *mixed SAMs at a 1:40 solution ratio.*

3.3.3 Contact angle and ellipsometry analysis of mixed SAMs

The formation of the mixed SAMs was analysed by means of contact angle and ellipsometry (**Table 3.1**). As expected, the water advancing (Adv) and receding (Rec) contact angles for the **biotin-4KC**:**C3TEG**, **biotin-4KC:C11TEG** and **biotin-4KC:C11HEG** SAMs revealed hydrophilic monolayers, exhibiting contact angles in between those observed for pure monolayers of either components.

Ellipsometry analysis confirmed the formation of **C3TEG**, **C11TEG** and **C11HEG** SAMs with an increasing trend of thickness values, which reflects the increase in molecular length of each OEG respectively. Furthermore, the thicknesses of the three mixed SAMs: **biotin-4KC**:**C3TEG**, **biotin-4KC:C11TEG** and **biotin-4KC:C11HEG** were all within the thickness ranges observed between the pure **C3TEG**, **C11TEG**, **C11HEG** and **biotin-4KC** monolayers within error.

As expected the ellipsometric thicknesses of the mixed **biotin-4KC**:**C3TEG**, **biotin-4KC:C11TEG** and **biotin-4KC:C11HEG** SAMs also showed a gradual increase in thickness. The formation of the pure **biotin-4KC** SAM was also confirmed with an ellipsometric thickness of 1.7 ± 0.4 which is significantly lower than the theoretical length of 5.2 nm. This difference can be explained due to the pure **biotin-4KC** SAM displaying a slightly folded conformation under OC conditions,[122] thus exhibiting a much lower surface thickness than expected. It is important to note that the ellipsometric thickness of all pure formed SAMs is less than the theoretical molecular length of the molecules (**Table 3.1**). This discrepancy, between molecular length and SAM thickness, is expected, in agreement with the literature, and can be ascribed to both the tilt angle and density of the SAM surfactants.[167]

Table 3.1. *Advancing and receding water contact angles and ellipsometric thickness for the different SAMs formed for 24 h. The theoretical molecular lengths were derived from ChemBio3D Ultra 12.0 in which the molecules were in fully extended conformations.*

SAM	**Contact Angle (^{0})**		**Thickness (nm)**	
	Adv.	*Rec.*	*Theor.*	*Exp.*
Biotin-4KC	43 ± 2	35 ± 3	5.2	1.7 ± 0.4
C3TEG	34 ± 2	27 ± 1	1.7	1.3 ± 0.3
C11TEG	29 ± 2	25 ± 3	2.6	1.7 ± 0.2
C11HEG	35 ± 1	32 ± 1	3.9	2.5 ± 0.1
Biotin-4KC:**C3TEG**	35 ± 3	32 ± 2	-	1.6 ± 0.1
Biotin-4KC:**C11TEG**	39 ± 2	32 ± 3	-	1.7 ± 0.1
Biotin4KC:C11HEG	40 ± 3	31 ± 5	-	2.0 ± 0.1

The pure OEGs SAMs were also analysed by contact angle and ellipsometry. The **C11TEG** SAM has smaller hysteresis (θ_{Adv} -θ_{Rec}) of 4^0 as compared with the 7^0 obtained for the **C3TEG** SAM. **C11HEG** SAMs has a slightly smaller hysteresis (θ_{Adv} -θ_{Rec}) of 3^0 than **C11TEG**, however all the pure OEGs showed hydrophilic properties. The pure **biotin-4KC** SAM also displayed hydrophilic properties and showed the biggest hysteresis (θ_{Adv} — θ_{Rec}) of 8^0 suggesting a less ordered monolayer in comparison to the other pure OEG SAMs. From these results, it can be inferred that the longer hydrocarbon chain for the **C11TEG** and **C11HEG** has led to a lower hysteresis, both indicating the presence of a more close-packed monolayer.

3.4 Comparison of anti-fouling properties between different OEGs

Initial investigations were performed to elucidate the interactions of the different complex media – DMEM, DMEM-FBS, and DMEM-FBS-HEPES – with the pure **biotin-4KC**, **C3TEG**, **C11TEG** and **C11HEG** SAMs. In the SPR experiments, the pure **biotin-4KC** and OEG SAMs were exposed to a flow of phosphate buffer saline (PBS) solution, to establish the baseline, followed by an injection of either DMEM, DMEM-FBS or DMEM-FBS-HEPES media into the SPR flow cell for 30 min at a flow rate of 8 µl/min. The SPR flow cell was then flushed with PBS to remove any loosely adsorbed material (**Figure 3.5**)

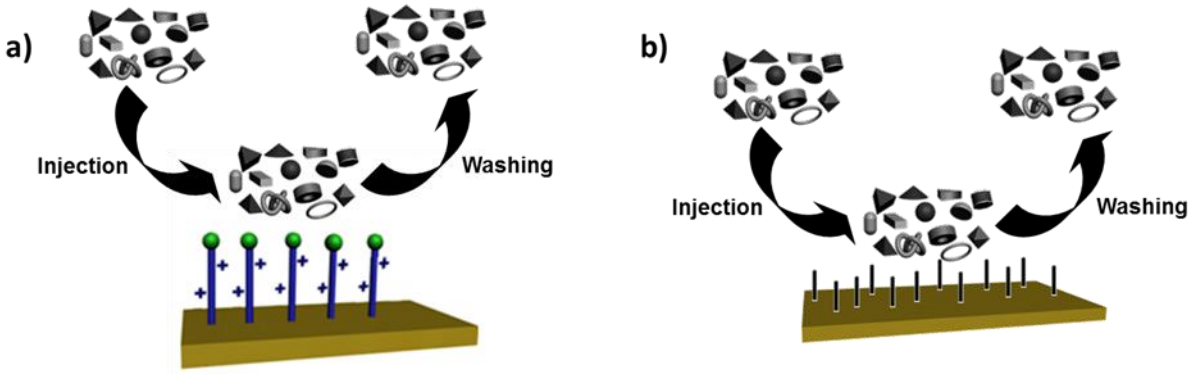

Figure 3.5 *Schematic showing the injection and washing procedure of complex media during SPR experiments using a) pure **biotin-4KC** SAM and b) oligo(ethylene glycol) SAMs.*

Figure 3.6 shows SPR sensorgrams carried out on four surfaces where upon the injection of different media over the SAM surface, showed a rapid response due to differences in the refractive indices of the PBS buffer and media solution, followed by a slower increase as the media components adsorbed to the surface. On re-

injection of PBS buffer into the flow cell, as indicated by the “washing” arrow, there was an immediate drop in the SPR signal due to the change from media solution back to PBS, which induces a change in the bulk refractive index. However, after the final washing, the signal remained elevated compared to the original baseline, in particular for both DMEM-FBS and DMEM-FBS-HEPES media.

The results shown in **Figure 3.6a** indicate that the pure **biotin-4KC** SAM does not prevent non-specific binding due to a high response of ~1600 response units. It is expected that charged molecules within the complex media including serum adsorb nonspecifically on the pure **biotin-4KC** SAM due to the presence of the charged lysine backbone. Thus, it is essential that any OEG used to form mixed SAMs for switching studies is long enough to mask the lysine backbone in order to minimise nonspecific binding from the complex media.

The first OEG to be investigated for protein inert properties was **C3TEG** SAM, which produced high responses of 1000 response units. This result indicates that the **C3TEG** is ineffective at preventing nonspecific serum adsorption (**Figure 3.6b**), which is expected to be detrimental to the specificity and efficiency of the switching system. Furthermore, the nonspecific response would hinder the evaluation of the switching performance as the adsorption of serum on the SAM surface would lead to a nonspecific SPR response, which would be undistinguishable from the response resulting from specific biomolecular interactions of neutravidin-biotin.

The next task was to assess the non-fouling characteristics of the more ordered **C11TEG** and **C11HEG** terminated SAMs. As shown in the representative SPR sensorgrams in **Figure 3.6c** and **3.6d**, the **C11TEG** and **C11HEG** SAMs showed much better performance with regard to limiting the non-specific signal

induced by either DMEM-FBS or DMEM-FBS-HEPES by a factor of 4-5 (see **Appendix III**), in comparison to the **C3TEG** SAM (**Figure 3.6b**). The **C11TEG** and **C11HEG** monolayers exhibited high resistance to non-specific adsorption from all three media, producing small SPR responses of less than 300 response units. The difference in nonspecific binding between the **C3TEG** (**Figure 3.6b**) and the two longer chain OEG SAMs can be viewed as a consequence of the better packing achieved with the **C11TEG** and **C11HEG** respectively (See **Appendix III** for response unit values for each sensogram trace)

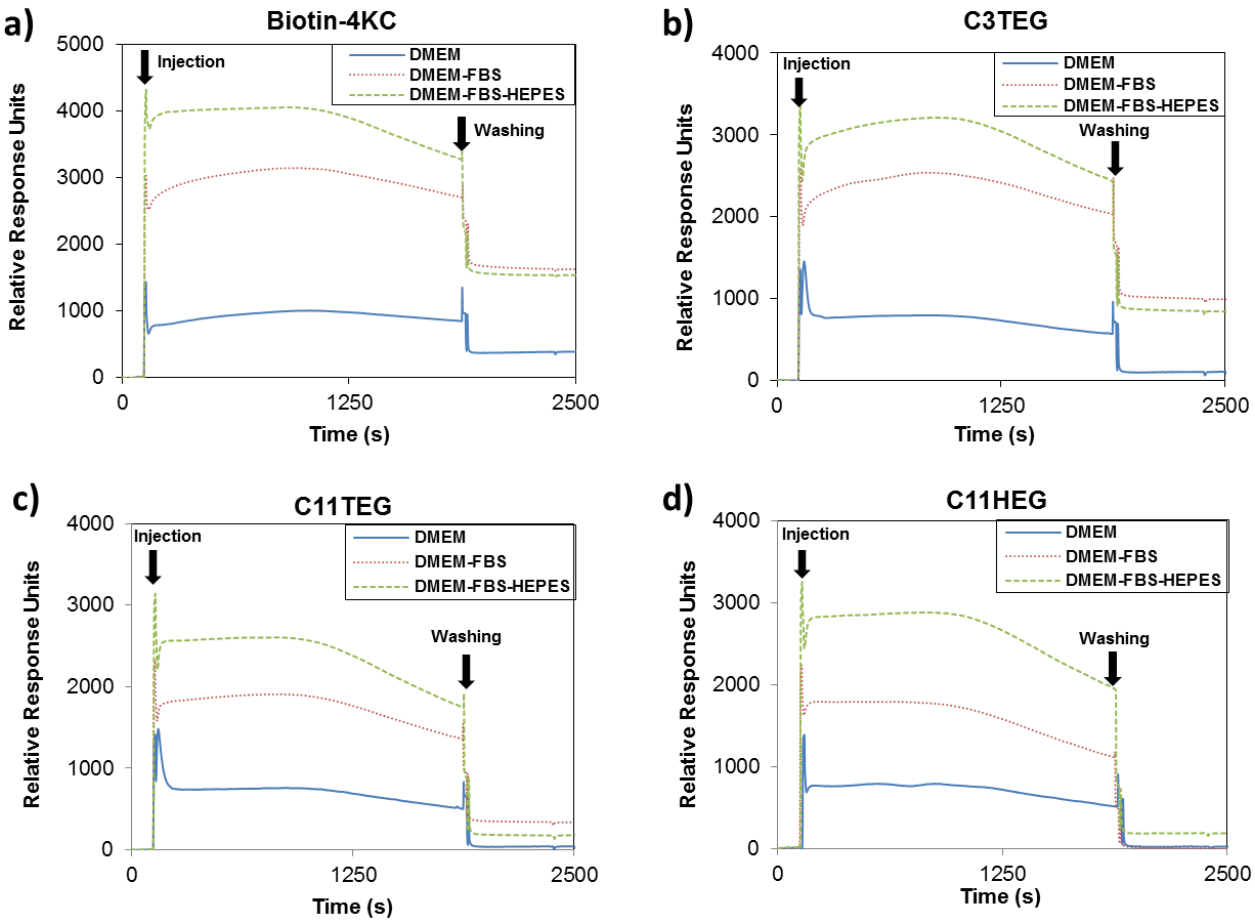

Figure 3.6 *SPR sensorgram traces for the interaction of a)* ***biotin-4KC*** *b)* ***C3TEG****, c)* ***C11TEG*** *and d)* ***C11HEG*** *SAMs with different complex media – DMEM, DMEM-FBS, and DMEM-FBS-HEPES.*

The results observed in **Figure 3.6b** demonstrate that the **C3TEG** was not inhibiting non-specific serum-surface interactions. It is believed that oligo(ethylene glycol) (OEG)-terminated alkanethiolate SAMs resist protein adsorption from solution via two possible mechanisms:[43,44] i) steric repulsion, resulting from compression of OEG chains as protein approaches the surface and ii) water barrier due to the formation of strong hydrogen bonds between the oxygen atoms in the ethylene oxide units and the hydrogen atoms in the water molecules. From these two proposed mechanisms, and as demonstrated by previous studies,[168-172] the molecular conformation and spatial arrangement of the OEG moieties as well as OEG surface density play an important role in imparting protein resistance. For instance, OEG SAMs have been shown to adsorb proteins when their surface OEG densities were too high or too low, yet non-fouling at appropriate OEG densities.[173] From the literature and the above contact angle and ellipsometry analysis (**Table 3.1**), it seems reasonable to infer that the presence of a short alkyl chain (i.e. C3) between the thiol group and the TEG moiety give rise to less ordered structures on the gold surface, implying lower surface packing density and coverage. This is perhaps not surprising, as previous studies[174] have shown that the structure of short-chain *n*-alkyl thiol assemblies is more disordered than that of the longer chain (above C9) assemblies. Thus, a longer alkyl chain between the thiol group with the TEG and HEG moieties were utilised that could excel at limiting non-specific binding (**Figure 3.6c and 3.6d**) but that would not be long enough that could interfere with the binding and switching ability of the oligopeptide. Taking these two factors into consideration, the tri(ethylene glycol)-terminated (**C11TEG**) and hexa(ethylene glycol)-terminated (**C11HEG**) alkanethiols with a 11 carbon chain were chosen for further study (**Figure 3.1**).

3.4.1 Neutravidin binding with oligopeptide mixed SAMs with different OEGs

After assessing the ability of the OEGs in preventing nonspecific binding with different complex media, it was important to ensure that the **C11TEG** and **C11HEG** did not interfere with the neutravidin-biotin binding. Thus, **biotin-4KC:C11TEG** and **biotin-4KC:C11HEG** were prepared to confirm that the OEGs in these mixed SAMs still allowed for maximum specific binding to neutravidin. To demonstrate the 'uninhibited' binding capacity (*i.e.* the binding capacity of the surface without proteins, amino acids, glucose and vitamins in the subphase) of **biotin-4KC**:**C11TEG** and **biotin-4KC:C11HEG** mixed SAMs, SPR experiments were performed by injecting neutravidin in PBS (**Figure 3.7a**) to the mixed SAMs (1:40 solution ratio), and monitoring the SPR response for 1800s (OC trace), before washing with PBS (arrow on right in **Figure 3.7**), noting only a small drop in the SPR signal upon washing. The binding capacity is defined as the difference in the SPR response units between the beginning of injection of protein and the end of washing with PBS.

Focusing firstly on the specific binding of neutravidinto the **biotin-4KC**:**C11TEG** SAM (1:40 solution ratio), a binding capacity of ~2700 RU was observed (**Figure 3.7a red line**). This response is slightly higher than the one previously[121] observed for the **biotin-4KC**:**C3TEG** mixed SAM (~2195 RU), likely due to the higher amount of biotinylated peptide on the surface as determined by XPS analysis. More importantly, these results indicate that the longer **C11TEG** shielding component does not interfere significantly with the binding capacity of the biotin ligand. In contrast, the binding capacity of the **biotin-4KC:C11HEG** SAM (1:40

solution ratio) was very low at only 332 RU (**Figure 3.7a biotin-4KC:C11HEG trace**).

In order to improve the low binding capacity of the **biotin-4KC:C11HEG** surface, the solution ratios of the **C11HEG** were varied between 1:10 and 1:100. However, **Figure 3.7b** clearly shows that varying the solution ratio does not increase the binding capacity significantly. For a solution ratio of 1:10 a response of 426 RU is observed, which is ~100 RU higher than the 1:40 ratio (332 RU). The increased response units observed in the **biotin-4KC:C11HEG** with a 1:10 ratio can be explained due to a higher ratio of **biotin-4KC** peptides, which was confirmed by XPS to give a surface ratio of 1:5 ± 1. The increased number of peptides present on the surface allows for slightly enhanced neutravidin binding. In contrast, the 1:100 solution ratio of **biotin-4KC:C11HEG** only has 232 RU due to there being significantly fewer **biotin-4KC** peptides, which was also confirmed by XPS data and showed a **biotin-4KC:C11HEG** surface ratio of 1:19 ± 4.

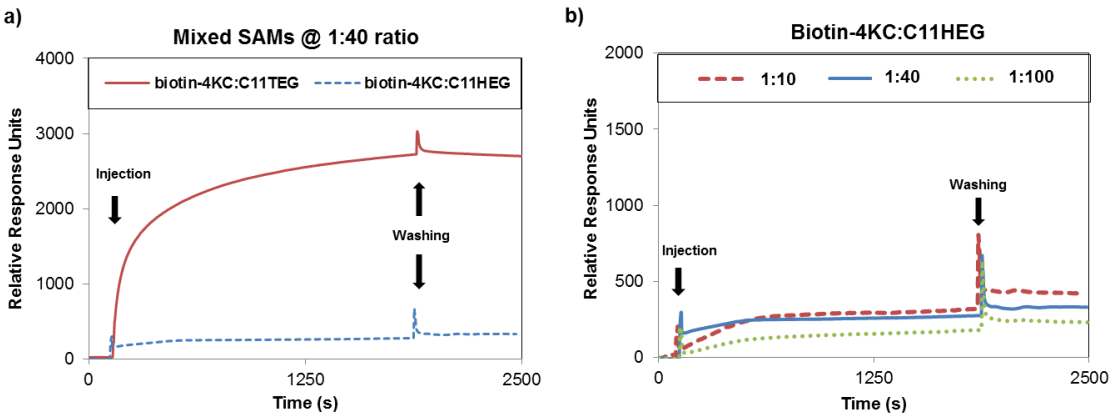

Figure 3.7 *SPR sensorgram traces for a) neutravidin binding with mixed SAMs of **biotin-4KC:C11TEG** and **biotin-4KC:C11HEG** at a 1:40 solution ratio and b) neutravidin binding with **biotin-4KC:C11HEG** mixed SAMs at solution ratios of 1:10, 1:40 and 1:100.*

The overall low binding capacity observed with the **biotin-4KC:C11HEG** mixed SAMs over a range of solution ratios (**Figure 3.7b**) suggested that the **C11HEG** interferes with the neutravidin-biotin binding interactions due to the presence of the longer 6 ethylene glycol group, which does not occur in the shorter **C3TEG** and **C11TEG**. The ellipsometry thickeness of the **biotin-4KC** was 1.7 ± 0.4 nm, whereas the **C11HEG** SAM was 2.5 ± 0.1 nm (as shown in **Table 3.1**), which supports the idea that the longer **C11HEG** is shielding the majority of neutravidin passing through the surface, thus not allowing sufficient access for the neutravidinto bind to the biotin binding sites. These findings were also supported by results obtained from molecular dynamic simulations (see **Section 3.5.1**) on the **biotin-4KC:C11HEG** mixed SAMs. To conclude the results in this section clearly show that the **C11HEG** is not suitable for further studies with the oligopeptide in mixed SAMs due to interference with the neutravidin-biotin binding activity.

3.4.2 Neutravidin binding under complex media conditions

The studies described above demonstrate that the oligo(ethylene glycol)-terminated thiol, **C11TEG**, offers the best low fouling characteristics (**Figure 3.6c**), while still capable of optimal neutravidin binding (**Figure 3.7a**). Thus, at this stage, it was important to assess if the **biotin-4KC**:**C11TEG** mixed SAM was inert to non-specific binding events while capable of maximum specific binding to neutravidin. Firstly, the resistance of the **biotin-4KC**:**C11TEG** mixed SAMs to non-specific adsorption was investigated by exposing them to the three media. In the SPR experiments, the surfaces were first exposed to PBS for 10 min, then a solution of either DMEM, DMEM-FBS or DMEM-FBS-HEPES was passed through the SPR flow

cell for 30 min, and finally the adsorbed layer formed on the mixed SAM was washed with PBS for 10 min. As evident in **Figure 3.8a**, the SPR responses following PBS rinsing for all three media was comparable to those of pure **C11TEG** SAMs (**Figure 3.6c**), showing that the **biotin-4KC**:**C11TEG** can successfully act as a serum resistant surface. In order to evaluate the binding capacity of the **biotin-4KC:C11TEG** mixed SAM under complex biological conditions, neutravidin binding to the biotin ligand on the mixed SAM was monitored in the presence of media (**Figure 3.8b**).

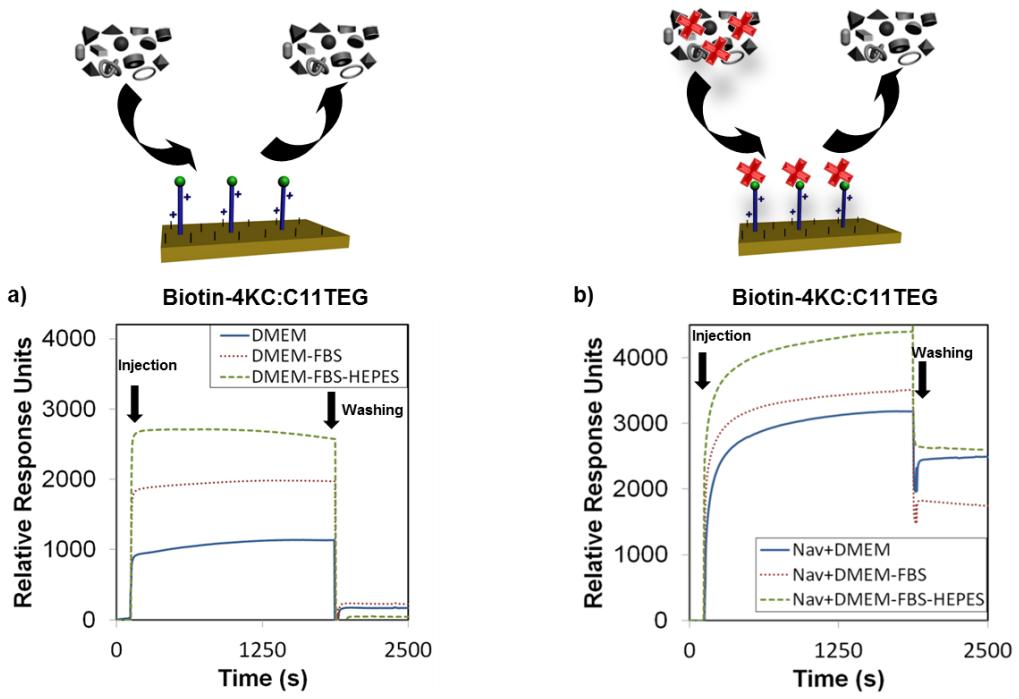

Figure 3.8 *SPR sensorgram traces for the interaction of* ***biotin-4KC*****:*****C11TEG*** *mixed SAMs with a) different complex media – DMEM, DMEM-FBS, and DMEM-FBS-HEPES and b) with neutravidin (Nav) in either DMEM, DMEM-FBS or DMEM-FBS-HEPES. After neutravidin binding for 30 min, the surfaces were washed with PBS for 10 minto remove any non-specifically adsorbed material. The two arrows in the graphs indicate the point of injection of neutravidin either in PBS or media and PBS washing buffer, respectively.*

In the SPR experiments shown in **Figure 3.8b**, the mixed SAMs were exposed to a flow of PBS, to establish the baseline, followed by an injection of neutravidin in either DMEM, DMEM-FBS or DMEM-FBS-HEPES into the SPR flow cell for 30 min. The SPR flow cell was then flushed with PBS to leave only the specifically bound neutravidin on the biotinylated mixed SAM. Following rinsing with PBS, the final SPR signal associated with neutravidin and DMEM (~2500 RU) and neutravidin and DMEM-FBS-HEPES (~2600 RU) was comparable to the response associated with neutravidin in PBS (~2700 RU), whereas a decrease in neutravidin binding was observed when the mixed SAM was exposed to neutravidin in DMEM-FBS (~1800 RU) (**Figure 3.8b Nav+DMEM-FBS trace**).

The differences observed in the representative SPR sensorgrams suggest that the presence of FBS to some extent interfered with the binding of neutravidin. The serum proteins are most likely non-specifically adsorbing to the surface alongside the specific adsorption of the neutravidin, and hence block some of the biotin moieties, not allowing them to bind to the neutravidin. Interestingly, the presence of HEPES buffer in the DMEM-FBS-HEPES solution allowed more neutravidin to bind to the biotinylated surface, which correlates well with the earlier reports which state that protein adsorption depends upon, among other factors, the medium in which the protein is found.[175] In this case the HEPES may be coating the serum proteins in the FBS, which in turn is inhibiting them from binding to the surface, and hence not blocking the biotins from binding to the neutravidin (**Figure 3.8b Nav+DMEM-FBS-HEPES trace**).

3.5 Switching efficiency of biotin-4KC:C11TEG mixed SAMs

The assays above demonstrated the efficacy of the **biotin-4KC**:**C11TEG** mixed SAM to excel at limiting non-specific adsorption and promoting specific biomolecule binding. Thus, switching efficiency was also assessed in terms of the **biotin-4KC**:**C11TEG** mixed SAM's ability to control the binding events between the surface-appended biotin and the neutravidin from the 'uninhibited' PBS solution (**Figure 3.9**). Switching efficiency studies were conducted by analysing the neutravidin binding to the biotinylated SAM under open circuit (OC) conditions (i.e. no applied potential - bio-active "ON" state) or to which a negative potential was applied (bio-inactive "OFF" state). Previously, it was demonstrated that the bio-inactive "OFF" state can be effected by application of –0.4 V, while not affecting the SAM integrity.[121] The neutravidin in PBS was injected (arrow on left **Figure 3.9 -0.4 V trace**) with the -0.4 V potential being applied for 30 min, after which the surface was rinsed with PBS. The switching efficiency (SE) was defined as the percent difference between the binding capacity at open circuit conditions (BC_{OC}) and the binding capacity at –0.4 V ($BC_{-0.4V}$) divided by BC_{OC}:

$$SE = 100 \times \frac{BC_{OC} - BC_{-0.4V}}{BC_{OC}}$$

Equation 3.2

Thus, given the binding capacity of ~2700 RU was observed under OC conditions (**Figure 3.9 OC trace**), whereas a negative potential of −0.4 V induced a

large reduction in binding affinity, with the SPR response decreasing to ~800 RU (**Figure 3.9 -0.4 V trace**). The switching efficiency of the **biotin-4KC**:**C11TEG** mixed SAMs in PBS was very high at 70%, thereby demonstrating the suitability of the **biotin-4KC**:**C11TEG** mixed SAM for efficiently controlling specific biomolecular interactions.

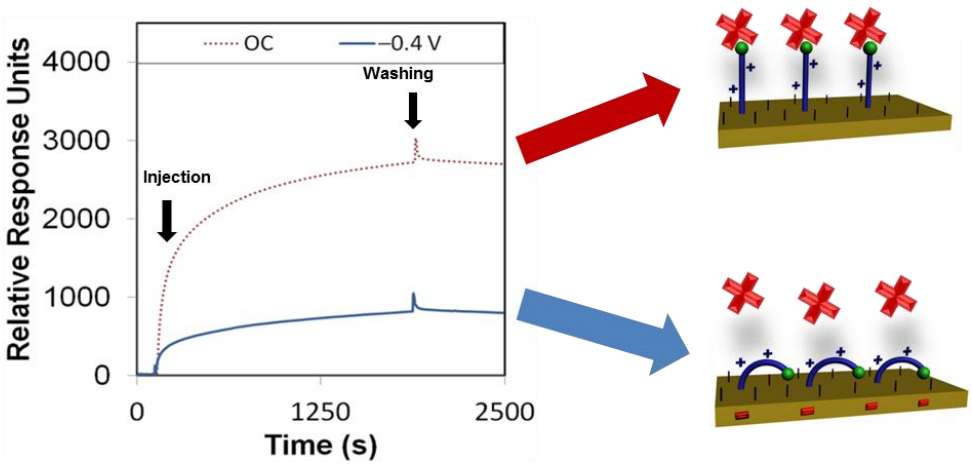

Figure 3.9 *SPR sensorgram traces showing the binding of neutravidin (Nav) to the* ***biotin-4KC*****:*****C11TEG*** *mixed SAMs. a) The mixed SAMs were exposed to neutravidin under OC conditions and an applied negative potential (− 0.4 V). SPR switching studies were carried out in triplicates to get an average switching efficiency.*

3.5.1 Using computational modeling to understand neutravidin-biotin interactions on biotin-4KC:C11HEG mixed SAMs

While SPR offers a system to retrieve information such as binding ability and binding switching efficiency, atomic molecular dynamic simulations provide molecular insights into the electrical-induced conformational changes of the oligolysines within the SAM. In this section molecular dynamics (MD) simulation was used for the **biotin-4KC:C11HEG** with collaborators from University of Nanjing, China to gain a better understanding of the neutravidin-biotin interactions on the surface under PBS like conditions.

The performance of MD simulations depends mainly on the force field selected, and thus three different force fields were tested, namely cvff (consistent-valence force field), compass (condensed-phase optimized molecular potentials for atomistic simulation studies) and pcff (polymer consistent force field (see **Section 5.2.6** for full details). The cvff force field performed best according to the test, and thus it was adopted in our simulations. The simulation models are shown in **Figure 3.10**. Two dimensional rhombic periodic boundary condition and slab models were applied throughout the simulations. Water molecules and chloride ions were adopted to simulate the PBS solution. Detailed model parameters are summarized in **Table 5.1** in **Chapter 5 Experimentals**. External electric fields were applied to model the electric potentials used in the experiment. In order to consider the polarization caused by the electric field, density functional theory-derived partial charge was used. Simulations were carried out for **biotin-4KC:C11HEG** and pure **biotin-4KC**.

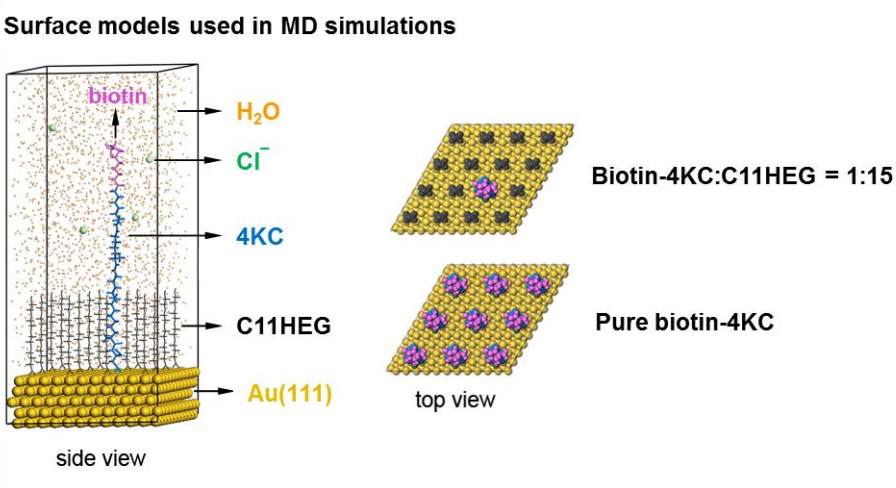

Figure 3.10 *The surface models used in the MD simulations. The purple, blue and dark green parts of the biotin-4KC chain represent the biotin motif, lysine and cysteine residues, respectively. The orange dots, light green balls, yellow balls and short grey chains denote water molecules, chloride ions, gold atoms and TEGT, respectively.*

Experiments conducted on mixed SAMs comprising the **biotin-4KC** and the longer ethylene glycol thiol – **C11HEG** in (**Figure 3.6**) – led to a greatly reduced binding of neutravidinto the biotinylated surface. When **biotin-4KC:C11HEG** solution ratios were varied between 1:10 and 1:100, surface ratios between 1:5 ± 1 and 1:19 ± 4 were observed respectively after XPS analysis (see **Appendix I**). The neutravidin binding amount was essentially independent of the surface ratio used, with SPR signals in the range of 232-426 response units for all the surfaces. Taking into consideration that the lengths of the **biotin-4KC** and **C11HEG**, in fully extended conformations, are 5.2 nm and 3.9 nm, respectively, to a certain extent the biotin functionalities are expected to protrude from a matrix of **C11HEG**s even if most likely both molecules adapt an unstretched form on the surface. Nevertheless, and based

on the SPR results observed in **Figure 3.7**, there is strong evidence that the biotin moieties were not accessible for binding. Therefore the suppression of biorecognition with the biotin-binding pockets of neutravidin is a result of the biotin moieties not standing further away from the **C11HEG** matrix, thus not allowing complete insertion of the biotin into the binding pockets.

This reasoning is in line with previous studies that showed that increasing the length of the biotin linker in a mixed SAM increased the protein binding efficiency.[176] Our hypothesis is also consistent with X-ray crystallographic analysis that revealed that the biotin is buried quite deeply inside the neutravidin barrel,[177] indicating that the binding of biotin by neutravidin requires the complete insertion of the ligand into the binding pocket of the protein. **C3TEG** and **C11TEG** in a fully extended conformation exhibit a length of 1.7 nm and 2.6 nm respectively. The **C3TEG** has a theoretical length approximately three-fold shorter than the **biotin-4KC** and the **C11TEG** is half of that of the **biotin-4KC** in a fully extended conformation, allowing complete insertion of the biotin into the binding pocket and efficient binding of the neutravidinto the biotinylated monolayer. Although ellipsometric thickness indicates that both the **C11TEG** (1.7 ± 0.2 nm) and **biotin-4KC** (1.7 ± 0.4 nm) are very similar in length on the surface, this had no impact on the binding capacity of the neutravidin.

In the case of **biotin-4KC:C11HEG** (**Figure 3.11**), the ethylene glycol chains were long enough to partially cover the biotin in the OC conditions (d < 0.5 nm). The biotin-4KC chain would extend to about 5.2 nm (using ChemDraw 3D) and reach neutravidin only when the E_z field was applied (d > 1.4 nm). This finding supports the interpretation that low neutravidin binding to the **biotin-4KC:C11HEG** mixed SAM is

an effect related with the biotin moieties standing too close to the ethylene glycol matrix thus, sterically shielding the biotin and making it inaccessible to the neutravidin.

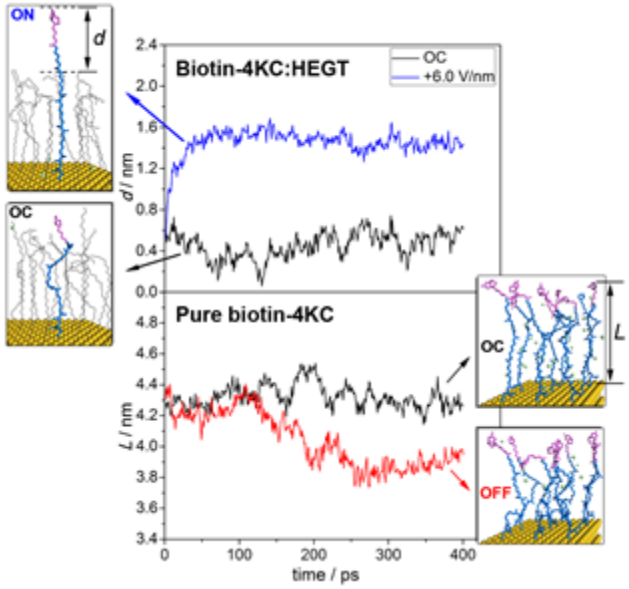

Figure 3.11 *The conformational changes of* ***biotin-4KC:C11HEG*** *(up) and pure* ***biotin-4KC*** *(down) under different electric fields, along with the MD simulation snapshots. L is defined as the gap distance variation between the biotin and gold surface.*

The oligopeptide density was also shown to affect the switching mechanism, and as a consequence, the binding switching efficiency. From **Figure 3.11**, it is noticeable that for the pure **biotin-4KC** SAM, the chains were closely packed on the surface and insufficient space was left for the chains to collapse. The biotin heads were always exposed, which would lead to a constant bioactivity. It can be inferred from these findings that a basic criterion in the design of the switching surfaces is to provide sufficient freedom for conformational transitions of surface confined oligopeptide chains.

3.5.2 Effects of electrical potential on complex media

Prior to carrying out switching studies under complex media, it was essential to ensure that the **biotin-4KC:C11TEG** surface does not display any artificial increase in protein adsorption from the complex media due to a negative potential as this could be detrimental to the effectiveness of the switching system. Complex media (DMEM-FBS-HEPES) was injected to the **biotin-4KC:C11TEG** surface under both OC conditions and -0.4 V applied potential as shown in **Figure 3.12**, thereafter the surface was washed with PBS (as shown by the arrow in **Figure 3.12**). A drop off in signal was observed representing a change in refractive index and the removal of serum proteins under both OC conditions (**Figure 3.12 blue line**) and -0.4 V applied potential (**Figure 3.12 red dashed line**). Thus, indicating that the application of a potential does not artificially increase serum adsorption on the surface, likely due to the highly protein inert properties of the **C11TEG**, hence providing a sound basis for testing switching efficiency under complex media.

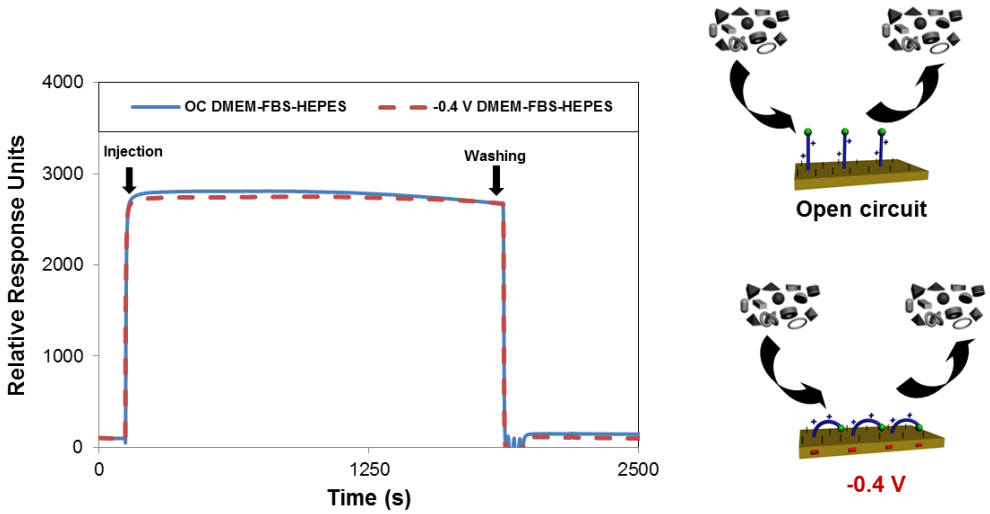

Figure 3.12 *SPR sensorgram traces showing the interaction of DMEM-FBS-HEPES on the* ***biotin-4KC:C11TEG*** *mixed SAMs under OC conditions and -0.4 V*

3.5.3 Effects of complex media on switching efficiency

The **biotin-4KC:C11TEG** mixed SAMs were further studied with respect to the switching efficiency in the presence of the three different media (**Figure 3.13a**). A similar efficiency to PBS was reached when DMEM was employed as the control media (~67%), whereas the presence of DMEM-FBS and DMEM-FBS-HEPES during the switching process had induced a drop off in efficiency to values close to 45%. The different behaviour observed for DMEM-FBS and DMEM-FBS-HEPES (**Figure 3.13a**) indicates that both FBS and HEPES might have an effect in the switching ability of the electrically switchable SAM surface (please see **Section 4.5.1** for a detailed discussion on the components of complex media including DMEM, FBS and HEPES buffer).

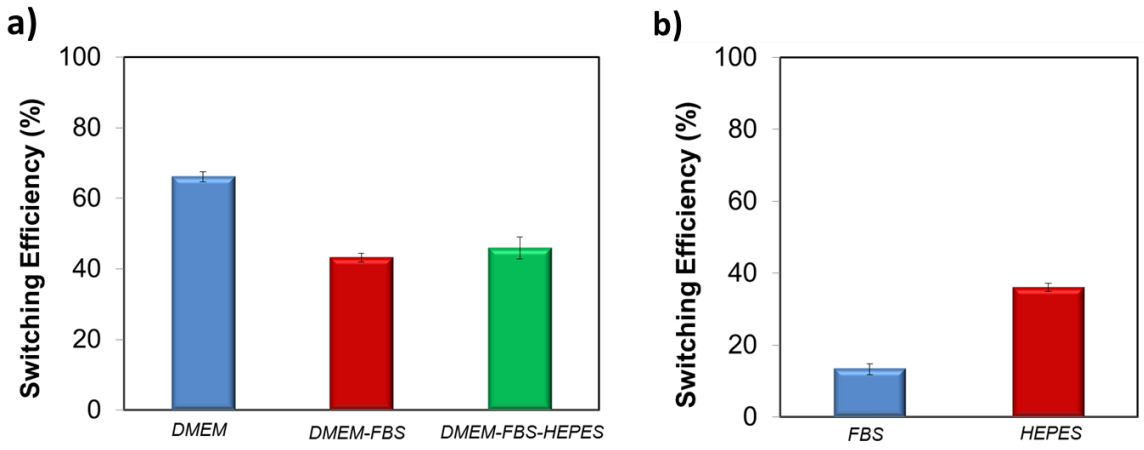

Figure 3.13 *Switching efficiency, as determined by SPR analysis under OC conditions and an applied negative potential (− 0.4 V), on* ***biotin-4KC:C11TEG*** *mixed SAMs which were exposed to neutravidin in a) DMEM, DMEM-FBS, DMEM-FBS-HEPES as well in b) FBS and HEPES. Error bars show standard deviations among three different substrates.*

Thus, in order to further delineate the respective roles of FBS and HEPES in the switching process, SPR switching studies were performed with these two individual components (**Figure 3.13b**). FBS and HEPES solutions in PBS were used at the same concentration as in the DMEM-FBS and DMEM-FBS-HEPES (i.e. 10% FBS and 24 mM HEPES). As before, the baseline for the **biotin-4KC:C11TEG** mixed SAM-modified gold chip was established using PBS, following which the neutravidin in either of the solutions mentioned above (i.e. 10% FBS and 24 mM HEPES) was introduced for 30 min. Subsequently, the surfaces were washed in PBS. These SPR experiments were conducted under OC conditions and -0.4 V in order to calculate the binding switching efficiency as described above using **Equation 3.2**. The binding switching efficiencies of the **biotin-4KC:C11TEG** mixed SAM in the presence of these 10% FBS or 24 mM HEPES are summarised in **Figure 3.13b**.

Interestingly, the switching behaviour of the mixed SAM on 10% FBS has led to efficiencies around 15%, indicating that the switching effect was largely absent. Remarkably, these values can be significantly enhanced, rising to ~45%, if the switching is performed using such FBS concentrations in the presence of HEPES as shown in **Figure 3.13a**. Nevertheless, it is clear that the presence of a significant amount of protein results in the partial inhibition of the switching process. This behaviour might be attributed to the interference of the FBS with the conformation changes in the oligopeptide. This reasoning is in line with the decreased specific binding capacity when the **biotin-4KC:C11TEG** mixed SAM was exposed to neutravidin in the presence of DMEM-FBS (**Figure 3.8b**), showing that non-specific interactions between FBS and the oligopeptide mixed SAM caused interference with the specific binding between neutravidin and the surface-appended biotin. From the

HEPES experiments, some valuable information can also be gathered. The switching efficiency is also affected by the presence of HEPES, which has led to efficiencies values of ~40%. It is therefore reasonable to presume that either the presence of FBS and/or HEPES in the DMEM solution had adversely affected the switching ability of the oligopeptide.

3.5.3.1 Effects of diluted complex media on switching efficiency

In order to adequately represent the factors influencing the switching ability, the oligopetide mixed SAMs were tested using the three media (i.e. DMEM, DMEM-FBS and DMEM-FBS-HEPES) at different dilutions in PBS buffer. Interestingly, a dilution in PBS to 10% of the different media had no effect on the switching efficiency of DMEM, while it had improved the efficiency of the DMEM-FBS and DMEM-FBS-HEPES systems at different rates. As seen in **Figure 3.14a**, switching efficiency increased roughly 35% as the DMEM-FBS concentration decreases from 100% to 10%, whereas the same decrease in concentration for the DMEM-FBS-HEPES has led to no differences in efficiency within the error. The analysis of the effect of concentration on the switching efficiency of the **biotin-4KC**:**C11TEG** mixed SAMs also indicate that 1% media solutions have negligible effect on the switching efficiency, with all three media showing values similar to those observed for PBS, i.e. of approximately 70%. At this point, it should be stressed that even though the switching is partly compromised when compared to more diluted media (i.e. 1%) or pure PBS buffer, the level of switching in 10% and 100% media is still relatively high and in all instances is higher than 45% (See **Appendices IV-VIII** for SPR sensogram representations).

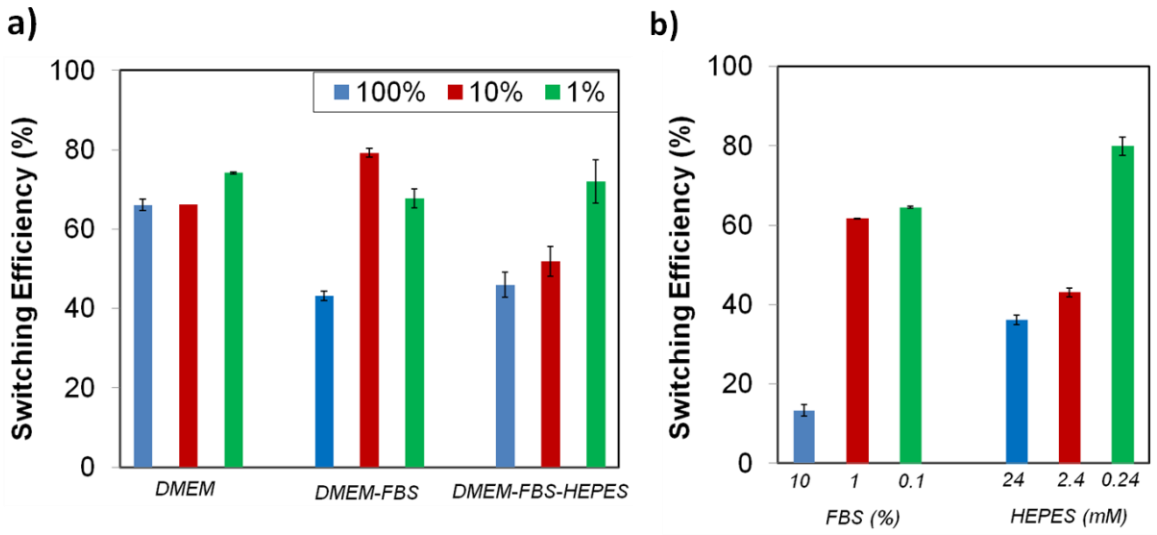

Figure 3.14 *Switching efficiency, as determined by SPR analysis under OC conditions and an applied negative potential (− 0.4 V), on biotin-4KC:C11TEG mixed SAMs which were exposed to neutravidin in a) DMEM, DMEM-FBS, DMEM-FBS-HEPES as well in b) FBS and HEPES. The switching efficiency of the different media was tested at different dilutions in PBS buffer. Error bars show plus or minus one standard deviation of the mean among three different substrates.*

Similar dilution studies were carried out with FBS and HEPES solutions in PBS at the same concentration as in the DMEM-FBS and DMEM-FBS-HEPES (i.e. 10% FBS and 24 mM HEPES), as well as diluted to 10% and 1% of the original concentrations. The FBS solutions are designated as 10% FBS, 1% FBS and 0.1% FBS, while the HEPES solutions are denominated as 24 mM HEPES, 2.4 mM and 0.24 mM HEPES. The switching behavior of the mixed SAM on 10% FBS differed strikingly from that observed on 1% and 0.1 % FBS (**Figure 3.14b**). Switching efficiency was pronounced for 1% and 0.1% FBS, with values in the range of 60-

65%, which are comparable to those observed for PBS. (See **Appendices VII-VIII** for SPR sensogram representations).

The HEPES buffer dilutions showed that the switching efficiency is strongly dependent on the concentration of HEPES, which by decreasing from 24 mM to 0.24 mM has led to a marked augmentation in switching efficiency from 35% to more than 75%. No major differences were found between 24 mM and 2.4 mM HEPES, which remained in the range of 35%-45%. HEPES contains both a very strong acid (sulfonic acid) and a relatively weak base (amine) and they are particularly prone to the formation of hydrogen bonds and electrostatic interactions with proteins as is seen in several protein crystal structures.[178,179] From the aforementioned results, and on the basis of the previous literature of the interactions of the zwitterionic HEPES with proteins, it could be suggested that the ability of the HEPES molecule to form stable intermolecular interactions with the peptide might restrict the oligopeptide from electrostatically interacting with the negatively charged gold surface and change its conformation, resulting in a decrease in switching efficiency. The noted protein-HEPES interactions can also explain the reduction in non-specific FBS adsorption (**Figure 3.8b**) when HEPES was present in the media. Thus, HEPES interactions with FBS might prevent nonspecific interactions between FBS and **biotin-4KC:C11TEG** mixed SAM. Taken together, these results clearly show the importance of selecting a buffer that has a minimal impact on the switching ability of the oligopeptide. Careful control of the media composition ensures that the switching can achieve levels of efficiency as high as 70%.

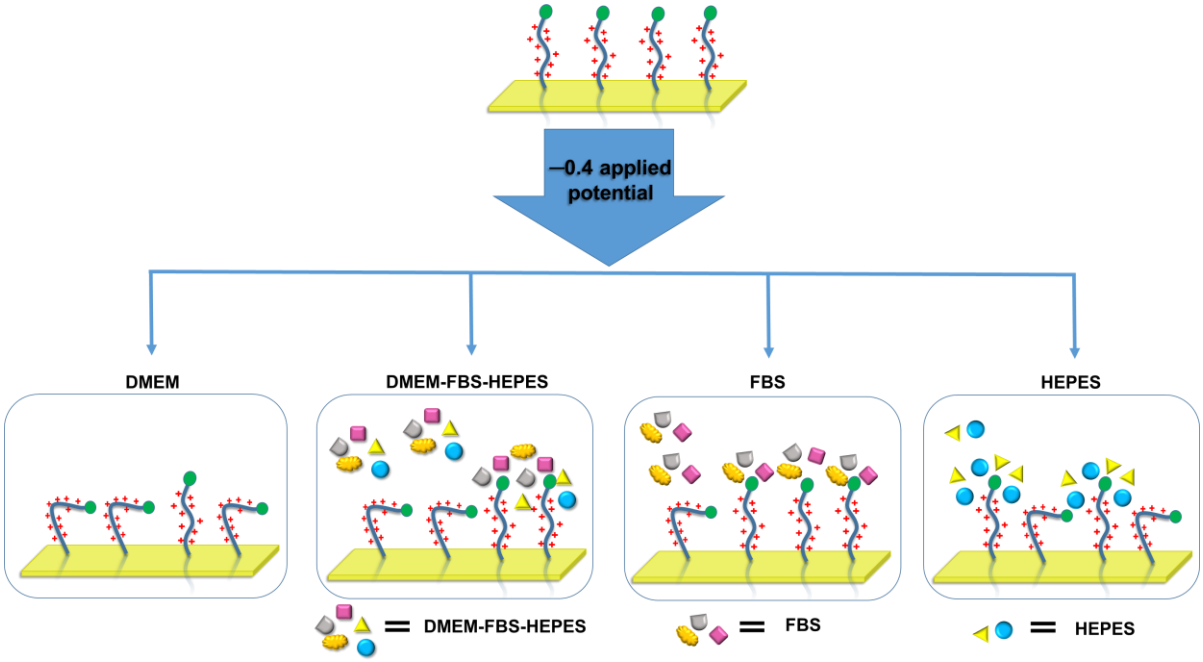

Figure 3.15 *Schematic showing that the characteristics of the media influence the performance of the switching of the electro-switchable oligopeptides. DMEM exhibits similar switching behaviour as PBS, whereas DMEM-FBS-HEPES induces a drop in switching efficiency. However, the switching ability is higher than when only FBS is used. We propose that the presence of HEPES in the DMEM-FBS-HEPES media allows for the formation of hydrogen bonds and electrostatic interactions between HEPES and the serum proteins, leading to a decrease in the interactions between the serum proteins and the switchable surface. High concentrations of HEPES also inhibit to a certain extent the switching of the oligopeptides likely as a result of intermolecular interactions between HEPES and the oligopeptides. Not to scale (see* ***Figure 3.1*** *for the description of the cartoons). The oligo(ethylene glycol) thiols have been removed for clarity.*

3.6 Conclusion

While substantial attention has been directed to construction and performance of biological switchable surfaces in simple biological systems, less effort has been directed to developing and understanding surfaces capable of switching under more practical biological applications. This is the first study to investigate and address such scientific issues and challenges associated with the underpinnings of biological switchable surfaces. In this work, a combined approach was taken for producing well-defined SAMs that prevent non-specific binding with the ability to electrically switch the SAM to allow control over biomolecular interactions under complex biological matrixes. Particularly, this SAM system can be dynamically modulated by an electrical potential under different commonly used biological media, ranging from DMEM to DMEM supplemented with FBS and HEPES. The work demonstrated that the performance of the switching on the electro-switchable oligopeptide is sensitive to the characteristics of the media, and in particular, its protein concentration and buffer composition. For instance, these studies demonstrated that higher concentrations of non-specific proteins affect the conformations changes of the oligopeptide and thus reduce the switching efficiency. The design of electrical stimuli-responsive surfaces and their operation under complex biological conditions must properly take these issues into account to assure maximum switching performance. However, it is important to point out that even though the switching is partly compromised when compared to very diluted media (i.e. 1%) or pure buffer, the level of switching in 10% and 100% DMEM is still relatively high and in all instances is higher than 45%.

Chapter 4: Regulating Cellular Interactions on Surfaces under Complex Biological Conditions

This chapter is based on the manuscript, "Electrically-driven modulation of surface-grafted RGD peptides for manipulation of cell adhesion" by *M. Lashkor, F. J. Rawson, J. A. Preece, P. M. Mendes, Chemical Communications,* ***2014****, 50, 15589.*

Abstract: *The ability to regulate cellular interactions on surfaces via an external stimulus is important in providing a greater understanding of the processes that take place between the cell and the ECM during cell adhesion and migration. The development of such surfaces has practical implications in biological and medical applications. This chapter reports a switchable surface that relies on electrically-induced conformational changes within surface-grafted arginine-glycine-aspartate (RGD) oligopeptides as the means of modulating cell adhesion.*

4.1 Introduction

Switchable surfaces have been scarcely used, thus far, to control biomolecular interactions on more complex systems such as those involving modulation of cell responsiveness.[99,107,123,180] Jonkheijm and co-workers have reported a cucurbit[8]uril-based SAM system to electrochemically control the release of cells. Charged end groups on SAM surfaces have been exploited to electrically control the early stages of bacterial cell adhesion[180] and form patterned surfaces with two independent dynamic functions for inducing cell migration.[123] In spite of these

efforts, given cellular complexity and diversity, such studies are very limited in number, as are the opportunities to further understand and control the complex interplay of events and interactions occurring within living cells.

The fundamental work carried out in **Chapter 3** provided useful insight into the switching mechanism and the interaction of **biotin-4KC:C11TEG** monolayer under complex biological conditions. This chapter follows on from the previous chapter wherein, a stimuli-responsive surface is reported that relies on electrically-induced conformational changes within surface grafted arginine–glycine–aspartate (RGD) oligopeptides as the means of modulating cell adhesion. RGD, which is present in most of the adhesive ECM proteins (*e.g.* fibronectin, vitronectin, laminin and collagen) and is specific for integrin-mediated cell adhesion,[18] is used here to dynamically regulate the adhesion of immune macrophage cells. The stimuli-responsive surface is fabricated on a gold surface and comprises a mixed SAM consisting of two components (**Figure 4.1**): i) an oligopeptide containing a terminal cysteine for attachment to the gold surface, three lysine residues as the main switching unit, and a glycine–arginine–glycine–aspartate–serine (GRGDS) as the recognition motif for cell adhesion – **GRGDS-KKKC**, and ii) an ethylene glycol-terminated thiol (**C11TEG**) space out the oligopeptides. Since the charged backbone of the oligopeptide can be potentially harnessed[118,122] to induce its folding on the surface upon an application of an electrical potential, it was reasoned that such conformational changes can be employed to selectively expose under open circuit (OC) conditions (bio-active state) or conceal under negative potential (bio-inactive state) the RGD to the cell and dynamically regulate cell adhesion.

The RGD peptide will act as the bioactive moiety that promotes cell adhesion through binding of the cell integrin receptors, when exposed during the bio-active state (OC conditions).[181] Moreover it is expected that there will be a reduction in cell adhesion upon the application of -0.4 V electrical potential by the concealment of the RGD moiety in the bio-inactive state (**Figure 4.1**). The RGD motif has been well documented as the minimum peptide sequence required for cell recognition and has been used in number of previous systems which were successfully able to control cell adhesion properties.[20,99,106,123]

The second component is the **C11TEG**, which has two key roles: 1) to act as a spacer group to provide sufficient spatial distribution for the conformational switching of the **GRGDS-KKKC** peptide and 2) to prevent non-specific binding of proteins from complex media as demonstrated in **Chapter 3**. The switching of the peptide will be monitored primarily through optical microscopy by comparing differences in cell counts on the surfaces under an applied electrical potential (-0.4 V) and OC conditions. The protein resistant component (**C11TEG**) on the surface is essential for surfaces that manipulate cell adhesion properties. In this case surfaces will be incubated under complex media containing an array of proteins as well as the adherent cells. If the antifouling properties of the surface are not sufficiently protein resistant then proteins within the media could adsorb on the surface with ease. The adsorption of proteins on the surface could potentially hinder cell adhesion or artificially increase cell adhesion due to the presence of additional motifs.[16] In addition the ethylene glycol molecules provide the required spacing for conformational switching, thus when the target ligand is switched off it will be masked by the ethylene glycol molecules which act as a protein and cell resistant surface.

The cells chosen for this chapter were RAW 264.7 macrophages. This cell line was established from a murine (*Mus musculus*) tumour induced by Abelson murine leukaemia virus (A-MuLV). The cells' semi-adherent nature to surfaces provides a good platform to carry out switching studies, where it will be easily distinguishable whether or not the cells have adhered to the surface. It is expected that the RAW 264.7 cell line will also adhere preferentially to RGD functionalised surfaces via cell integrin receptors.[182] Macrophage cell adhesion to biomaterial surfaces plays a key role in mediating immune response to foreign materials.[183] Thus, development of dynamic *in vitro* model systems that can control macrophage cell adhesion on demand are likely to provide new opportunities to understand adhesion signalling in macrophages[184] and develop effective approaches for prolonging the life-span of implantable medical devices and other biomaterials.[185]

4.1.1 Objectives

1) To fabricate low density mixed SAMs using **GRGDS-KKKC** peptide and **C11TEG** to prevent non-specific binding and provide sufficient space for switching of the positively charged oligolysine chain in order to conceal RGD moiety.

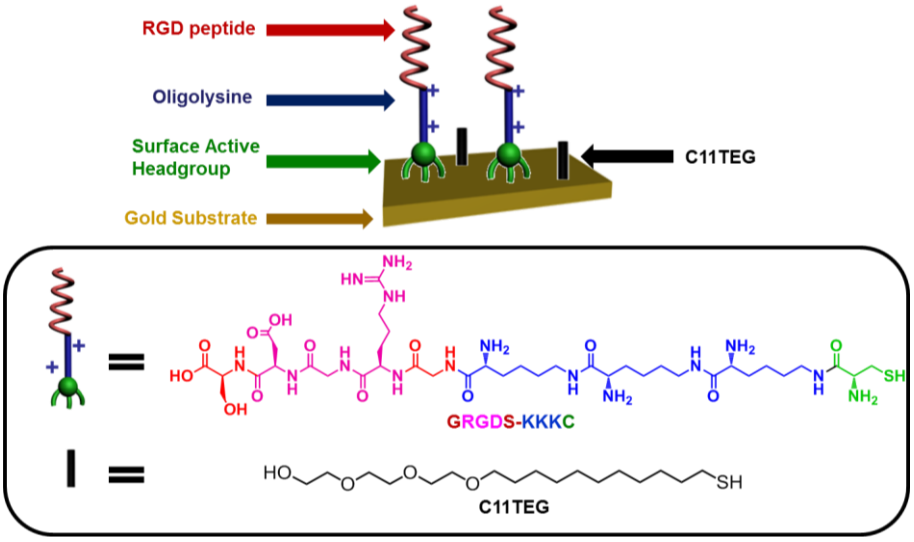

Figure 4.1 *Schematic showing gold substrate functionalised with* ***GRGDS-KKKC:C11TEG*** *mixed monolayer and the structure of each component.*

2) To compare the extent of cell adhesion of RAW 264.7 cells on both RGD and non-RGD functionalised surfaces and to ensure the C11TEG is effective at preventing non-specific binding.

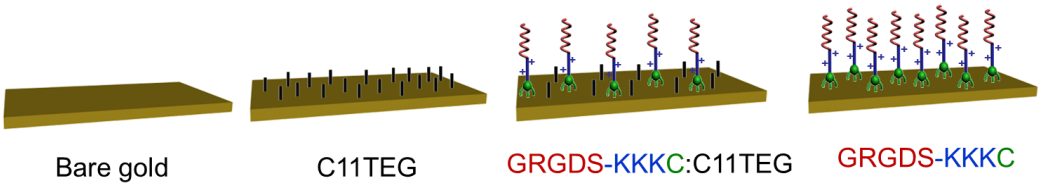

Figure 4.2 *Schematic showing the different surfaces that will be used to examine cell adhesion.*

3) Investigate the switching properties of the mixed SAMs by monitoring the interactions between the cells and the RGD functionalised surface upon the application of a negative electrical potential.

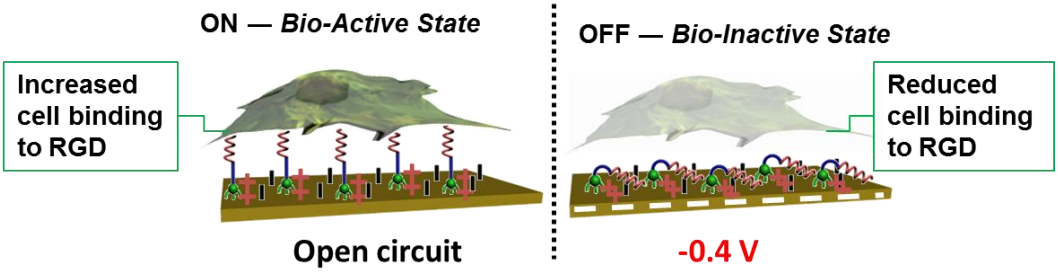

Figure 4.3 *Schematic representation of the **GRGDS-KKKC:C11TEG** mixed SAMs and the attachment of cells on electro-switchable oligopeptide surfaces. Depending on the electrical potential applied, the peptide can expose or conceal the RGD domain and regulate its binding to integrin receptors on cells.*

4) To carry out control studies by comparing the attached number of cells under -0.4 V applied potential and OC conditions with a pure **C11TEG** monolayer and **GRGDS-HEGC** and **C11TEG** mixed SAMs. **GRGDS-HEGC** (**Figure 4.4**) will be used as a substitute to **GRGDS-KKKC** by replacing the positively charged lysine backbone with six non-switchable ethylene glycols. Thus, it is expected that cells will adhere under both OC conditions and a negatively (-0.4 V) applied potential.

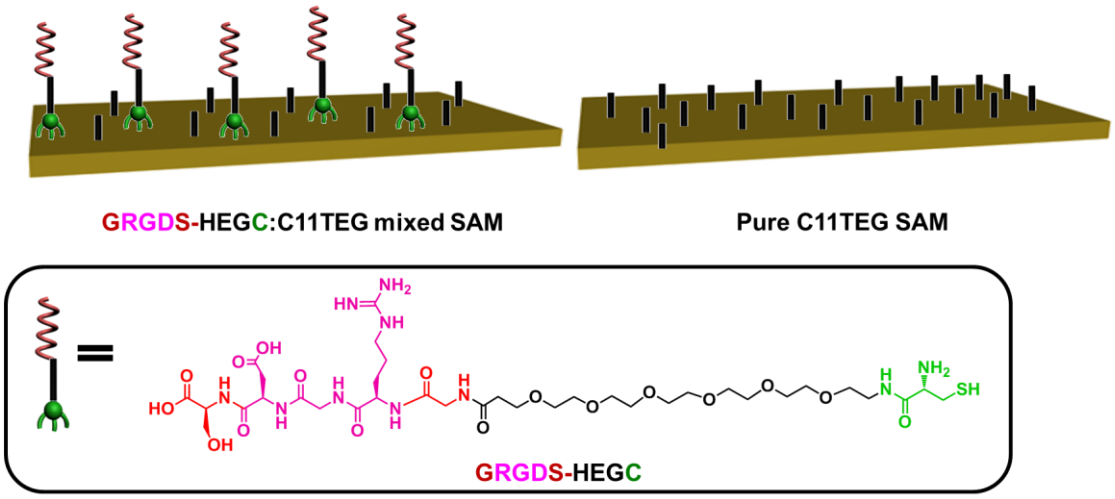

Figure 4.4 *Schematic representation of two control monolayers:* ***GRGDS-HEGC:C11TEG*** *mixed SAM and* ***C11TEG*** *SAM.*

5) To test for reversible switching with the mixed SAMs, by varying the surface potential from off-on and on-off.

a)

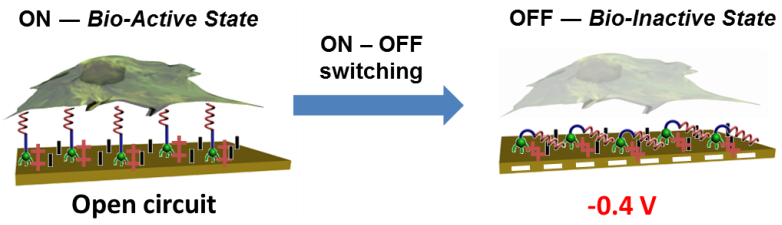

b)

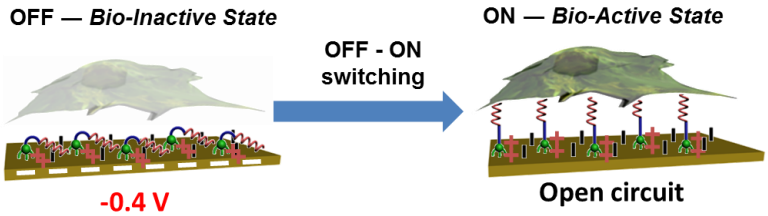

Figure 4.5 *a) ON-OFF switching and b) OFF-ON switching where "ON" represents a cell adhesive state and "OFF" represents a cell resistant state.*

The advantages of using **GRGDS-KKKC:C11TEG** as a switchable surface to control cell adhesion over other surfaces include the surfaces ability to prevent non-specific binding in the presence of complex media in which there are many proteins that have the potential to non-specifically bind to the surface. In addition, it is well established that the positively charged oligolysine chain can switch upon the application of a negative potential, thus allowing for an efficient switching mechanism. It is expected the switching mechanism will occur similar to that of the computational model mentioned in **Chapter 3**, whereby a collapse of the positively charged lysine chain occurs due to the application of an electrical potential which in-turn conceals the RGD binding ligands from cell receptors thus, preventing cell attachment.

4.2 Results and Discussion

4.3 Formation and characterisation of mixed SAMs on gold substrates

4.3.1 Formation of mixed GRGDS-KKKC:C11TEG SAMs

Cleaned gold surfaces were functionalized with a two-component mixed SAM of **GRGDS-KKKC** peptide and **C11TEG** as shown in **Figure 4.6**.The RGD peptide consists of a cysteine group, three lysines and a RGD functional group. The RGD peptide will be immobilised to the gold surface via the cysteine group, which contains a thiol moiety that binds to gold. The three lysine groups provide a flexible backbone, similar to the **biotin-4KC** peptide, which provides ample manoeuvrability to switch conformations between the on and off states. The main role of the **C11TEG,** in addition to providing spatial distribution for the **GRGDS-KKKC** peptide to switch, is to prevent non-specific binding from complex media and cells.

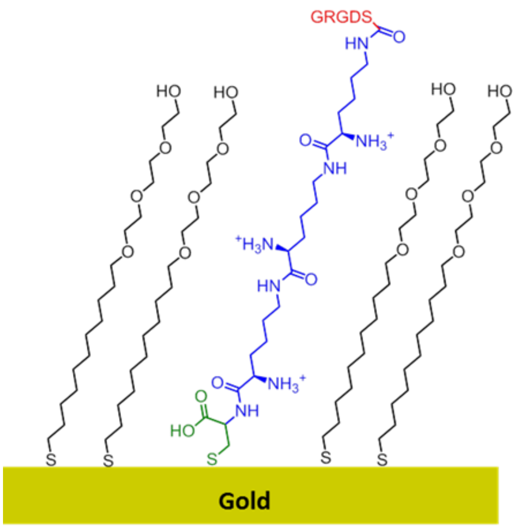

Figure 4.6 *Schematic of the formation of **GRGDS-KKKC:C11TEG** mixed SAMs.*

Our previous work carried out with **biotin-4KC:TEGT** and **biotin-4KC:C11TEG** mixed SAMs indicated that the optimal solution ratio for switching was 1 **biotin-4KC** peptide to 40 **TEGT** molecules. In order to fabricate novel mixed SAMs using a peptide with a RGD functional group (**GRGDS-KKKC**) and **C11TEG** molecules, solution ratios from our previous studies with **biotin-4KC:TEGT** and **biotin-4KC:C11TEG** were used as a guide. Hence, the solution ratio chosen to form a mixed SAM of **GRGDS-KKKC:C11TEG** was 1:40. From previous studies it was assumed that 1:40 would provide sufficient spatial distribution and allow for efficient switching of the **GRGDS-KKKC** peptide. However, as suggested in the literature,[55] the two components in a solution ratio are rarely similar to the ratio of the SAM formed on the surface. Thus, surface characterisation techniques such as ellipsometry, contact angle and XPS were used to determine the surface ratio and characteristics of the SAM.

4.3.2 XPS analysis of mixed GRGDS-KKKC:C11TEG SAMs on gold substrates

XPS was used to investigate the surface ratio of the **GRGDS-KKKC:C11TEG** monolayer in a 1:40 solution ratio. Gold substrates were cleaned by piranha solution, then rinsed with UHQ water, HPLC ethanol and finally immersed in a mixed SAM solution of **GRGDS-KKKC** (0.1 mM) and **C11TEG** (0.1 mM) for 24 h to allow the formation of the monolayers. The mixed SAM solution also contained 3% (v/v) $N(CH_2CH_3)_3$, which prevents multilayer formation between NH_2 functional groups of the adsorbed thiolate peptide on the surface and the free thiol peptide in the bulk solution.[186] After 24 h had elapsed, the SAM functionalised gold substrates were rinsed initially with an ethanolic solution with acetic acid to rinse any $N(CH_2CH_3)_3$ that

may have remained on the surface. Thereafter, the substrates were rinsed further using HPLC grade ethanol and finally dried under argon gas. The substrates were then stored under an argon gas atmosphere prior to XPS analysis.

XPS analysis confirmed the formation of the **GRGDS-KKKC:C11TEG** mixed monolayer and displayed signals from S, N, C and O. The chemical state of the sulfur atom was probed using the XPS spectra of the S 2p emission (binding energy range of 160 eV to 170 eV) (**Figure 4.7a**). The S 2p spectrum (**Figure 4.7a**) consists of two doublet peaks, with one doublet peak at 163.2 eV (S $2p_{1/2}$) and 162.0 eV (S $2p_{3/2}$), indicating that the sulphur is chemisorbed on the gold surface.[162] The second doublet peak can be observed at 163.8 eV and 165.0 eV, which is assignable to the S-H bond indicating a small presence of unbound sulphur.

The N 1s spectrum (**Figure 4.7b**) can be deconvoluted into two peaks, which support the presence of the peptide on the surface. The first peak centred at 400.5 eV is attributed to amino (NH_2) and amide (CONH) moieties. The second peak centred at 402.8 eV is ascribed to protonated amino groups.[165] The C 1s spectrum (**Figure 4.7c**) can be deconvoluted into three peaks, which are attributed to five different binding environments. The peak at 285.0 eV is attributed to C-C bonds,[166] while the peak at 286.7 eV corresponds to C 1s of the three binding environments of C-S, C-N and C-O.[166] The third and smaller peak (288.6 eV) is assigned to the C 1s photoelectron of the carbonyl moiety, C=O.[166] The O 1s spectrum (**Figure 4.7d**) is de-convoluted into two different peaks, corresponding to two different binding environments, arising from the C-O (533.3 eV) and C=O (532.0 eV) bonds.[166]

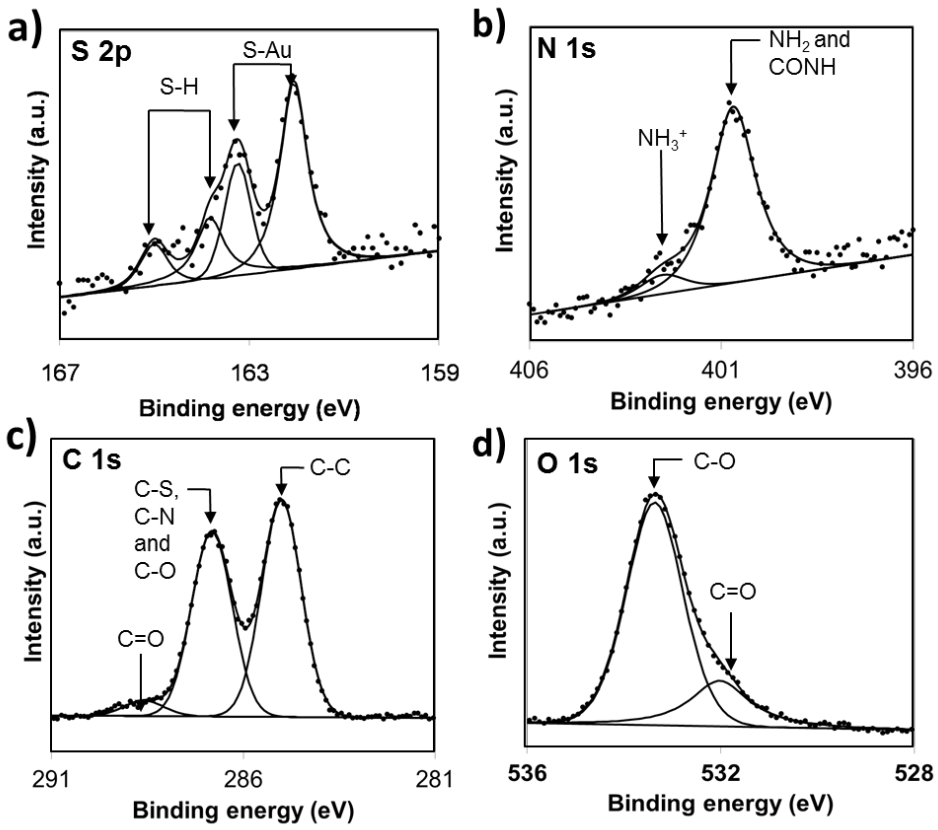

Figure 4.7 *XPS spectra of the a) S 2p, b) N 1s, c) C 1s and d) O 1s peak regions of* ***GRGDS-KKKC:C11TEG*** *mixed SAMs at a 1:40 solution ratio.*

Furthermore, by taking into consideration that the **GRGDS-KKKC** oligopeptide consists of 15 N atoms and 1 S atom and C11TEG has no N and 1 S atom only, the number of **C11TEG** molecules per **GRGDS-KKKC** peptide on the surface was calculated by integrating the area of the S 2p and N 1s peaks. Thus, it was possible to infer that the ratio of **GRGDS-KKKC:C11TEG** on the surface is 1:10 ± 2 using **Equation 3.1**.

In comparison to the **biotin-4KC:C11TEG** mixed SAM (1:8 ± 4), the ratio for the **GRGDS-KKKC:C11TEG** (1:10 ± 2) is very similar and within the error. Thus, the surface ratio for the **GRGDS-KKKC:C11TEG** (1:10 ± 2) is within the error margins

of that obtained for the original **biotin-4KC**:**C3TEG** monolayer (1:16 ± 4),[121] and therefore remains favorable to carry out switching studies. Thus, the mixed monolayer solution ratios being used in this chapter have been chosen on the basis of optimising the switching capacity of the monolayer.

4.3.3 GRGDS-KKKC:C11TEG contact angle and ellipsometry analysis

Analysis by contact angle and ellipsometry also supported the formation of the **GRGDS-KKKC:C11TEG** mixed SAM. **C11TEG** SAMs as mentioned in **Section 3.2.2** has a small hysteresis (θ_{Adv} -θ_{Rec}) value of 4**⁰** indicating a hydrophilic, closely-packed monolayer. The overall contact angle for the pure **GRGDS-KKKC** monolayer is hydrophilic in accordance with previous reports of RGD terminated SAMs.[187] Pure **GRGDS-KKKC** SAMs has a hysteresis contact angle of 8**º** indicating the monolayer is less ordered than the **C11TEG** SAM. However, in the **GRGDS-KKKC:C11TEG** mixed SAM has a hysteresis value of 19**⁰**, which indicates a less ordered and more sparsely packed monolayer, which is understandable due to the presence of the larger RGD headgroup and lysine backbone with charged amine groups.

The ellipsometric thickness of the pure monolayers is less than the theoretical molecular length of the molecules (**Table 4.1**). This discrepancy, between molecular length and SAM thickness, is expected, in agreement with the literature, and it is ascribed to both the tilt angle and density of the SAM surfactants.[30,188] The thickness measurements acquired using ellipsometry for the **GRGDS-KKKC:C11TEG** mixed SAMs was 2.0 ± 0.1 nm which is between the thickness of the pure monolayers of both components. This suggests the successful formation of the **GRGDS-KKKC:C11TEG** mixed SAMs.

Table 4.1 *Contact angle and ellipsometry measurements of Pure **GRGDS-KKKC**, **C11TEG** monolayers and **GRGDS-KKKC:C11TEG** mixed SAMs at a 1:40 solution ratio.*

SAM	Contact Angle (^{0})		Thickness (nm)	
	Adv.	*Rec.*	*Theor.*	*Exp.*
GRGDS-KKKC	21 ± 1	13 ± 3	4.7	2.3 ± 0.1
C11TEG	29 ± 2	25 ± 3	2.6	1.7 ± 0.2
GRGDS-KKKC:C11TEG	40 ± 3	21 ± 0.5	-	2.0 ± 0.1

4.4 Antifouling properties of GRGDS-KKKC:C11TEG mixed SAM

The antifouling properties of the mixed monolayer were examined using SPR by measuring the amount of non-specific binding from two types of complex media onto a mixed SAM of **GRGDS-KKKC:C11TEG**. A high level of non-specific binding would indicate the mixed SAMs have insufficient antifouling properties, which may impede cell adhesion due to adsorption of other proteins from within the cell suspension. The lack of antifouling properties could artificially increase cell adhesion due to the presence of additional motifs.[189] Furthermore, a protein layer could be responsible for differences in cell adhesion behavior,[58,190] which could give false positives. The importance of fabricating a surface with effective antifouling properties

will determine the effectiveness of switching as it is essential to observe a clear difference between the bio-active and bio-inactive states.

Figure 4.8 shows the response of **GRGDS-KKKC:C11TEG** mixed SAM with two complex media solutions: supplemented DMEM (Dulbecco's Modified Eagle Medium, 10% FBS, 24 mM HEPES and 1% pen/strep) and DMEM. Surfaces were incubated in the respective media for 30 minutes then rinsed with PBS for 10 minutes to remove any remaining media on the surface.The incubation of DMEM on the RGD functionalised surface showed low levels of non-specific binding at 46.5 RIU, which correlates well with previous data from **Chapter 3** where minimal non-specific binding was also observed on the **biotin-4KC:C11TEG** monolayer. In the case of the supplemented DMEM non-specific binding significantly increased on the surface giving a response unit of 496 RIU after the final PBS rinse. The increase in non-specific binding primarily due to the presence of high levels of protein from FBS within the supplemented DMEM. The low level of non-specific binding observed for DMEM on **GRGDS-KKKC:C11TEG** mixed SAMs (**Figure 4.8**) provides support for using DMEM as an electrolyte during switching studies. Supplemented DMEM is important in the culturing of cells, however evidence from **Figure 3.13** in **Chapter 3** suggests that during switching experiments, a complex media of only DMEM allows for efficient switching in the region of 67%. Thus during the short duration of switching experiments (1-2 h), it is expected that DMEM would provide sufficient nutrients to support cell adhesion.

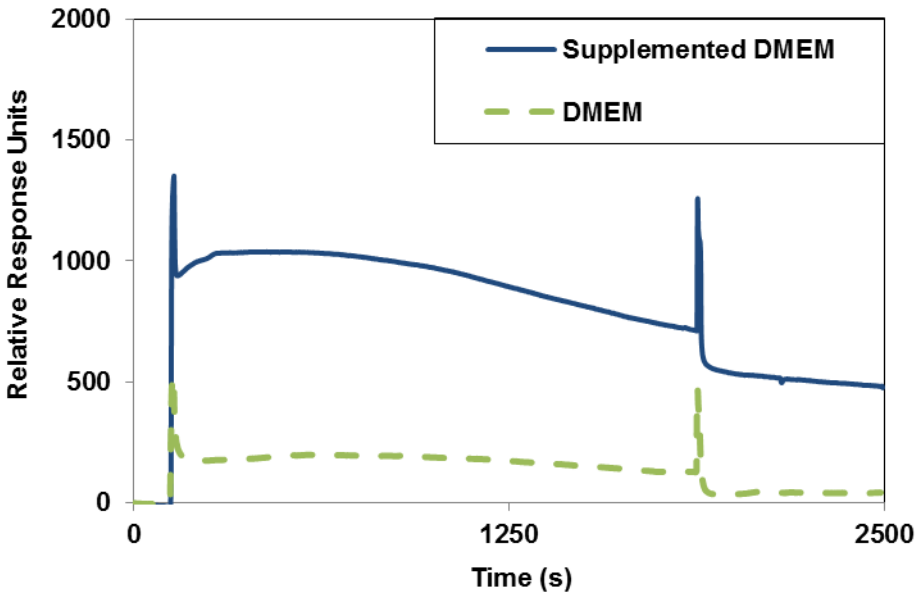

Figure 4.8 *SPR sensograms showing the comparison of non-specific binding of supplemented DMEM and DMEM to an* ***GRGDS-KKKC:C11TEG*** *mixed SAM.*

4.5 Cell adhesion studies

4.5.1 Passaging and preparation of RAW 264.7 macrophages for cell adhesion

The supplemented DMEM used to culture RAW 264.7 cells consisted of a number of components, similar to those mentioned in **Chapter 3**, including DMEM, 10% FBS, 1% penicillin and streptomycin (pen/strep) and 24 mM of HEPES buffer. DMEM, the primary component of most cell cultures, contains all the required essential nutrients for cells to survive in-vitro conditions. FBS contains growth supplements and other proteins**,** with a typical cell culture containing 10% FBS. Pen/strep is added as an antibiotic to help prevent bacterial growth, however excessive amounts can inhibit cell growth thus, 1% pen/strep is commonly used.[191] HEPES buffer is a well-known buffering reagent used to maintain the physiological

pH of medium between pH 7.2 and 7.6 of the culture media even if there are changes in the carbon dioxide concentration.

RAW 264.7 cells are known to adhere to tissue culture plastic through integrin receptors[192] and are extremely sensitive to lipopolysaccharides (LPS) endotoxin[193] from gram-negative bacteria, therefore, only sterile disposable tissue culture ware and solutions, buffers, and media with endotoxin tested distilled deionized water were used. RAW 264.7 macrophage cells were grown in supplemented DMEM for 2-3 days at 37^0C in 5% CO_2 atmosphere, reaching approximately 80% confluency. For experiments, cells were harvested from tissue culture flasks then re-suspended in supplemented DMEM, checked for viability and counted. Finally cells were diluted with supplemented DMEM to yield a solution of 1 x 10^6 cell/mL and adhered to surfaces (See **Chapter 5** for cell culture method).

4.5.2 Cell adhesion on RGD and non-RGD functionalised surfaces

It has been well documented in literature that cells are well known to adhere preferentially to RGD peptides via integrins receptors in cells, due to the cellular recognition properties of RGD.[2,15,18] In order to demonstrate that the RAW 264.7 cell line displays preferential cell adhesion towards RGD peptides, an initial study was carried out by attaching cells to a number of different surfaces with and without RGD. The surfaces used were: bare gold, pure **C11TEG**, **GRGDS-KKKC:C11TEG** mixed SAM and a pure **GRGDS-KKKC** which was used to normalise the cell counts.

Substrates were rinsed with HPLC ethanol after monolayer formation, dried with Argon gas and placed in sterile petri dishes. The Petri dishes containing the

substrates were then taken to a sterile hood and immersed in supplemented DMEM. Finally, a cell suspension of 1 x 10^6 cell/mL was added to the Petri dishes containing the substrates, which were then allowed to incubate for 24 h at 37.5^{0}C and 5% CO_2. Care was taken to ensure all work involving the transfer and incubation of cells was carried out under sterile conditions to prevent contamination. An incubation time of 24 h was selected in order to allow sufficient time for cell attachment and proliferation.

Supplemented DMEM was chosen to culture the RAW 264.7 cells on substrates, in preference to other complex media such as DMEM and DMEM-FBS in order to provide optimal conditions for the formation of focal adhesions and cell proliferation on the surfaces. It is expected that there will be similar levels of non-specific binding from proteins present within the supplemented DMEM in relation to **Figure 4.8**, which is low enough to overlook at this stage as we are primarily concerned with the adhesion of cells. However, the effects of non-specific binding of proteins will be more important to consider when carrying out switching studies.

After 24 h of incubation, substrates with adhered cells were then removed from the supplemented DMEM and rinsed with DMEM to remove loosely adhered cells on the surface. Prior to rinsing, DMEM was warmed to 37.5^{0}C to prevent accidental cell death due to sudden changes in culture medium and temperature**.**[58] Thereafter, substrates were mounted on microscope slides and observed via an optical microscope to determine if preferential cell adhesion to surfaces functionalised with RGD peptide could be observed. Surfaces were prepared in triplicates and images were taken at a 20x magnification at 5 random spots on each substrate. Cell counts shown in **Figure 4.9**, were normalised to a pure **GRGDS-**

KKKC monolayer in order to make the cell densities of different surfaces comparable.

Figure 4.9 clearly indicates that cells adhere preferentially to RGD functionalised SAMs. In the case of **GRGDS-KKKC:C11TEG** mixed SAMs at a solution ratio of 1:40 the number of cells that adhere was only 15% less than the pure RGD surface. A 15% decrease in cell adhesion in the mixed SAM is consistent with the presence of ethylene glycol molecules, causing a reduction in the number of RGD binding sites on the surface. In both the mixed SAM and pure RGD SAM numerous cases of cell proliferation can be observed as labelled in **Figure 4.9**. However, in the case of bare gold and pure **C11TEG** surfaces there were fewer adherent cells and cell proliferation was rare, which can be attributed to the lack of cell-specific binding sites. Cell adhesion was lowest in the pure **C11TEG** monolayer with 60% less cells when compared to the pure **GRGDS-KKKC** monolayer. This was in agreement with previously reported behavior of cells in response to EG-based monolayers[58,194-197] and indicates that the **C11TEG** monolayer decreases overall cell adhesion. The bare gold surface had 50% less adherent cells compared to the pure **GRGDS-KKKC** monolayer. These results agree with previous reports[190] and confirm that cells are able to adhere to bare gold due to the secretion of proteins which form part of the extra-cellular matrix (ECM).

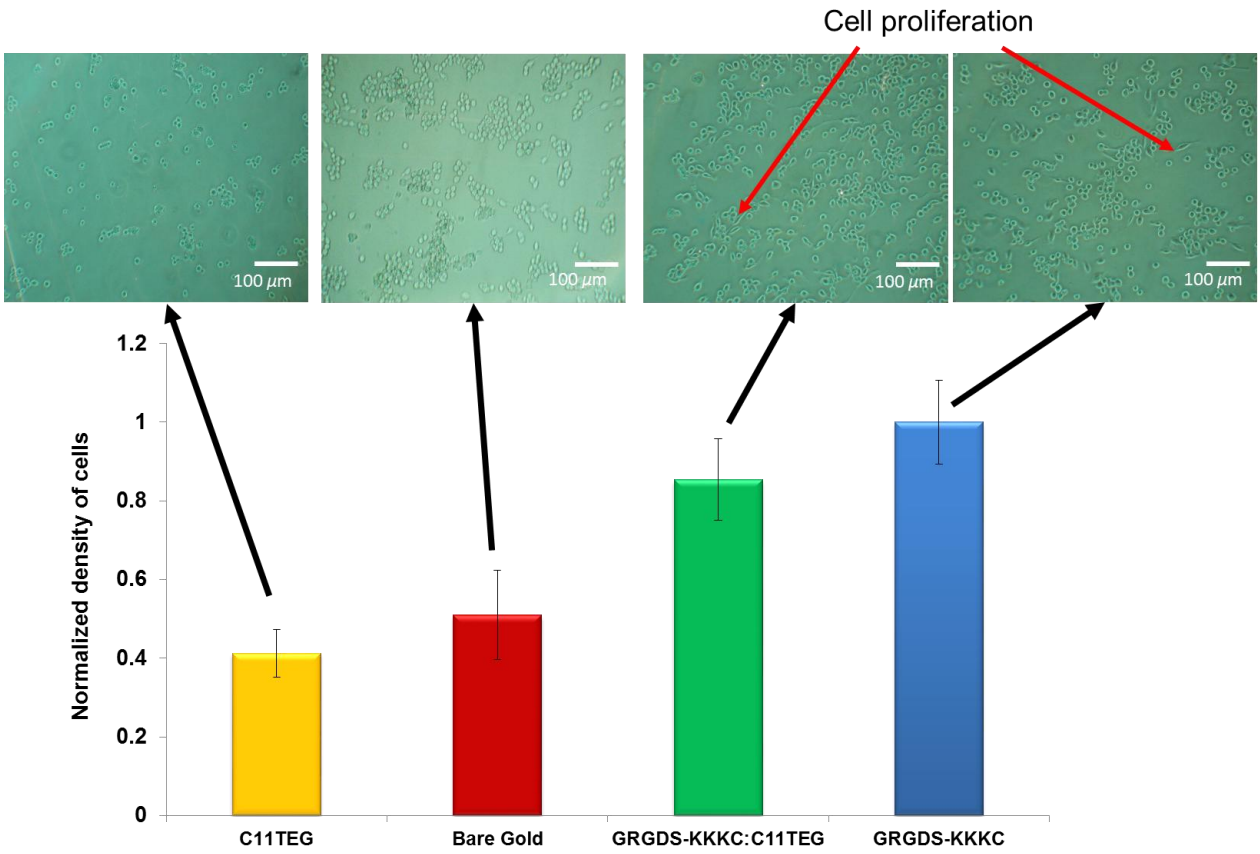

Figure 4.9 *Normalized density of cells for 24 h cell adhesion on pure* ***C11TEG*** *SAMs, bare gold,* ***GRGDS-KKKC:C11TEG*** *mixed SAMs and pure* ***GRGDS-KKKC*** *SAMs. The density was normalized against the density of cells adherent onto pure* ***GRGDS-KKKC*** *SAMs.*

The cell counts observed on the two RGD functionalised monolayers provides sufficient evidence to suggest that the **GRGDS-KKKC** peptide was present and had an active role in promoting cell adhesion on the surface. Thus, we can conclude that increased cell adhesion occurred due to cellular recognition of the monolayers containing RGD peptides. The difference in cell counts observed in the mixed SAMs compared to the pure **GRGDS-KKKC** peptide monolayer shows a >95 % confidence

level using a t-test. This indicates that the amount of cell adhesion on the mixed SAMs shows a significant difference compared to the pure **GRGDS-KKKC** monolayer which can be attributed to the presence of **C11TEG** in the mixed SAMs.

It should be noted that the relative surface ratio of **GRGDS-KKKC** to **C11TEG** will contribute to the inter-distance spacing of RGD cell binding sites thus, directly impacting cell adhesion. It has been shown that RGD ligand-ligand inter-distance is an essential part of cell adhesion.[198] From the cell count data in **Figure 4.9** we can deduce that the high cell counts observed in the two RGD functionalised SAMs (pure **GRGDS-KKKC** and **GRGDS-KKKC:C11TEG**) are due to the RGD ligands being sparsely packed providing sufficient spacing for integrin receptors to access the RGD binding sites. If however the pure **GRGDS-KKKC** SAM had been a very densely packed monolayer, this would have hindered the ability of cells to bind via the integrin receptors and a low overall cell count would have been observed.[199]

4.6 Cell adhesion kinetic studies

A kinetic time study was carried out in order to better understand the optimum incubation time of the **GRGDS-KKKC:C11TEG** monolayers and the length of time required for cell spreading. **GRGDS-KKKC:C11TEG** functionalised substrates were immersed in supplemented DMEM (**Figure 4.10**) followed by 1 x 10^6cells for 45 min, 3 h, 6 h, 12 h, 24 h, 48 h.

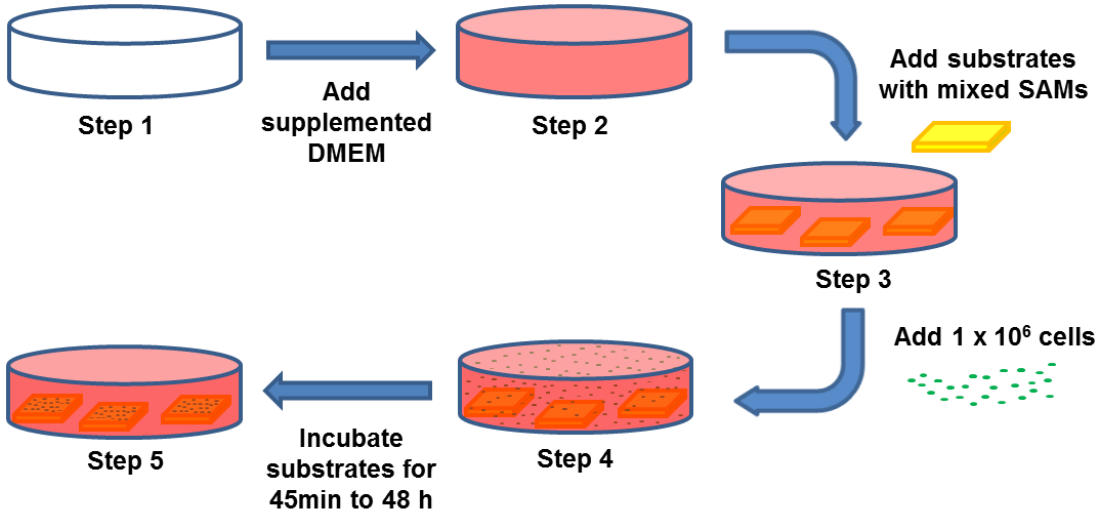

Figure 4.10 *Schematics showing the method of incubating functionalised substrates in cells.*

The results obtained from the cell adhesion time study shown in **Figure 4.11** indicates a clear trend of increased cell adhesion from 45 min to 24 h. Cell adhesion peaks at 24 h of incubation with an average of 1615 ± 51 cells/mm^2. Thereafter the number of adhered cells decreases to 795 ± 75 cells/mm^2 after 48 h of incubation. From this data we can deduce that the optimal incubation time to gain the highest cell adhesion at 1 x 10^6 cells is 24 h. It has been commonly reported that 24 h is the amount of time required for cell spreading to take place. After 24 h the supplemented DMEM requires replacement due to cells utilizing the contents of the DMEM. Hence it is assumed that due to the lack of fresh DMEM, a significant drop in cell adhesion is observed at 48 h. It is important to note here that the differences in the overall number of cells throughout this work can be attributed to batch to batch variations. In order to make reliable conclusions, the necessary controls for each set of experiments were all done in the same day with the same batch of cells.

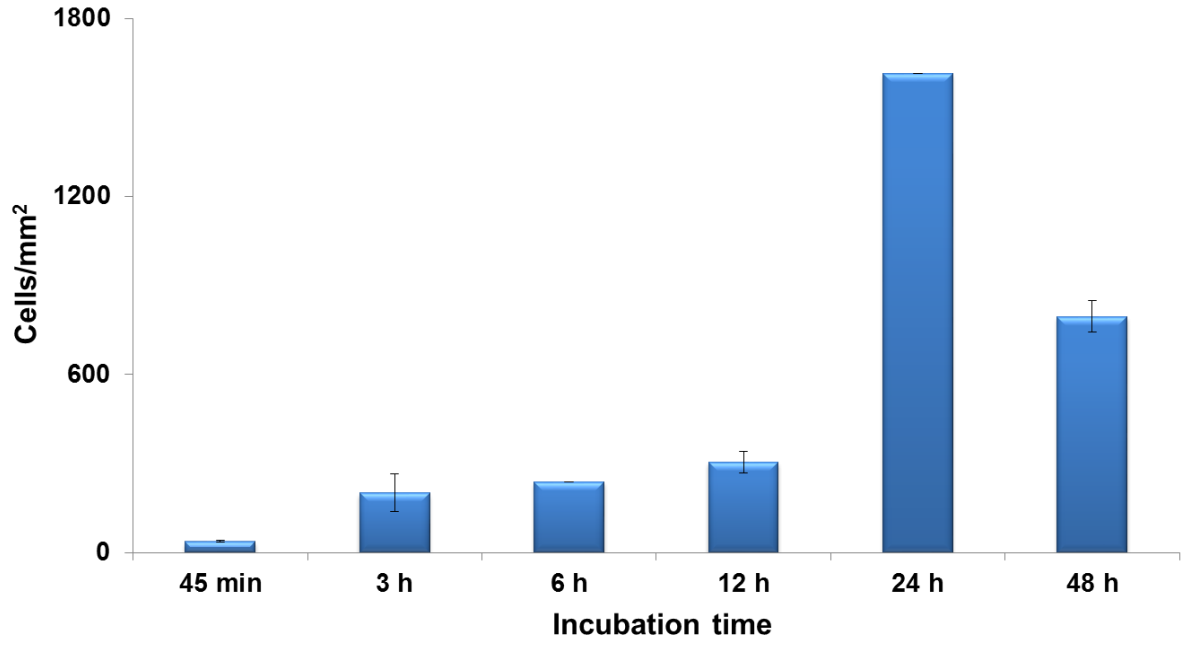

Figure 4.11 *Cell density based on a kinetic study of cell adhesion times between 45 minto 48 h on* ***GRGDS-KKKC:C11TEG*** *functionalised substrates at 1:40 ratio.*

4.7 Switching studies of GRGDS-KKKC:C11TEG mixed SAMs after 24 h cell adhesion time

In order to investigate the switching properties of the **GRGDS-KKKC:C11TEG** mixed SAM, cells were adhered to **GRGDS-KKKC:C11TEG** mixed SAMs (1:40 solution ratio) in DMEM at a -0.4 V negative potential and OC conditions. The electrolyte selected for the switching experiments was DMEM, based on previous results in **Chapter 3** which resulted in high switching efficiency and low non-specific binding via SPR (**Figure 4.8**). Firstly, cells were adhered to functionalised **GRGDS-KKKC:C11TEG** substrates over a 24 h incubation in supplemented DMEM. The substrates with adhered cells were then exposed to a surface potential of -0.4 V for

30 min. Thereafter, surfaces were rinsed with PBS to remove any unattached cells. Cell binding activity, as a result of switching induced by electrical potential, was observed by an optical microscope.

High cell counts were observed under OC conditions as expected with an average cell count of 1753 ± 49 cells/mm^2 (**Figure 4.12**). In the case of an -0.4 V applied negative potential, the cell count remained high at 1764 ± 102 cells/mm^2. The high cell counts observed for both OC conditions and -0.4 V indicate that after substrates have been incubated for 24 h, cells cannot be detached by means of switching with a negative potential. The lack of cell detachment after an applied negative potential can be explained by one of two reasons: 1) the **GRGDS-KKKC** peptides are unable to switch due to the cells secreting proteins that inhibit the switching or 2) the binding of the adhered cells cannot be disrupted once they are attached due to the strength of multiple RGD ligands and integrin receptor interactions mediating cell adhesion.[200] Other factors that could be causing the lack of cell detachment maybe due to the proteins within the supplemented DMEM that may have deposited over the 24 h period, in effect nullifying the antifouling properties of the surface.

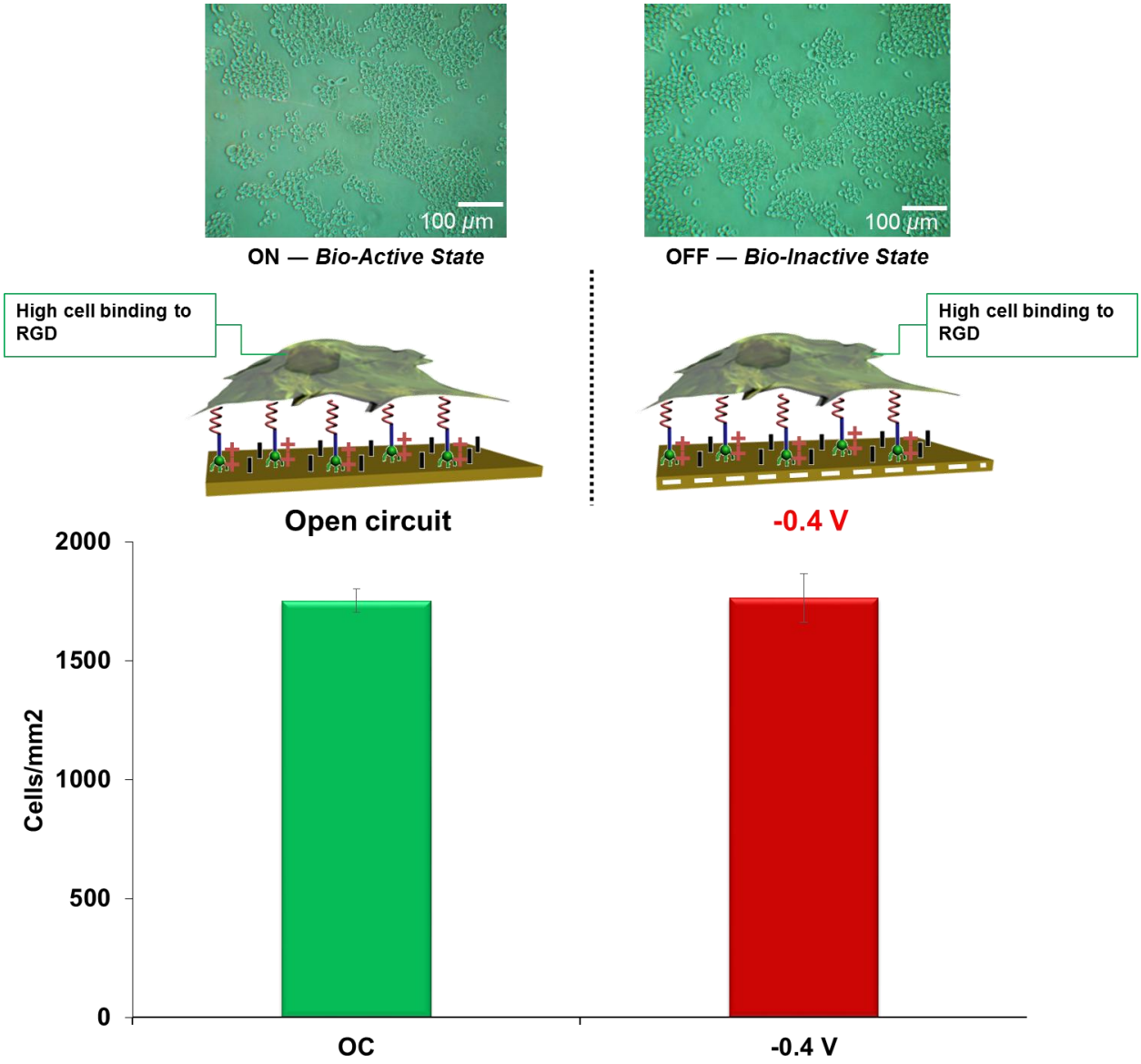

Figure 4.12 *Cell densities of* ***GRGDS-KKKC:C11TEG*** *mixed SAMs under OC conditions and -0.4 V after 24 h incubation in cells.*

It has been well documented that cells secrete proteins as part of the ECM on surfaces.[201,202] Thus, the possibility of cells not detaching from the surface due to an electric potential appears very likely. These results are not surprising as there has until now been no reports of any switchable surfaces that can detach cells once they have been adhered. All literature of switchable surfaces working with cells have only

reported switching from concealed to exposed systems or antifouling to fouling states. Although Liu *et al.*[106] fabricated a photochemically switchable SAMs which appears reversible. However, this system is ultimately an off-on system and cannot use switching as a mechanism for cell detachment. Instead Liu *et al.* relied on the use of a soluble RGD peptide solution to remove cells from the surface. Furthermore, Ng *et al.* also reported a similar lack of cell detachment after adhesion had taken place using an electrical potential as a stimulus.[123]

4.7.1 Testing mechanical detachment of cells and re-adhesion on substrates

The purpose of this study was to test the re-usability of the mixed SAMs. Cells were adhered onto a **GRGDS-KKKC:C11TEG** monolayer after a 24 h incubation. The adhered cells were then removed by forcefully rinsing with UHQ water. The substrates were then sterilized with 70% HPLC Ethanol. Finally the substrate was re-immersed in a new batch of cells and incubated again for a 24 h period in order to promote cell adhesion for a second time. The results shown in **Figure 4.13** illustrate that after cells have been removed by rinsing with 70% Ethanol and UHQ water, cell adherence for a second time on the same RGD functionalised substrate is reduced almost 80%. This indicates that it is not possible to re-use functionalised substrates with a **GRGDS-KKKC:C11TEG** monolayer. Thus, once cells have been removed from the substrate surface this renders the surface void of repeated usage for cell adhesion. This can be explained by considering that the cells secrete proteins as part of the ECM formed on a surface.[201,202] Removal of the cells does not necessitate the removal of secreted proteins, which are non-specifically bound to the surface, hence the remaining protein residues maybe an obstacle to repeated cell adhesion.

In addition it can be assumed that due to the nature of cell interactions the quality of the monolayer may have been compromised, further hindering repeated attempts of cell adhesion on the same surface.

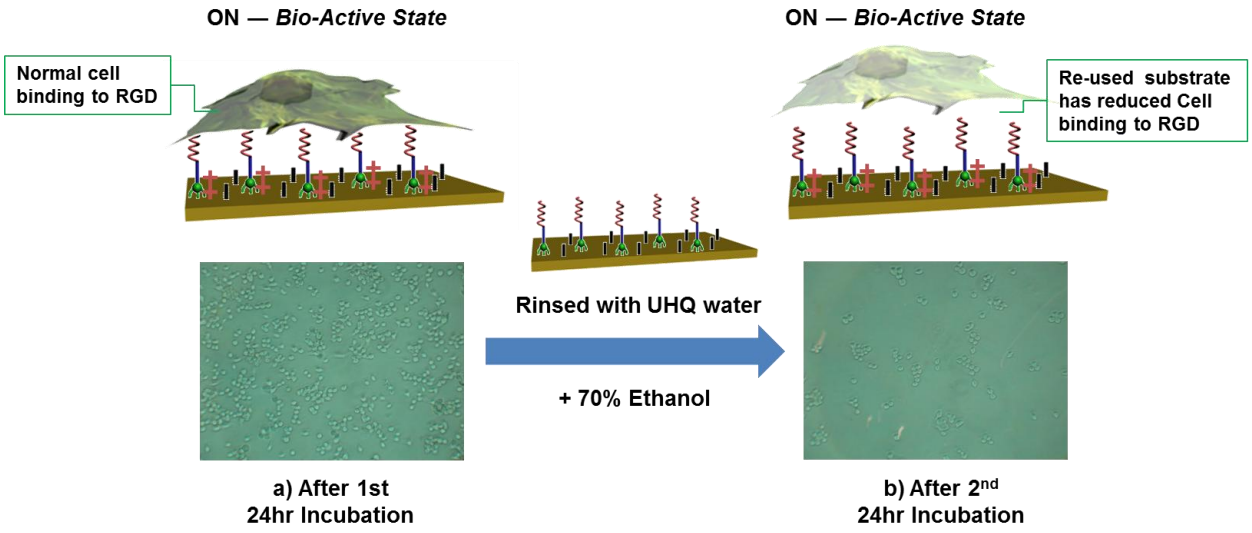

Figure 4.13 *a)* ***GRGDS-KKKC:C11TEG*** *functionalised substrate after a 24 h incubation in cells showing normal cell adhesion and b) after removal then re-adhesion of cells to the surface.*

4.8 GRGDS-KKKC:C11TEG cell adhesion and ratio optimisation study for 1 h incubation

After confirming the unfeasibility of cell detachment from mixed SAMs via the application of a negative potential after a 24 h incubation, an alternative method for controlled cell adhesion was investigated. The chosen route to achieve a viable switchable surface, from the “ON” state (OC conditions) to the “OFF” state (-0.4 V potential), was to reduce the incubation time to 1 h. By reducing the incubation time

to 1 h, cells would still have sufficient time to attach on the surface in the cell adhesive “ON” state which would then be compared to a substrate in the cell resistant “OFF” state. A lower cell count from the substrate in the “OFF” state would indicate that successful switching has occurred with additional control surfaces. Thus, 1 h is a more suitable incubation time in testing the ability of the **GRGDS-KKKC:C11TEG** mixed SAMs to control cell adhesion via an applied negative potential (**See section 4.9**).

Prior to carrying out switching studies under a 1 h incubation period, a ratio study was carried out with the **GRGDS-KKKC:C11TEG** mixed SAM in order to compare the number of cells attached on a 1:10, 1:20 and 1:40 ratio. A pure **GRGDS-KKKC** substrate was used to normalise the cell densities. As mentioned in previous literature,[203] ratios of RGD ligand to ethylene glycol groups have a significant impact on the number of cells that attach on a surface. The results in **Figure 4.9** showed that a pure RGD monolayer gives the highest cell count on a surface. Hence the primary aim for carrying out this ratio study was to understand how ratios between pure RGD and 1:40 mixed SAMs would affect cell attachment.

Surfaces for each mixed SAM ratio were prepared in triplicates and incubated for 1 h in RAW 264.7 cells. The substrates were then rinsed with DMEM and placed under a microscope to observe the number of attached cells. Images were taken at a 20x magnification at 5 random spots on each substrate. Cell counts shown in **Figure 4.14**, were normalised to a pure **GRGDS-KKKC** monolayer in order to make the cell counts between surfaces easily comparable.

Figure 4.14 shows that the pure **GRGDS-KKKC** monolayer has the highest cell density, which is in agreement with results from **Figure 4.9**. Interestingly a clear

trend of increased cell counts appears from the 1:10 to the 1:40 ratio. In comparison to the pure RGD monolayer, the 1:40 ratio had a reduced cell count of 32%, whereas the 1:10 and 1:20 ratio had a 60% and 54% reduction in cell count respectively. The lower cell counts on the 1:10 and 1:20 surfaces can be attributed to the increased number of RGD ligands which form a more ordered monolayer in the presence of ethylene glycol molecules. As a result a more ordered mixed monolayer could reduce the spacing between RGD ligands which, negatively impacts the ability of cell integrins to bind to the specific RGD binding sites thus, a lower cell count is observed for the 1:10 and 1:20 ratios. In the case of the 1:40 mixed SAM, the RGD ligands are fewer in number and can be said to be more sparsely packed, which is in agreement with the contact angle data, thus allowing for more integrin receptors to access the RGD binding sites. This data further reinforces the need to take into consideration RGD ligand spacing and solution ratio in order to ensure optimal cell adhesion.[198]

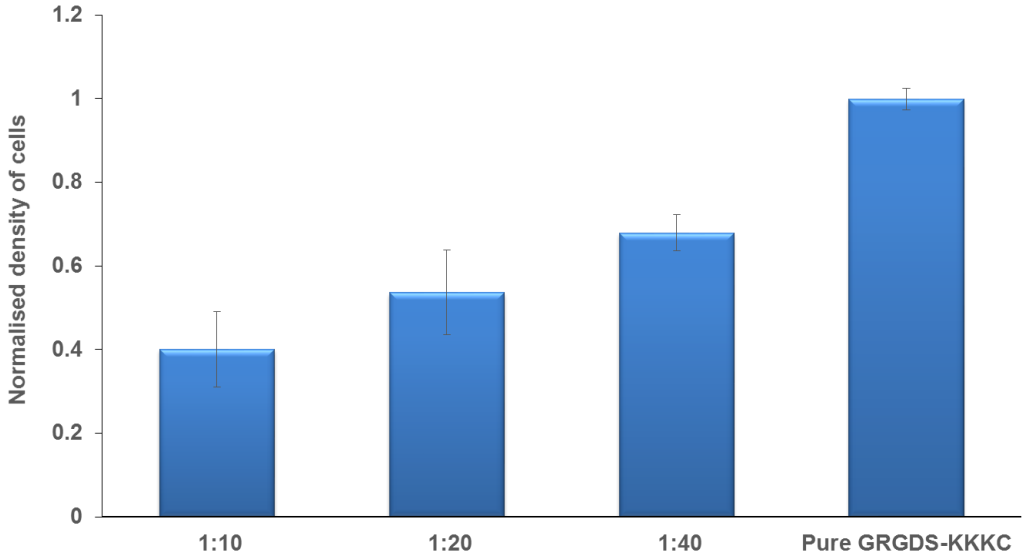

Figure 4.14 *Normalised cell densities of* ***GRGDS-KKKC:C11TEG*** *mixed SAMs at solution ratios of 1:10, 1:20, 1:40 and pure* ***GRGDS-KKKC***

4.9 Effects of electrical potential on GRGDS-KKKC:C11TEG mixed SAMs and cells after 1 h cell adhesion time

In order to demonstrate that the **GRGDS-KKKC:C11TEG** mixed SAMs can support or resist cell adhesion on demand, the macrophage cells were cultured on the **GRGDS-KKKC:C11TEG** mixed SAM in DMEM medium under OC conditions and applied negative (-0.4 V) potential for a period of 1 h. In contrast to the procedure carried out in **section 4.7** cells were not pre-adhered to the **GRGDS-KKKC:C11TEG** monolayer. By reducing the incubation time to 1 h, cells were still given sufficient time to attach to the surface in the “ON” state under OC conditions. In the “OFF” state a negative potential (-0.4 V) was applied on the surface in order to switch the **GRGDS-KKKC** peptide in real time during the 1 h cell incubation. Incubation of substrates under a -0.4 V potential (OFF state) would indicate if the RGD peptide could be switched and therefore prevent cell adhesion. Switching experiments were carried out by pre-conditioning SAM functionalised substrates with a negative potential of -0.4 V for 10 min under a DMEM electrolyte, chosen for its high switching efficiency and low non-specific binding. The -0.4 V potential was then continued for 1 h with the addition of cells (**Figure 4.15**). A similar procedure was carried out for OC conditions without electrical potential.

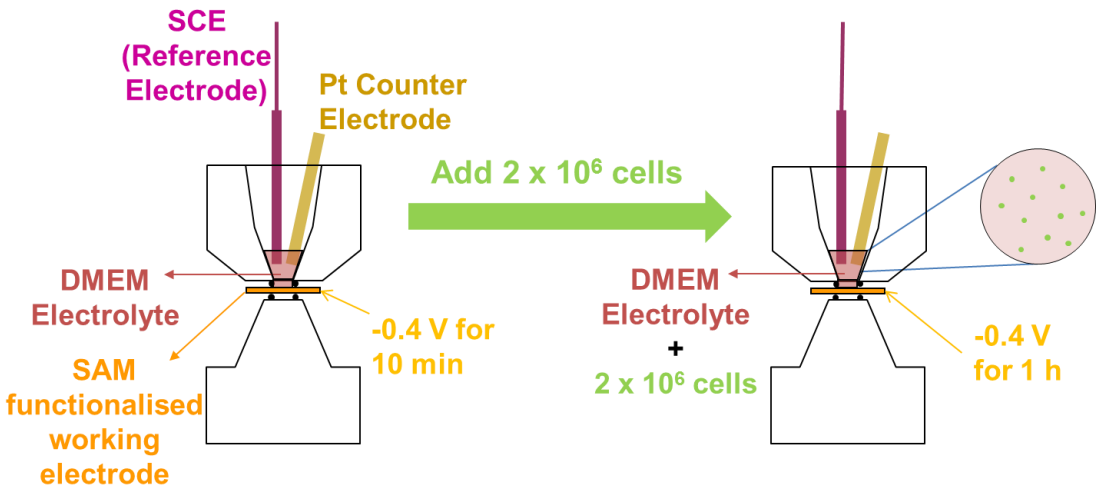

Figure 4.15 *Schematic of experimental setup for incubating cells during 1 h switching.*

Focusing firstly on **GRGDS-KKKC:C11TEG** functionalised substrates under OC conditions where the RGD head group remained exposed allowing for cell adhesion. The number of adhered cells was 1421 ± 103 cells/mm^2 as shown in **Figure 4.16a**. In contrast when surfaces were poised at -0.4 V, such that RGD ligands were concealed, the number of adhered cells decreased significantly to 432 ± 102 cells^2 (**Figure 4.16b**), which equates to a switching efficiency of 70%. Although the incubation time of cells on substrates was reduced to 1 h, due to the higher density of cells per substrate in the Teflon cell (2 x 10^6 cells) it was possible to induce sufficient cell binding to clearly distinguish between the "ON" and "OFF" states. These findings implied that conformational changes occurred at the gold surface, and that the cells sensed the presence or the absence of the RGD moieties to the extent that cell adhesion can be reduced to 70% of its bioactive state (**Figure 4.17**).

In the bio-inactive state the RGD headgroup remained concealed from adherent cells thus, exposing the anti-fouling properties of the **C11TEG** present within the mixed SAM. Furthermore, the **C11TEG** masks the RGD headgroup rendering the surface cell resistant and unavailable for cell attachment. As a result, the majority of cells were unable to adhere during the 1 h incubation period. The remaining cells on the surface were either adhered via non-specific interactions or specific interactions through RGD ligands which were unable to switch due to unequal spatial distribution possible due to island formation.[51] Island formation is a known phenomenon in mixed SAMs and can occur due to the presence of clusters of peptide binding sites.

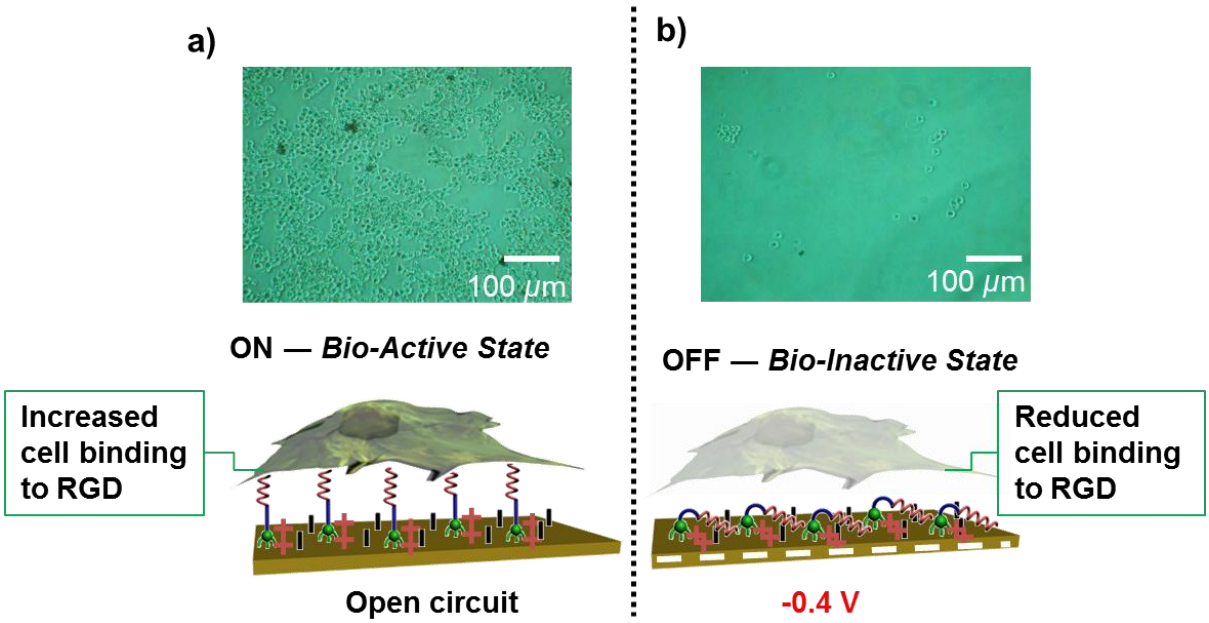

Figure 4.16 *Schematic of the **GRGDS-KKKC:C11TEG** mixed SAMs during a) cell adhesive "ON" state under OC conditions and b) cell resistant "OFF" state under -0.4 negative potential.*

It is important to also consider the effects of an electrical potential on cell viability, as they are living organisms and may be affected by such stimuli. Thus, one of the factors that may be causing the removal of cells is the influence of electrical potential directly on the cells. Previous researchers such as Ng *et al.* and Mrksich *et al.* showed that it was perfectly safe to apply potentials between ±300 mV and ±500 mV without affecting the cells.[39,40,109,204]

In order to verify that the changes in adhesion upon application of a negative surface potential occur due to changes in the conformational orientation of the RGD instead of cell repulsion or cell damage due to the presence of an electrical potential, control mixed SAMs were also prepared using **C11TEG** and a peptide where the 3 lysine residues as the switching unit were replaced by 6 non-switchable ethylene glycol units – **GRGDS-HEGC**. **Figure 4.17** demonstrates that cells adhered in similar numbers to the **C11TEG** and **GRGDS-HEGC:C11TEG** mixed SAMs under OC conditions and an applied negative potential. These results provide strong evidence that control over cell adhesion using the **GRGDS-KKKC:C11TEG** mixed SAM is due to a conformational behaviour of the lysine-containing oligopeptide that can either expose or conceal the RGD moiety.

The overall low cell counts observed for the **C11TEG** SAM under OC conditions and a negatively applied potential (**Figure 4.17**) indicate that **C11TEG** has good anti-fouling properties and the applied potential does not affect cell adhesion. In the case of the **GRGDS-HEGC:C11TEG** mixed SAM cell counts were between 20-30% less than the **GRGDS-KKKC:C11TEG** mixed SAMs under OC conditions. XPS data for the **GRGDS-HEGC:C11TEG** showed that a solution ratio of 1:40 translated to a 1:6 ± 1 ratio on the surface (see **Appendix II**), which is less than the

1:10 ± 2 surface ratio observed for the **GRGDS-KKKC:C11TEG** mixed SAMs. The lower ratio observed in **GRGDS-HEGC:C11TEG** suggests an increase in RGD ligand density which may provide insufficient spacing for cells to bind efficiently to integrins in the cell membrane.[198]

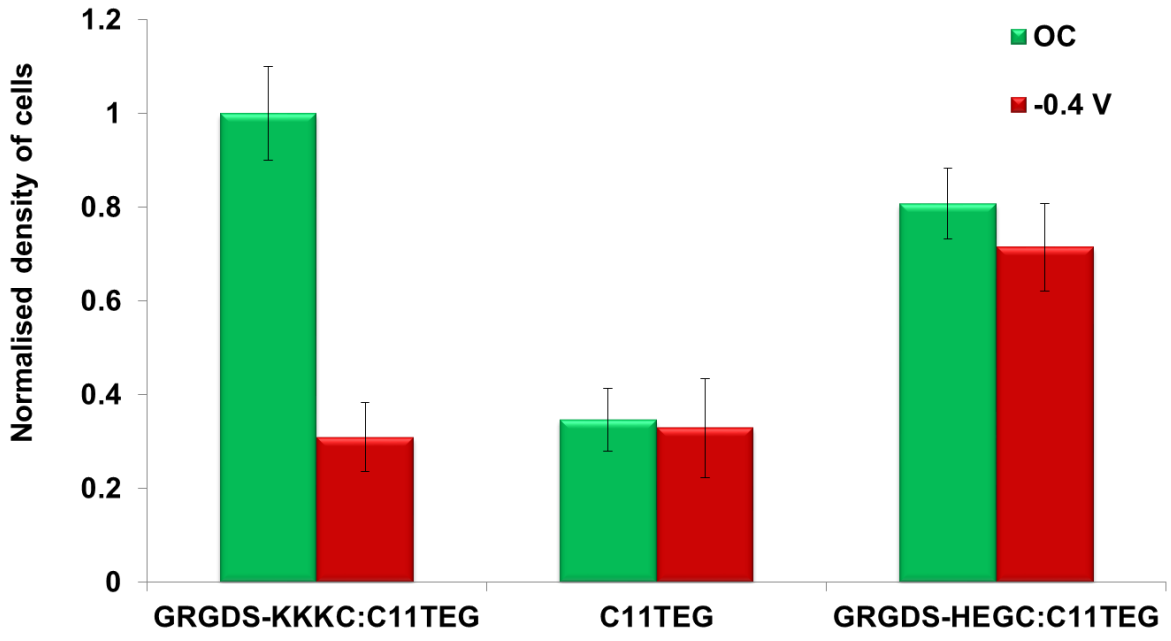

Figure 4.17 *Density of adhered cells on **GRGDS-KKKC:C11TEG** mixed SAMs, pure **C11TEG** and **GRGDS-HEGC:C11TEG** mixed SAMs that were incubated with cells for 1 h under OC conditions and -0.4 V applied potential.*

Previous studies have shown that small conformational and orientational changes in proteins and peptides modulate the availability and potency of the active sites for cell surface receptors.[205-207] Thus, in a similar manner, small changes in the conformation/orientation of the RGD peptide on the surface induced by application of an electrical potential are able to affect the binding activity of the peptide. Based on

previous theoretical and experimental studies aimed at understanding the switching mechanism of these electrically switchable oligopeptide surfaces,[118,122] it can be assumed that when a negative potential is applied to the surface, the oligopeptide chain adopts a collapsed conformation on the surface and the RGD binding motif is partially embedded on the **C11TEG** matrix, thus showing no bioactivity ("OFF" state).

In order to determine the percentage of cells that were viable after switching in this system, trypan blue solution, which is commonly used to detect cell viability, was used on cells attached to the substrates after a 1 h applied potential. Uptake of the trypan blue would indicate cells were dead, and a lack of uptake of the blue dye would indicate cells were still alive (**Figure 4.18**). Results suggested that cell viability was above 98%, which indicates that the application of a negative potential did not affect cell viability.

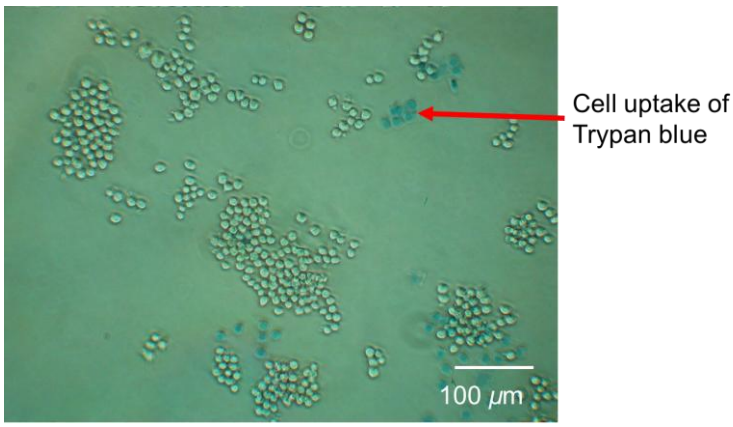

Figure 4.18 *Image of cells adhered to a RGD functionalised surface after an application of a -0.4 V negative potential. Uptake up Trypan blue indicates cell death as shown by the arrows.*

4.10 Reversible switching studies of GRGDS-KKKC:C11TEG mixed SAMs

The question of whether the **GRGDS-KKKC:C11TEG** surfaces could be switched between different cell adhesive states (cell-resistant and cell-adhesive states) was then addressed. To begin with, we investigated the switching from a cell-adhesive state to a cell-resistant state, and the possibility to detach the cells from the substrate upon the application of a negative potential. Cells were incubated in the **GRGDS-KKKC:C11TEG** mixed SAMs for 1 h under OC conditions, thereby exposing the RGD moiety and allowing for cell attachment. This step was followed by the application of a potential of -0.4 V for 1 h in order to detach the cells from the surface, by concealing the RGD moieties.

Cell counts showed no significant differences between the OC and OC to -0.4 V samples (**Figure 4.19 OC green bar and OC to -0.4 V red bar**) suggesting that the electrostatic force generated by the applied negative electrical potential might not be sufficient to disrupt the RGD-integrin interactions. Thus, indicating that after cells adhere to the **GRGDS-KKKC:C11TEG** mixed SAMs after a 1 h incubation under OC conditions, cells cannot be detached from the substrate. These results were to a certain extent expected since adherent cells are able to withstand strong detachment forces due to the adhesion being mediated by multiple RGD-integrin bonds in parallel.[200] The reference substrate in which a -0.4 V potential was applied (**Figure 4.19 OC blue bar**) still showed a reasonable switching efficiency and displayed 60% reduction in cell adhesion compared to the OC and OC to -0.4 V substrates.

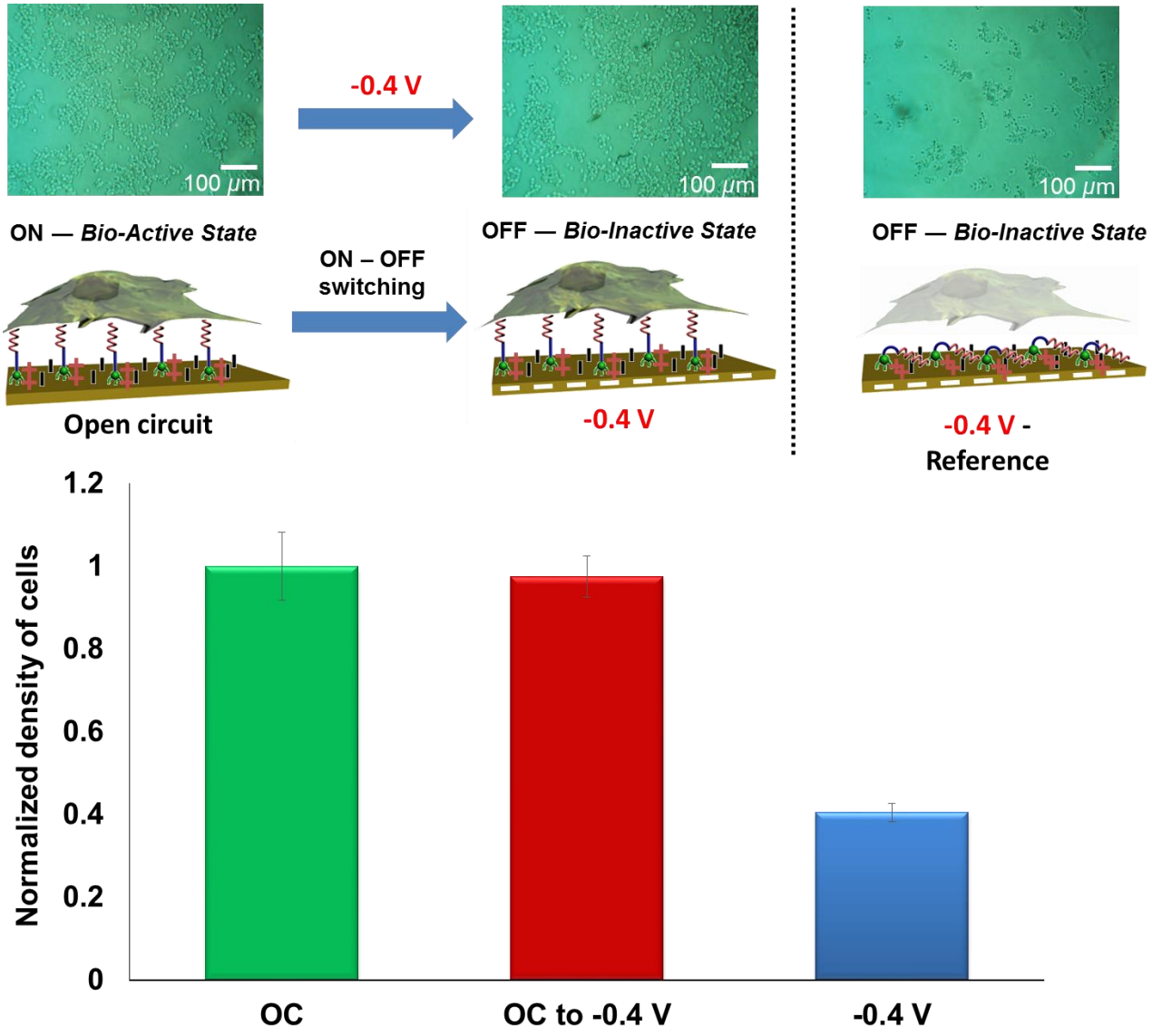

Figure 4.19 *Microscopic images and density of adhered cells on* ***GRGDS-KKKC:C11TEG*** *mixed SAMs that were incubated with cells for 1 hour under OC conditions and subsequently under an applied -0.4 V potential for 1 hour. The density was normalized against the density of cells adherent onto* ***GRGDS-KKKC:C11TEG*** *mixed SAMs that were incubated with cells in OC conditions for 1 hour.*

In contrast, a reversal of the switching sequence demonstrated that the surfaces can be dynamically switched from a non-adhesive to cell-adhesive state

(**Figure 4.20**). Cells were incubated in the **GRGDS-KKKC:C11TEG** mixed SAMs for 1 h while holding the potential at –0.4 V for 1 h making the RGD peptide inaccessible for recognition by the corresponding integrin. The number of adherent cells when a negative potential of –0.4 V was applied was 70% lower (**Figure 4.20 -0.4 V blue bar**) than that adhered to the **GRGDS-KKKC:C11TEG** mixed SAMs under OC condition (**Figure 4.20 OC green bar**). By then shifting to open circuit conditions for 1 h, a dramatic increase of 67% in adherent cells was observed as a result of the exposure of the RGD moiety to the cells (**Figure 4.20 -0.4 V to OC red bar**). These values were similar to those obtained for the samples that were only incubated for 1 hour under OC conditions (**Figure 4.20 OC green bar**), indicating that the surfaces were highly effective at switching from a non-adhesive to cell-adhesive state.

In order to gauge the effectiveness of the **GRGDS-KKKC:C11TEG** mixed SAM switchable system it is important to compare it with other switchable surfaces. The electrically switchable oligopeptide surface developed by Yeung *et al.* displayed a switching efficiency of *ca.* 90% in the OFF state, where the binding site was concealed, in comparison to the ON binding state. This high switching efficiency can be attributed to the fact PBS was used as the electrolyte for switching and proteins were used as opposed to cells used in this system.[121] The photoswitchable surfaces developed by Kessler *et al.* exhibited *ca.* 50% switching efficiency between the fouling and antifouling states.[107] This system outperforms Kessler's photoswitchable system which may be due to the lack of antifouling component. Building on from Kessler's system, Liu *et al.* introduced an antifouling component into their switchable system to which was also controlled by different wavelengths of light. Liu's system significantly increased the switching efficiency reaching 90%. However, Liu's system does not take into consideration the effects of media culture and uses a system that

relies on prolonged periods of irradiation of light. Hence, it can be argued this system still has a high switching efficiency and switching experiments can be carried out with observable results within a significantly shorter period of time.

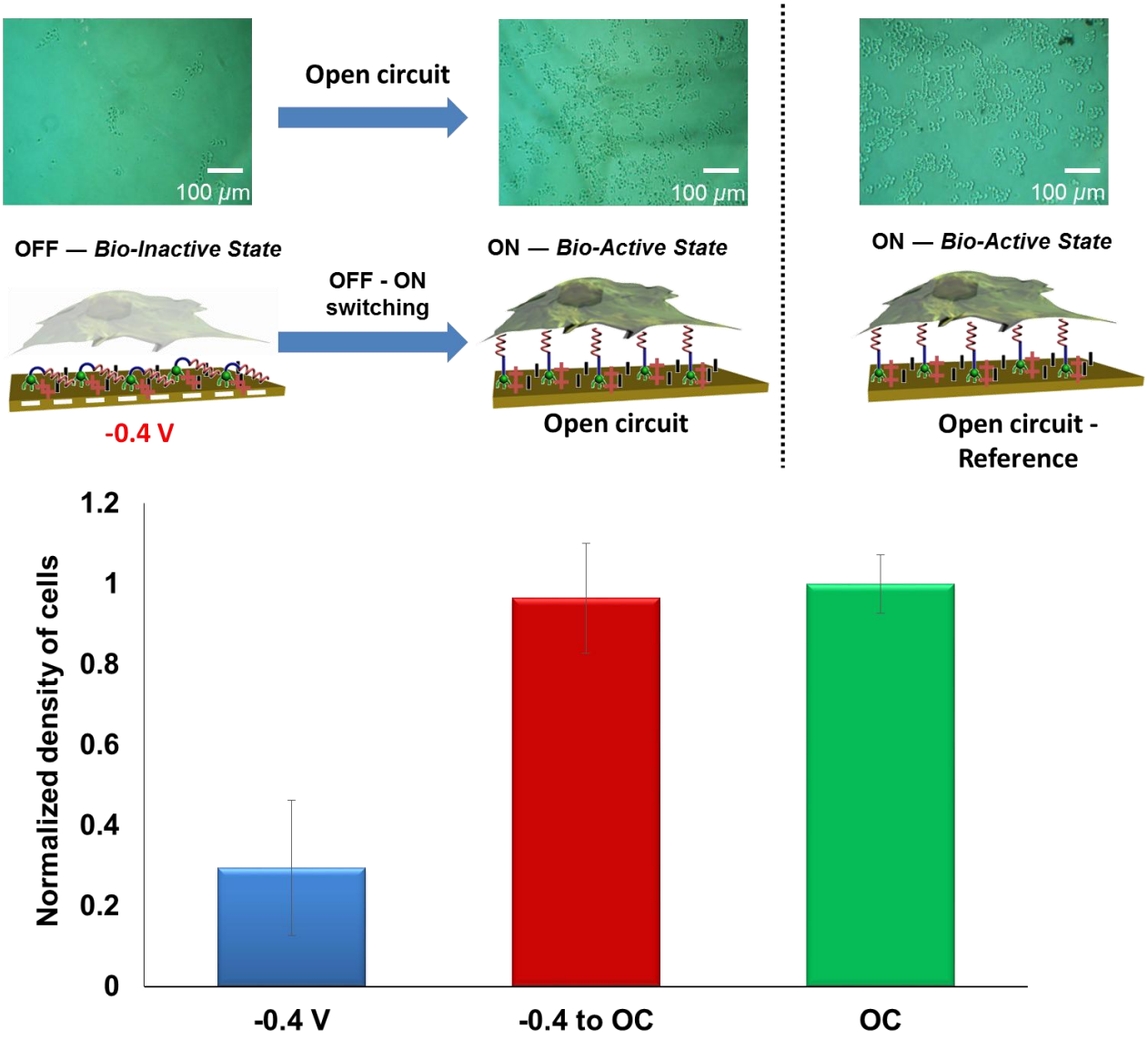

Figure 4.20 *Microscopic images and density of adhered cells on* ***GRGDS-3KC:C11TEG*** *mixed SAMs that were incubated with cells for 1 hour while applying -0.4 and subsequently in OC conditions for 1 hour. The density was normalized against the density of cells adherent onto* ***GRGDS-3KC:C11TEG*** *mixed SAMs that were incubated with cells in OC conditions for 1 hour.*

Ng *et al.* were able to control cell adhesion via an electrical potential resulting in switching efficiencies of 85%.[123] The charged groups on the distal moeity of the sulphonate and ammonium SAMs used as the switching mechanism introduces the possibility that these charged groups will interfere with cellular interactions which depend on for example cationic interactions.[192] The system used in this current study significantly reduces the risk of interference of nonspecific cellular interactions with charged groups in a SAM by instead utlilising a charged backbone as the switching mechanism rather than a distal moiety. The backbone is masked by the **C11TEG** antifouling component at all times further reducing the risk of non-specific cell adhesion. In addition the **GRGDS-KKKC:C11TEG** system retains the benefits of using **C11TEG** as an antifouling component to reduce nonspecific binding, while maintaining a high switching efficiency of 70%, which is more than sufficient to distinguish between the antifouling and fouling states.

4.11 Conclusion

In summary, we have successfully fabricated a switchable surface capable of both a cell adhesive and cell resistant state, which prevents cell adhesion under an applied -0.4 V potential due to the exposure of the antifouling components of the mixed SAMs masking the RGD binding moiety. Further switching studies were carried out to test the ability of the surface to change between cell adhesive and cell resistant states. It was shown that when going from a cell adhesive state to a cell resistant state, cells cannot be removed once adhered due to the strength of multiple integrin receptors binding to numerous RGD ligands. However, experiments carried out testing a cell resistant to cell adhesive state showed that cells are still able to adhere

to the surface as the RGD moiety is exposed and thus, allows for controlled cell adhesion. Ratio studies of the **GRGDS-KKKC:C11TEG** mixed SAMs also provided important insight into the effects of ratio on cell adhesion and that the ratio of any RGD functionalised surface must take into consideration the inter-distance of RGD ligands which if too sparsely packed or too densely packed may hinder optimal cell adhesion. This study will no doubt be useful in developing more realistic dynamic extracellular matrix models and is certainly applicable in a wide variety of biological and medical applications.

Chapter 5: Experimental Procedures and Protocols

Abstract: *This chapter describes the materials, methods and different experimental techniques used during the work carried out for this projects. Experimental protocols and data analysis by various types of equipment have also been described.*

5.1 Materials and Methods

5.1.1 Gold substrates

Polycrystalline gold substrates were purchased from George Albert PVD, Germany and consisted of a 50 nm gold layer deposited onto glass covered with a thin layer (5 nm) of chromium as the adhesion layer. Polycrystalline gold substrates employed in SPR were purchased from Reichert Technologies, USA, consisted of 49 nm gold with 1 nm chromium.

5.1.2 Chemicals and Materials

Commercially available chemicals and solvents were purchased from Aldrich Chemicals and Fisher Chemicals and were used as received. The oligopeptide **biotin-4KC**, **GRGDS-KKKC:C11TEG** and **GRGDS-HEGC:C11TEG** were synthetised by Peptide Protein Research Ltd. (Wickham, UK) to > 95% purity and verified by HPLC and mass spectrometry. The (3-mercaptopropyl)tri(ethylene glycol) (**C3TEG**) was prepared as previously described.[121] The (11-mercaptoundecyl)tri(ethylene glycol) (**C11TEG**), (11-mercaptoundecyl)hexa(ethylene glycol) (**C11HEG**), Fetal Bovine Serum (FBS) and 4-(2-hydroxyethyl)-1-

piperazineethanesulfonic acid (HEPES) buffer (1 M) were purchased from Sigma Aldrich and used as received (**Figure 5.1**). Neutravidin and DMEM were obtained from Invitrogen Life Technologies. Phosphate buffered saline (PBS) solution was prepared from a 10× concentrate PBS solution (1.37 M sodium chloride, 0.027 M potassium chloride, and 0.119 M phosphate buffer) from Fisher BioReagents. DMEM-FBS contains DMEM with 10% (v/v) FBS. DMEM-FBS-HEPES contains 10% FBS and 24 mM HEPES. Polycrystalline gold substrates were purchased from George Albert PVD, Germany and consisted either of a 50 nm gold layer deposited onto glass covered with a thin layer of chromium as the adhesion layer (used for contact angle and XPS analysis) or 100 nm gold layer on 100-4 inch-silicon wafer, precoated with titanium as the adhesion layer (for ellipsometry analysis). SPR gold chips were purchased from Reichert Technologies, US.

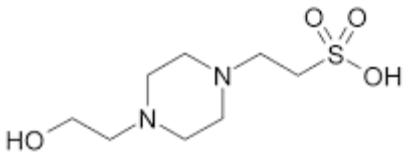

Figure 5.1 *Structure of HEPES buffer*

5.2 Experimental procedures

5.2.1 Preparation of Mixed Self-Assembled Monolayers (SAMs)

The gold substrates were cleaned by immersion in piranha solution (3:1, H_2SO_4 :30% H_2O_2) at room temperature for 10 min, rinsing with Ultra High Pure (UHP) H_2O and then HPLC grade EtOH thoroughly for 1 min. (*Caution: Piranha*

solution reacts violently with all organic compounds and should be handled with care). For the preparation of the pure biotin-4KC SAMs, the clean gold substrates were immersed for 24 h in ethanolic 0.1 mM solution of biotin-4KC containing 3% (v/v) $N(CH_2CH_3)_3$. For the preparation of the biotin-4KC:C3TEG, biotin-4KC:C11TEG, biotin-4KC:C11HEG, GRGDS-3KC:C11TEG or GRGDS-HEGC:C11TEG mixed SAMs, solutions of the oligopeptide (0.1 mM) and either C3TEG or C11TEG or C11HEG (0.1 mM) were prepared in HPLC EtOH containing 3% (v/v) $N(CH_2CH_3)_3$, and mixed at the volume ratio of 1:40. Subsequently, the clean gold substrates were immersed in the mixed solutions for 24 h to form the mixed SAMs on the gold surfaces. The substrates were rinsed with HPLC EtOH, an ethanolic solution containing 10% (v/v) CH_3COOH, and UHP H_2O. Note that the mixed SAMs were deposited in the presence of $N(CH_2CH_3)_3$ to prevent the formation of hydrogen bonds between the NH_2 functional groups of the bound thiolate peptide on gold and that of free thiol peptide in the bulk solution.[208] The pure C3TEG or C11TEG SAMs were prepared by immersing the clean gold substrates in ethanolic 0.1 mM solution of the respective ethylene glycol thiols for 24 h, followed by rinsing with HPLC EtOH. After 24 h of immersion in either mixed SAMs or pure SAM that gold substrate was dried

5.2.2 X-ray Photoelectron Spectroscopy (XPS)

The gold substrates approximately 0.5 cm by 0.5 cm were prepared as mentioned in **Section 5.2.1**. Thereafter, the substrates were rinsed further using HPLC grade ethanol and finally dried under argon gas. The substrates were then stored in a petry dish sealed with parafilm under an argon gas atmosphere prior to

XPS analysis. The gold substrates were adhered to a plate with carbon tape prior to insertion into the XPS. XPS spectra were obtained on the VG Escalab 250 instrument based at University of Leeds EPSRC Nanoscience and Nanotechnology Facility, UK. XPS experiments were carried out using a monochromatic Al K α X-ray source (1486.7 eV) and a take-off angle of 15°. High-resolution scans of N 1s and S 2p were recorded using a pass energy of 150 eV at a step size of 0.05 eV. Fitting of XPS peaks was performed using the Avantage V 2.2 processing software. Sensitivity factors used in this study were: S 2p, 2.08; N 1s, 1.73; C 1s, 1.00; O 1s 2.8; Au 4f 7/2, 9.58 and Au 4f 5/2, 7.54. The averages and standard errors reported were determined from at least four different XPS measurements.

5.2.3 Elipsometry

The thickness of the deposited monolayers was determined by spectroscopic ellipsometry using gold on silicon substrates with a gold thickness of 50 nm. A Jobin-Yvon UVISEL ellipsometer with a xenon light source was used for the measurements. The angle of incidence was fixed at 70^0. A wavelength range of 280–820 nm was used. The DeltaPsi software was employed to determine the thickness values and the calculations were based on a three-phase ambient/SAM/Au model, in which the SAM was assumed to be isotropic and assigned a refractive index of 1.50. The thickness reported is the average of six measurements, with the errors reported as standard deviation.

5.2.4 Contact Angle

Gold-glass substrates were prepared with a glass cutter approximately 1 cm by 1 cm. A black marker pen was used to mark the side of the gold substrate facing the camera in order to better determine the surface from the water droplet. Contact angles were determined using a home-built contact angle apparatus, equipped with a charged coupled device (CCD) KP-M1E/K camera (Hitachi) that was attached to a personal computer for video capture. The dynamic contact angles were recorded as a micro-syringe was used to quasi-statically add liquid to or remove liquid from the drop. The drop was shown as a live video image on the PC screen and the acquisition rate was 4 frames per second. FTA Video Analysis software v1.96 (First Ten Angstroms) was used for the analysis of the contact angle of a droplet of UHP H_2O at the three-phase intersection. The averages and standard errors of contact angles were determined from five different measurements made for each type of SAM.

5.2.5 Surface Plasmon Resonance (SPR)

SPR switching experiments were performed with a Reichert SR7000DC Dual Channel Spectrometer (Buffalo, NY, USA) at 25 °C using a three-electrode electrochemical cell (**Figure 5.2**) and a Gamry PCI4/G300 potentiostat. The SAMs prepared on Reichert gold sensor chips served as the working electrode, the counter electrode was a Pt wire, and a standard calomel electrode (SCE) was used as the reference electrode. Prior to the binding studies, the sensor chips were equilibrated by flowing degassed PBS at 50 µl/min, followed by application of – 0.4 V or open circuit conditions for 10 min while passing degassed PBS through the

electrochemical cell at a flow rate of 50 µl/min. While still applying a potential, neutravidin (500 µL, 54.4 µg/mL) or neutravidin with DMEM, DMEM-FBS or DMEM-FBS-HEPES were injected over the sensor chip surface for 10 sec at 1500 µl/min and then 30 min at 8 µl/min (the decrease in flow rate from 1500 to 8 µl/minto ensure that sufficient exposure time was provided for binding to occur between the biotin on the surface and neutravidin in solution). In order to remove any unbound material, the sensor chips were washed with degassed PBS for 10 sec at a flow rate of 1500 µl/min, followed by 10 min at a flow rate of 50 µl/min while still applying a potential to the chips. The same procedure was used for OC experiments without applying a potential.

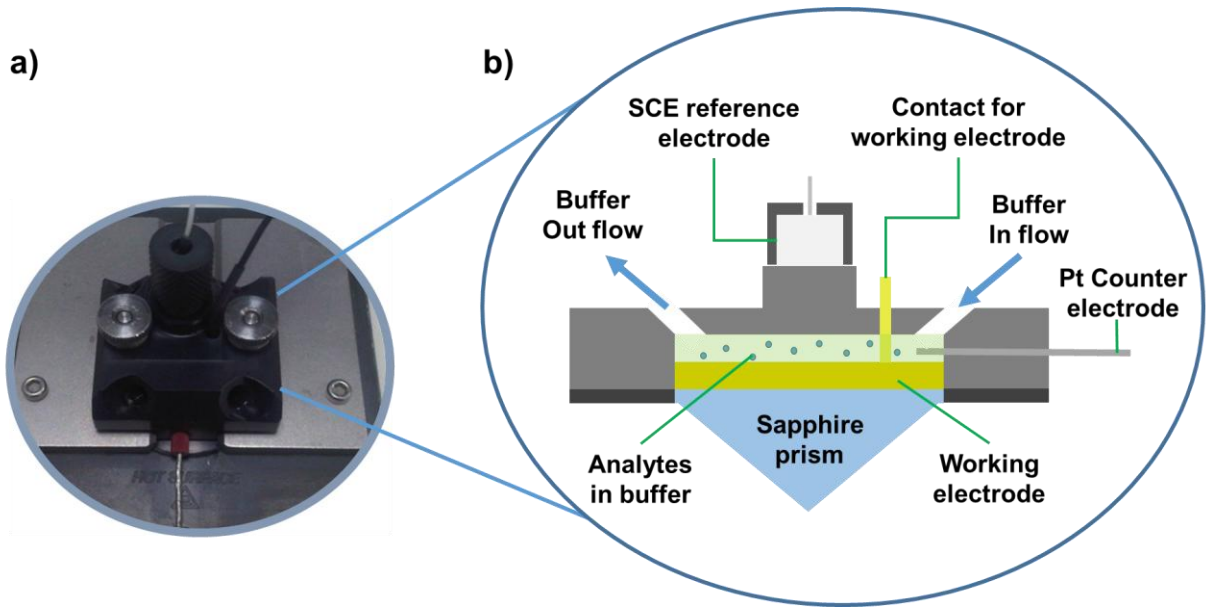

Figure 5.2 *Shows the experimental setup for a) an image of the electrochemical SPR using a Reichert custom designed electrochemical cell and b) a diagram showing a side view of the electrochemical SPR cell during experiments.*

5.2.6 Force field test

Since the conformational switching of biotin-4KC chains mainly results from the rotation of the C-C bonds, the energy scan for biotin-4KC molecule with different C1-C2-C3-C4 dihedrals (**Figure 5.3**) was carried out by both force field methods and density functional theory (DFT) calculations with the B3LYP functional and 6-31G(d) basis set. Three kinds of force fields, cvff, compass and pcff were tested. The result is shown in **Figure 5.3**. The cvff force field shows the best performance. Although it overestimates the energies compared to the DFT result, it displays the right shape of the energy curve. In contrast, both compass and pcff force fields result in a significant deviation from the DFT result. So the cvff force field was adopted throughout our simulations.

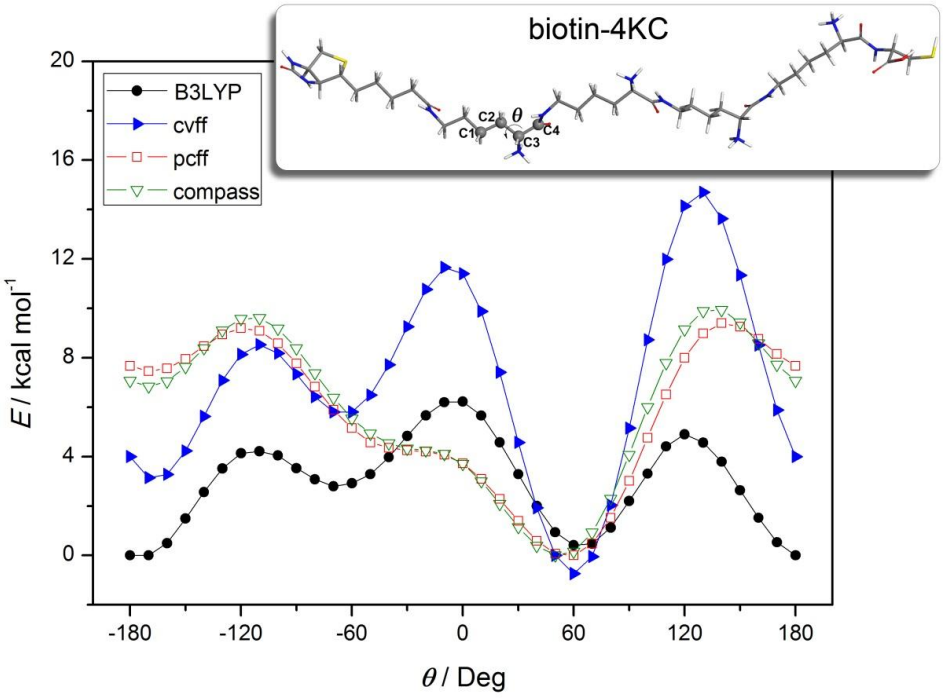

Figure 5.3 *The energy scanning for biotin-4KC molecule with different C1-C2-C3-C4 dihedrals, obtained by both force field methods and DFT calculations.*

Table 5.1 *Parameters for the surface models used in the simulations.*

Surface chains	Solvent molecules (H_2O)	Ions (Cl^-)	Cell parameters ($Å^3$)
Biotin-4KC/15(TEGT)	2115	4	34.60 × 34.60 × 77.42
Biotin-4KC/15(HEGT)	1974	4	34.60 × 34.60 × 77.42
9(Biotin-4KC)	1982	36	34.60 × 34.60 × 77.42

5.2.7 Computational details

Five layers of gold atoms cut from the Au(111) surface were adopted to model the gold substrates used in the experiment and they were fixed during the simulations. All MD simulations were performed in the canonical (NVT) ensemble using the cvff force field. The temperature was set to 298 K by using the Andersen thermostat.[3] The equations of the motion were integrated using the velocity Verlet algorithm[4] with the time step of 1fs. The atomic charges for the biotin-*4*KC molecules were updated every 100ps by DFT calculations, at the M06-2X/6-31G(d,p) level of theory. The Discover module in the Materials Studio package[5] was employed to run all the MD simulations. All DFT calculations were carried out with the Gaussian 09 program package.[6]

5.2.8 Cell culture

Cryovials of RAW 264.7 macrophage cells (ATCC# TIB-71) were taken out from the liquid nitrogen following standard operating procedure for liquid nitrogen. After thawing for 3 minutes in a water bath at 37^{o}C, the cell suspension was then transferred from the cryovial to a 50mL centrifuge tube with 10 mL of supplemented DMEM (10% FBS, 1% penicillin/streptomycin and 24 mM HEPES buffer) and centrifuged twice at 1500 rpm for 5 minutes at a time. The cell pellet was re-suspended in 10 mL of fresh supplemented DMEM and transferred into a Corning tissue culture flask. Cells were cultured at 37^{0}C, 5% CO_2 and in humidified atmosphere. When cells reached approximately 80% confluency (**Figure 5.4**), they were ready to be sub-cultured.

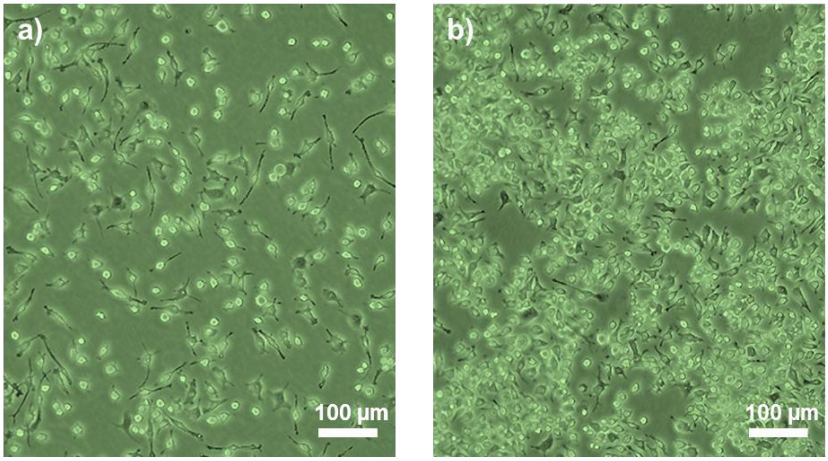

Figure 5.4 *Optical images of RAW 264.7 cells showing a) low density and b) high density.*

The procedure to sub-culture cells required some of the used medium to be aspirated using a cell culture vacuum pump and some medium to remain in the culture flask (approximately 2 mL). The cells were dislodged from the flask with a cell scraper and aspirated using a pipette. Appropriate aliquots of the cell suspension were added to new tissue culture flasks and cells were sub-cultured with 5 mL of new supplemented DMEM for every ~1 x 10^6 cell/mL. The cell culture medium was replaced every 2 to 3 days or until cells reached 80% confluency. All cell sub-culturing procedures were carried out inside a sterile laminar flow hood to minimise any possible contamination from exposure to the atmosphere.

5.2.9 Counting cells using a haemocytometer

Cells were dislodged from tissue culture flasks using a cell scraper after reaching 80% confluency as mentioned in section **5.2.8**. Cells were then transferred to a 50 mL centrifuge tube and suspended in sufficient supplemented DMEM. The cell suspension was mixed by gentle agitation of the tube in order to ensure cells were distributed evenly in the suspension. A 20 µL aliquot of the cell suspension was then pipetted into a vial and mixed with an additional 60 µL of trypan blue to check cell viability. Uptake of the trypan blue dye indicates cells are nonviable (dead) and non-uptake of the blue dye indicates cells are viable (alive).

The cells were then counted using a haemocytometer, which was first cleaned using 70% ethanol and dried using tissue. The shoulders of the haemocytometer were slightly moistened to affix the coverslip with gentle pressure. A 20 µL sample of the cell suspension and trypan blue mixture was pipetted into either side of the coverslip on the haemocytometer. The haemocytometer was then placed on a

microscope stage and the grid lines of the haemocytometer were brought into focus using an inverted microscope at a 10x magnification. The four sets of 16 corner squares were counted using a manual cell counter (**Figure 5.5**). Only live cells that looked healthy (unstained by trypan blue) were counted. Cells were counted within the square and any position on the right hand or bottom boundary line. Dead cells which were stained blue were counted separately for viability counts. The haemocytometer is designed so that the number of cells in one set of 16 corner squares is equivalent to the number of cells x 10^4/mL. To convert this cell count into cells/mL, the total cell count from four sets of 16 corner squares was:

1. Divided by 4 to get an average cell count for each set of 16 corner squares.
2. Then multiplied by 4 to adjust for the 1:4 dilution in trypan blue.
3. Multiplied by 10^4/mL to give number of cells/mL.

Finally, the initial cell suspension in the 50 mL centrifuge tube was diluted with supplemented DMEM yielding a solution of 1 x 10^6 cells/mL.

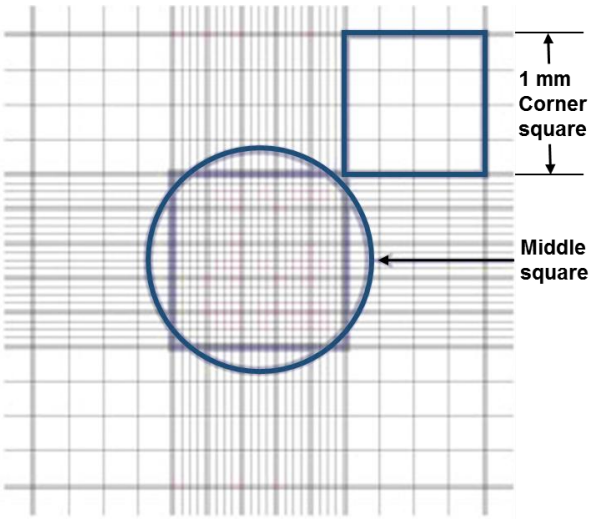

Figure 5.5 *Standard haemocytometer chamber used for counting cells.*

5.2.10 Cell adhesion on different SAMs

Gold substrates were prepared using a glass cutter to approximately 1 cm by 1 cm. The pure C11TEG and GRGDS-3KC:C11TEG mixed SAMs and bare gold substrates were prepared in triplicates and placed in sterile Petri dishes. The substrates were then immersed in 4 mL of supplemented DMEM using a pipette. An aliquot with 1 mL of RAW 264.7 cell suspension at 1 x 10^6 cells/mL was then added to the Petri dishes to give a final cell suspension of 2 x 10^5 cells/mL in each Petri dish. The substrates were incubated for 24 h at 37^0C in 5% CO_2 to allow time for cell adhesion. Substrates were then rinsed in DMEM (warmed to 37^0C) to ensure loosely bound cells were removed. Substrates were then mounted on a microscope slide and the cells were counted using an optical microscope (**see Section 5.2.12**).

5.2.11 Cell switching studies

Electrical potentials were applied to the SAM functionalised gold substrates using a Gamry PCI4/G300 potentostat with a custom designed Teflon cell, equipped with the functionalised gold substrate as the working electrode, a Pt wire as the counter electrode and a SCE as the reference electrode as shown in **Figure 4.15**. For the bio-inactive state (cell resistant state), an electrical potential of -0.4 V was applied for 10 min on the gold substrate in 4 mL of DMEM, followed by adding a RAW 264.7 cell suspension of 2 x 10^6 cells/mL, whilst maintaining the -0.4 V potential for a further 1 h. The substrates were then placed in a petry dish and immersed in DMEM warmed to 37^0C to gently rinse loosely bound cells were removed. Thereafter, cell viability was checked under a microscope to ensure an applied potential of -0.4 V was not causing cell death. A drop (~0.1 mL) of trypan blue was pipetted onto the surface of

the substrate that had undergone switching and was left for 1-2 minutes. The substrate was then rinsed again by immersing in a petri dish with DMEM to remove the trypan blue from the surface in preparation for cell counting under a microscope. For the bioactive state (cell adhesive state), the same procedure was used but under OC conditions with no applied potential.

5.2.12 Counting cells on gold substrates

Gold substrates that had cells adhered for 24 h or had undergone switching experiments were taken out of the petri dish containing DMEM using tweasers and attached to a microscope slide using a double sided adhesive. The microscope slide with the gold substrate was then placed on the microscope stand and cells were visualised with an optical microscope (Zeiss SM-LUX) using 20x objective lens. It was essential for the gold substrates to remain moist after being removed from DMEM in order for cells to be observed clearly using the microscope. Images were collected with a Canon Powershot G5 monochrome camera. Cell numbers were quantified using cell counts on the remaining cells per field of view at 5 random locations on each substrate. A microscope scale bar was used to measure the area of each image in μm^2 which was then converted to cells/mm^2.

Chapter 6: Conclusion and Future Work

6.1 Conclusion

The work carried out in this thesis provides new insights into the switchablility of surfaces under complex biological conditions. **Chapter 3** focused on the optimisation of mixed SAMs to prevent nonspecific adsorption, which were still capable of displaying high switching efficiencies. It was shown that the combination of electro-switchable oligopeptide SAMs with ethylene glycols (EG_3) of an appropriate length, high levels of switching efficiency can be achieved under complex biological conditions, utilising the biotin-neutravidin interactions. A shorter chain ethylene glycol molecule (C3TEG) was shown to be ineffective at preventing nonspecific adsorption. SPR sensorgrams provided evidence to confirm that longer EG chains (EG_6) are advantageous in preventing nonspecific binding, however they can be detrimental to specific protein binding due to interference and shielding of the binding sites. These results were confirmed using theoretical models via molecular dynamic simulations, thus proving that the EG_6 chain does not allow neutravidin to bind to biotin due to the biotin being partially concealed in the EG_6 matrix.

Dilution studies provided further information about the switching efficiency of the oligopeptide mixed SAMs. At highly concentrated media solutions of DMEM-FBS-HEPES, DMEM-FBS, DMEM only, FBS only and HEPES only, switching efficiency was shown to be much lower reaching between 15-45%. However, dilutions down to 1% of the original media solutions can increase the switching efficiency up to 70%. The presence of FBS and HEPES appeared to cause a partial inhibition in switching. FBS has high protein content and hence displayed high nonspecific binding to surfaces, which was understood to be the primary reason for

the occurrence of compromised switching. Similarly it was shown that HEPES buffer also affects the switching, which may be due to its strong sulfonic acid and weak base that can form hydrogen bonds with proteins.

In **Chapter 4** the discussion was based around controlling macrophage cell adhesion under complex media. The knowledge gained from **Chapter 3** was used to design and fabricate electrically switchable RGD terminated mixed SAMs in order to adhere and repel cells via an electrical stimulus. After characterising the surfaces, initial studies were carried out to ensure cells were adhering preferably to the RGD functionalised surfaces as opposed to nonspecific adhesion to non-RGD functionalised surfaces. The results indicated that cells were capable of recognising surfaces functionalised with RGD. Thereafter, switching studies were carried out by applying a -0.4 V potential to cell adhered surfaces, in order to determine the possibility of detaching cells via switching. However, it was shown that the cell integrin receptor interactions were such that it was not possible to detach cells from a suface after an incubation period of 24 h.

Subsequently, the experimental setup was re-designed with the aim of testing switching under an incubation time of 1 h. Under OC conditions the RGD group was exposed for cell adhesion, resulting in high cell counts, thus generating a cell adhesive surface. Alternatively, by applying a negative potential to the surface the positively charged lysine chains were attracted to the surface thus partially concealing the RGD. As a result the cell count was significantly reduced and an overall switching efficiency of 70% was achieved, indicative of an effective cell resistant surface. The system was also shown to change between cell resistant and cell adhesive states allowing for a significant degree of control over cell adhesion.

6.2 Future work

The next step of this project would be to further optimise switching conditions by varying concentrations of culture media and fine-tuning the applied potentials on the surface. For example switching capacity of the **GRGDS-3KC:C11TEG** mixed SAMs could be investigated under 1-100% dilutions of different medium to find out if switching efficiency can be improved from the current 70%. In addition, tweaking the the potentials applied to the surface could also improve the switching efficiency significantly. One possibility would be to use a positively applied potential of +0.3 V, which could alter the configuration of the positively charged oligolysine chain to a stretched out conformation. Thus, further enhancing cell adhesion due to the increased availability of RGD sites in comparison to OC conditions. However, the application of such potentials and their effects on cells would also need to be considered to ensure cells are not being adversely affected. In addition, changing the length of the switchable lysine chain of **GRGDS-3KC** to include 4-6 lysine units, in order to improve switching efficiency could also be a possible route for further investigation.

These studies could contribute to significant work in cell signaling in addition to cell adhesion due to the ability of the RGD functionalised surface to modulate surface ligand availability in real-time in a spatially controlled manner. For instance, intracellular signaling mediated by specific cell surface receptors could also be used to monitor the interaction of controlled ligands and surface receptors, in real-time using a fluorescent reporter for Ca^{2+} flux.

Other alternative routes to this project could be to replace the RGD headgroup with other bioactive moieties such as progesterone to form novel

switchable surfaces. In such a system the application of an electrical potential could regulate the progestrone moeity and thus be used to investigate the stimulus activated signal in human sperm cells for determining the quality of human sperm cells and also the potential to study human infertility. Another important line of study could be to use bioactive moieties such as boronic acids capable of detecting glucose and other saccharides to facilitate the development of diagnostic tools for the early detection of diabetes.

The fabrication of a new generation of well-defined surfaces consisting of multiple ligands could offer more selective and precise methods for controlling specific cellular interactions in addition to more biologically relevant biomolecules such as glycoproteins. For example in an “ON” state the surface could bind to cells, however in an “OFF” state the cells would be unable to bind due to specifically bound biomolecules to the surface preventing cell adhesion. Some of the key aspects that would need to be considered in assembling a well-defined multi-ligand switchable surface are: the bioactive moieties, ligand length, EG_n components for preventing nonspecific binding and electrically active chains required for the switching mechanism. The binding of biomolecules could be detected via SPR, whereas the presence of cells on the surface could be observed by utilising fluorescently labelled cells via a confocal microscope. SFG could also be used to further investigate the ways in which each ligand is affected by an electrical stimulus.

A key application for these dynamic surfaces could be the development of more selective capture and release of cells and also controlling the location of cell adhesion on surfaces. Furthermore a detailed analysis of cell function, precise manipulation of cell response and monitoring of intracellular processes via the

uptake of nanomaterials such as carbon nanotubes would be of great interest to cell biologists. The fabrication of surfaces that can mimick the natural environment will provide new insights into the pathway through which cells sense, adapt and respond to changes to their surroundings. Surfaces that can be dynamically controlled in this manner have the huge potential to be developed into simple and efficient diagnostic tools for the early detection of many diseases such as cancer, immunodeficiency diseases and diabetes.

Finally one of the novel features of this research project was to use an RGD functionalised surface to regulate the adhesion of macrophage cells. It is well known that macrophages form an integral part of the immune system, which mediates immune response to foreign materials. Thus, development of such novel dynamic *in vitro* systems to control macrophage cell adhesion in particular could provide new insights into macrophage cell signaling and aid the advancement of implantable devices and other biomaterials in order to prolong their lifespan.

References

(1) Sheetz, M. P.; Felsenfeld, D. P.; Galbraith, C. G.: Cell migration: regulation of force on extracellular-matrix-integrin complexes. *Trends in cell biology* **1998**, *8*, 51-54.

(2) Ruoslahti, E.: RGD and other recognition sequences for integrins. *Annual review of cell and developmental biology* **1996**, *12*, 697-715.

(3) Alberts, B.; Bray, D.; Hopkin, K.; Johnson, A.; Lewis, J.; Raff, M.; Roberts, K.; Walter, P.: *Essential cell biology*; Garland Science, 2013.

(4) Kato, M.; Mrksich, M.: Using model substrates to study the dependence of focal adhesion formation on the affinity of integrin-ligand complexes. *Biochemistry* **2004**, *43*, 2699-2707.

(5) Pytela, R.; Pierschbacher, M. D.; Ginsberg, M. H.; Plow, E. F.; Ruoslahti, E.: Platelet membrane glycoprotein IIB/IIIA - member of a family of Arg-Gly-Asp specific adhesion receptors. *Science* **1986**, *231*, 1559-1562.

(6) Pytela, R.; Pierschbacher, M. D.; Ruoslahti, E.: A 125/115-KDa cell-surface receptor specific for vitronectin interacts with the arginine-glycine-aspartic acid adhesion sequence derived from fibronectin. *Proceedings of the National Academy of Sciences of the United States of America* **1985**, *82*, 5766-5770.

(7) Dedhar, S.; Ruoslahti, E.; Pierschbacher, M. D.: A cell-surface receptor complex for collagen type-I recognizes the Arg-Gly-Asp sequence. *Journal of Cell Biology* **1987**, *104*, 585-593.

(8) Wagner, D.; Hynes, R.: Domain structure of fibronectin and its relation to function. Disulfides and sulfhydryl groups. *Journal of Biological Chemistry* **1979**, *254*, 6746-6754.

(9) Hynes, R. O.; Yamada, K. M.: Fibronectins: multifunctional modular glycoproteins. *The Journal of cell biology* **1982**, *95*, 369-377.

(10) Weibel, D. B.; Garstecki, P.; Whitesides, G. M.: Combining microscience and neurobiology. *Current Opinion in Neurobiology* **2005**, *15*, 560-567.

(11) Chen, C. S.; Mrksich, M.; Huang, S.; Whitesides, G. M.; Ingber, D. E.: Geometric control of cell life and death. *Science* **1997**, *276*, 1425-1428.

(12) Huang, S.; Chen, C. S.; Ingber, D. E.: Control of cyclin D1, p27(Kip1), and cell cycle progression in human capillary endothelial cells by cell shape and cytoskeletal tension. *Mol. Biol. Cell* **1998**, *9*, 3179-3193.

(13) McBeath, R.; Pirone, D. M.; Nelson, C. M.; Bhadriraju, K.; Chen, C. S.: Cell shape, cytoskeletal tension, and RhoA regulate stem cell lineage commitment. *Developmental Cell* **2004**, *6*, 483-495.

(14) Hynes, R. O.: Integrins - versatility, modulation and signaling in cell-adhesion. *Cell* **1992**, *69*, 11-25.

(15) Pierschbacher, M. D.; Ruoslahti, E.: Variants of the cell recognition site of fibronectin that retain attachment-promoting activity. *Proceedings of the National Academy of Sciences* **1984**, *81*, 5985-5988.

(16) Mrksich, M.: A surface chemistry approach to studying cell adhesion. *Chemical Society Reviews* **2000**, *29*, 267-273.

(17) Mrksich, M.: What can surface chemistry do for cell biology? *Current Opinion in Chemical Biology* **2002**, *6*, 794-797.

(18) Ruoslahti, E.; Pierschbacher, M. D.: New perspectives in cell adhesion: RGD and integrins. *Science* **1987**, *238*, 491-497.

(19) Choi, I.; Yeo, W. S.: Self-Assembled Monolayers with Dynamicity Stemming from (Bio) Chemical Conversions: From Construction to Application. *ChemPhysChem* **2013**, *14*, 55-69.

(20) Robertus, J.; Browne, W. R.; Feringa, B. L.: Dynamic control over cell adhesive properties using molecular-based surface engineering strategies. *Chemical Society Reviews* **2010**, *39*, 354-378.

(21) Hautanen, A.; Gailit, J.; Mann, D.; Ruoslahti, E.: Effects of modifications of the RGD sequence and its context on recognition by the fibronectin receptor. *Journal of Biological Chemistry* **1989**, *264*, 1437-1442.

(22) Massia, S. P.; Hubbell, J. A.: An RGD spacing of 440 nm is sufficient for integrin alpha V beta 3-mediated fibroblast spreading and 140 nm for focal contact and stress fiber formation. *The Journal of cell biology* **1991**, *114*, 1089-1100.

(23) Maheshwari, G.; Brown, G.; Lauffenburger, D. A.; Wells, A.; Griffith, L. G.: Cell adhesion and motility depend on nanoscale RGD clustering. *Journal of cell science* **2000**, *113*, 1677-1686.

(24) Selhuber-Unkel, C.; Erdmann, T.; Lopez-Garcia, M.; Kessler, H.; Schwarz, U.; Spatz, J.: Cell adhesion strength is controlled by intermolecular spacing of adhesion receptors. *Biophysical Journal* **2010**, *98*, 543-551.

(25) Huang, J.; Grater, S. V.; Corbellini, F.; Rinck, S.; Bock, E.; Kemkemer, R.; Kessler, H.; Ding, J.; Spatz, J. P.: Impact of order and disorder in RGD nanopatterns on cell adhesion. *Nano letters* **2009**, *9*, 1111-1116.

(26) Lutolf, M. P.; Hubbell, J. A.: Synthetic biomaterials as instructive extracellular microenvironments for morphogenesis in tissue engineering. *Nat. Biotechnol.* **2005**, *23*, 47-55.

(27) Ulman, A.: *An introduction to ultrathin organic films: from Langmuir-Blodgett to self-assembly*; Academic press New York, 1991; Vol. 45.

(28) Nuzzo, R. G.; Allara, D. L.: Adsorption of bifunctional organic disulfides on gold surfaces. *Journal of the American Chemical Society* **1983**, *105*, 4481-4483.

(29) Onclin, S.; Ravoo, B. J.; Reinhoudt, D. N.: Engineering silicon oxide surfaces using self-assembled monolayers. *Angew. Chem.-Int. Edit.* **2005**, *44*, 6282-6304.

(30) Ulman, A.: Formation and structure of self-assembled monolayers. *Chemical Reviews* **1996**, *96*, 1533-1554.

(31) Schwartz, D. K.: Mechanisms and kinetics of self-assembled monolayer formation. *Annual Review of Physical Chemistry* **2001**, *52*, 107-137.

(32) Love, J. C.; Estroff, L. A.; Kriebel, J. K.; Nuzzo, R. G.; Whitesides, G. M.: Self-assembled monolayers of thiolates on metals as a form of nanotechnology. *Chemical Reviews* **2005**, *105*, 1103-1169.

(33) Mendes, P. M.: Stimuli-responsive surfaces for bio-applications. *Chemical Society Reviews* **2008**, *37*, 2512-2529.

(34) Schreiber, F.: Structure and growth of self-assembling monolayers. *Progress in surface science* **2000**, *65*, 151-257.

(35) Schreiber, F.: Self-assembled monolayers: from 'simple' model systems to biofunctionalized interfaces. *Journal of Physics-Condensed Matter* **2004**, *16*, R881-R900.

(36) Wang, Q.; Geil, P.; Padua, G.: Role of hydrophilic and hydrophobic interactions in structure development of zein films. *Journal of Polymers and the Environment* **2004**, *12*, 197-202.

(37) Lahann, J.; Mitragotri, S.; Tran, T. N.; Kaido, H.; Sundaram, J.; Choi, I. S.; Hoffer, S.; Somorjai, G. A.; Langer, R.: A reversibly switching surface. *Science* **2003**, *299*, 371-374.

(38) Hayashi, G.; Hagihara, M.; Dohno, C.; Nakatani, K.: Photoregulation of a peptide-RNA interaction on a gold surface. *Journal of the American Chemical Society* **2007**, *129*, 8678-+.

(39) Yousaf, M. N.; Houseman, B. T.; Mrksich, M.: Turning on cell migration with electroactive substrates. *Angew. Chem.-Int. Edit.* **2001**, *40*, 1093-+.

(40) Yeo, W. S.; Hodneland, C. D.; Mrksich, M.: Electroactive monolayer substrates that selectively release adherent cells. *ChemBioChem* **2001**, *2*, 590-+.

(41) Mendes, P. M.; Christman, K. L.; Parthasarathy, P.; Schopf, E.; Ouyang, J.; Yang, Y.; Preece, J. A.; Maynard, H. D.; Chen, Y.; Stoddart, J. F.: Electrochemically controllable conjugation of proteins on surfaces. *Bioconjugate Chemistry* **2007**, *18*, 1919-1923.

(42) Mu, L.; Liu, Y.; Cai, S.; Kong, J.: A smart surface in a microfluidic chip for controlled protein separation. *Chemistry-A European Journal* **2007**, *13*, 5113-5120.

(43) Strong, L.; Whitesides, G. M.: Structures of self-assembled monolayer films of organosulfur compounds adsorbed on gold single crystals - electron diffraction studies. *Langmuir : the ACS journal of surfaces and colloids* **1988**, *4*, 546-558.

(44) Bain, C. D.; Troughton, E. B.; Tao, Y. T.; Evall, J.; Whitesides, G. M.; Nuzzo, R. G.: Formation of monolayer films by the spontaneous assembly of organic thiols from solution onto gold. *Journal of the American Chemical Society* **1989**, *111*, 321-335.

(45) Vericat, C.; Vela, M. E.; Benitez, G.; Carro, P.; Salvarezza, R. C.: Self-assembled monolayers of thiols and dithiols on gold: new challenges for a well-known system. *Chem Soc Rev* **2010**, *39*, 1805-34.

(46) Shao, H. B.; Yu, H. Z.; Cheng, G. J.; Zhang, H. L.; Liu, Z. F.: Formation kinetics and electrochemical behavior of an azobenzene self-assembled monolayer

on a gold electrode. *Berichte der Bunsengesellschaft für physikalische Chemie* **1998**, *102*, 111-117.

(47) Humbert, C.; Buck, M.; Calderone, A.; Vigneron, J. P.; Meunier, V.; Champagne, B.; Zheng, W. Q.; Tadjeddine, A.; Thiry, P. A.; Peremans, A.: In situ monitoring of the self-assembly of p-nitroanilino terminated thiol on gold: a study by IR-vis sum-frequency generation spectroscopy. *Physica Status Solidi a-Applications and Materials Science* **1999**, *175*, 129-136.

(48) Sun, L.; Crooks, R. M.: Imaging of Defects Contained within n-Alkylthiol Monolayers by Combination of Underpotential Deposition and Scanning Tunneling Microscopy: Kinetics of Self-Assembly. *Journal of the Electrochemical Society* **1991**, *138*, L23-L25.

(49) Tamada, K.; Hara, M.; Sasabe, H.; Knoll, W.: Surface phase behavior of n-alkanethiol self-assembled monolayers adsorbed on Au (111): An atomic force microscope study. *Langmuir : the ACS journal of surfaces and colloids* **1997**, *13*, 1558-1566.

(50) Fruböse, C.; Doblhofer, K.: In situ quartz-microbalance study of the self-assembly and stability of aliphatic thiols on polarized gold electrodes. *Journal of the Chemical Society, Faraday Transactions* **1995**, *91*, 1949-1953.

(51) Bain, C. D.; Whitesides, G. M.: Modeling Organic Surfaces with Self-Assembled Monolayers. *Angewandte Chemie International Edition in English* **1989**, *28*, 506-512.

(52) Nelson, K. E.; Gamble, L.; Jung, L. S.; Boeckl, M. S.; Naeemi, E.; Golledge, S. L.; Sasaki, T.; Castner, D. G.; Campbell, C. T.; Stayton, P. S.: Surface characterization of mixed self-assembled monolayers designed for streptavidin immobilization. *Langmuir : the ACS journal of surfaces and colloids* **2001**, *17*, 2807-2816.

(53) Hays, H. C.; Millner, P. A.; Prodromidis, M. I.: Development of capacitance based immunosensors on mixed self-assembled monolayers. *Sensors and Actuators B: Chemical* **2006**, *114*, 1064-1070.

(54) Prime, K. L.; Whitesides, G. M.: Adsorption of proteins onto surfaces containing end-attached oligo(ethylene oxide) - a model system using self-assembled monolayers. *Journal of the American Chemical Society* **1993**, *115*, 10714-10721.

(55) Laibinis, P. E.; Fox, M. A.; Folkers, J. P.; Whitesides, G. M.: Comparisons of self-assembled monolayers on silver and gold: mixed monolayers derived from HS(CH2)21X and HS(CH2)10Y (X, Y = CH3, CH2OH) have similar properties. *Langmuir : the ACS journal of surfaces and colloids* **1991**, *7*, 3167-3173.

(56) Bain, C. D.; Whitesides, G. M.: Formation of monolayers by the coadsorption of thiols on gold - variation in the length of the alkyl chain. *Journal of the American Chemical Society* **1989**, *111*, 7164-7175.

(57) Senaratne, W.; Andruzzi, L.; Ober, C. K.: Self-assembled monolayers and polymer brushes in biotechnology: current applications and future perspectives. *Biomacromolecules* **2005**, *6*, 2427-2448.

(58) Zhu, B.; Eurell, T.; Gunawan, R.; Leckband, D.: Chain-length dependence of the protein and cell resistance of oligo(ethylene glycol)-terminated self-assembled monolayers on gold. *J. Biomed. Mater. Res.* **2001**, *56*, 406-416.

(59) Petrie, T. A.; Capadona, J. R.; Reyes, C. D.; Garcia, A. J.: Integrin specificity and enhanced cellular activities associated with surfaces presenting a recombinant fibronectin fragment compared to RGD supports. *Biomaterials* **2006**, *27*, 5459-5470.

(60) Keselowsky, B. G.; Collard, D. M.; Garcia, A. J.: Surface chemistry modulates focal adhesion composition and signaling through changes in integrin binding. *Biomaterials* **2004**, *25*, 5947-5954.

(61) Ladd, J.; Zhang, Z.; Chen, S.; Hower, J. C.; Jiang, S.: Zwitterionic polymers exhibiting high resistance to nonspecific protein adsorption from human serum and plasma. *Biomacromolecules* **2008**, *9*, 1357-1361.

(62) Esseghaier, C.; Helali, S.; Ben Fredj, H.; Tlili, A.; Abdelghani, A.: Polypyrrole-neutravidin layer for impedimetric biosensor. *Sensors and Actuators B-Chemical* **2008**, *131*, 584-589.

(63) Sun, H.; Choy, T. S.; Zhu, D. R.; Yam, W. C.; Fung, Y. S.: Nano-silver-modified PQC/DNA biosensor for detecting E. coli in environmental water. *Biosens. Bioelectron.* **2009**, *24*, 1405-1410.

(64) Hall, W. P.; Ngatia, S. N.; Van Duyne, R. P.: LSPR Biosensor Signal Enhancement Using Nanoparticle-Antibody Conjugates. *Journal of Physical Chemistry C* **2011**, *115*, 1410-1414.

(65) Bashir, R.; Gomez, R.; Sarikaya, A.; Ladisch, M. R.; Sturgis, J.; Robinson, J. P.: Adsorption of avidin on microfabricated surfaces for protein biochip applications. *Biotechnology and Bioengineering* **2001**, *73*, 324-328.

(66) Lazcka, O.; Del Campo, F. J.; Munoz, F. X.: Pathogen detection: A perspective of traditional methods and biosensors. *Biosens. Bioelectron.* **2007**, *22*, 1205-1217.

(67) Zhavnerko, G. K.; Yi, S. J.; Chung, S. H.; Yuk, J. S.; Ha, K. S.: *Oriented immobilization of c-reactive protein on solid surface for biosensor applications*, 2004; Vol. 152.

(68) Barton, A. C.; Davis, F.; Higson, S. P. J.: Labeless Immunosensor Assay for the Stroke Marker Protein Neuron Specific Enolase Based upon an Alternating Current Impedance Protocol. *Analytical Chemistry* **2008**, *80*, 9411-9416.

(69) Cooper, M. A.: Optical biosensors in drug discovery. *Nature Reviews Drug Discovery* **2002**, *1*, 515-528.

(70) Wayment, J. R.; Harris, J. M.: Biotin-Avidin Binding Kinetics Measured by Single-Molecule Imaging. *Analytical Chemistry* **2009**, *81*, 336-342.

(71) Grunwell, J. R.; Glass, J. L.; Lacoste, T. D.; Deniz, A. A.; Chemla, D. S.; Schultz, P. G.: Monitoring the conformational fluctuations of DNA hairpins using single-pair fluorescence resonance energy transfer. *Journal of the American Chemical Society* **2001**, *123*, 4295-4303.

(72) Wennmalm, S.; Edman, L.; Rigler, R.: Conformational fluctuations in single DNA molecules. *Proceedings of the National Academy of Sciences of the United States of America* **1997**, *94*, 10641-10646.

(73) Ladd, J.; Boozer, C.; Yu, Q. M.; Chen, S. F.; Homola, J.; Jiang, S.: DNA-directed protein immobilization on mixed self-assembled monolayers via a Streptavidin bridge. *Langmuir : the ACS journal of surfaces and colloids* **2004**, *20*, 8090-8095.

(74) Green, N. M.: Avidin. *Advances in protein chemistry* **1975**, *29*, 85-133.

(75) Wolny, P. M.; Spatz, J. P.; Richter, R. P.: On the Adsorption Behavior of Biotin-Binding Proteins on Gold and Silica. *Langmuir : the ACS journal of surfaces and colloids* **2010**, *26*, 1029-1034.

(76) Delange, R. J.: Egg white avidin . 1. Amino acid composition-sequence of amino-terminal and corboxyl-terminal cyanogen bromide peptides. *Journal of Biological Chemistry* **1970**, *245*, 907-&.

(77) Green, N. M.: Avidin and streptavidin. *Methods in Enzymology* **1990**, *184*, 51-67.

(78) Claesson, P. M.; Blomberg, E.; Fröberg, J. C.; Nylander, T.; Arnebrant, T.: Protein interactions at solid surfaces. *Advances in Colloid and Interface Science* **1995**, *57*, 161-227.

(79) Ricci, F.; Lai, R. Y.; Heeger, A. J.; Plaxco, K. W.; Sumner, J. J.: Effect of molecular crowding on the response of an electrochemical DNA sensor. *Langmuir : the ACS journal of surfaces and colloids* **2007**, *23*, 6827-6834.

(80) Fan, C. H.; Plaxco, K. W.; Heeger, A. J.: Electrochemical interrogation of conformational changes as a reagentless method for the sequence-specific detection of DNA. *Proceedings of the National Academy of Sciences of the United States of America* **2003**, *100*, 9134-9137.

(81) Immoos, C. E.; Lee, S. J.; Grinstaff, M. W.: DNA-PEG-DNA triblock macromolecules for reagentless DNA detection. *Journal of the American Chemical Society* **2004**, *126*, 10814-10815.

(82) Xiao, Y.; Lubin, A. A.; Baker, B. R.; Plaxco, K. W.; Heeger, A. J.: Single-step electronic detection of femtomolar DNA by target-induced strand displacement in an electrode-bound duplex. *Proceedings of the National Academy of Sciences of the United States of America* **2006**, *103*, 16677-16680.

(83) Liu, J.; Zhou, H.; Xu, J.-J.; Chen, H.-Y.: An effective DNA-based electrochemical switch for reagentless detection of living cells. *Chem. Commun.* **2011**, *47*, 4388-4390.

(84) Liu, J.; Zhou, H.; Xu, J.-J.; Chen, H.-Y.: Switchable 'on–off–on'electrochemical technique for direct detection of survivin mRNA in living cells. *Analyst* **2012**, *137*, 3940-3945.

(85) Iqbal, P.; Rawson, F. J.; Ho, W. K.-W.; Lee, S.-F.; Leung, K. C.-F.; Wang, X.; Beri, A.; Preece, J. A.; Ma, J.; Mendes, P. M.: Surface Molecular Tailoring using pH-Switchable Supramolecular Dendron-Ligand Assemblies. *Acs Applied Materials & Interfaces* **2014**.

(86) Chan, E. W. L.; Park, S.; Yousaf, M. N.: An electroactive catalytic dynamic substrate that immobilizes and releases patterned ligands, proteins, and cells. *Angew. Chem.-Int. Edit.* **2008**, *47*, 6267-6271.

(87) Hoover, D. K.; Lee, E.-J.; Chan, E. W. L.; Yousaf, M. N.: Electroactive nanoarrays for biospecific ligand mediated studies of cell adhesion. *ChemBioChem* **2007**, *8*, 1920-+.

(88) Chan, E. W. L.; Yousaf, M. N.: Immobilization of ligands with precise control of density to electroactive surfaces. *Journal of the American Chemical Society* **2006**, *128*, 15542-15546.

(89) Luo, W.; Westcott, N. P.; Pulsipher, A.; Yousaf, M. N.: Renewable and Optically Transparent Electroactive Indium Tin Oxide Surfaces for Chemoselective Ligand Immobilization and Biospecific Cell Adhesion. *Langmuir : the ACS journal of surfaces and colloids* **2008**, *24*, 13096-13101.

(90) Westcott, N. P.; Yousaf, M. N.: Synergistic microfluidic and electrochemical strategy to activate and pattern surfaces selectively with ligands and cells. *Langmuir : the ACS journal of surfaces and colloids* **2008**, *24*, 2261-2265.

(91) Yousaf, M. N.; Houseman, B. T.; Mrksich, M.: Using electroactive substrates to pattern the attachment of two different cell populations. *Proceedings of the National Academy of Sciences of the United States of America* **2001**, *98*, 5992-5996.

(92) Artzy-Schnirman, A.; Blat, D.; Talmon, Y.; Fishler, R.; Gertman, D.; Oren, R.; Wolchinsky, R.; Waks, T.; Benhar, I.; Eshhar, Z.; Sivan, U.; Reiter, Y.:

Electrically controlled molecular recognition harnessed to activate a cellular response. *Nano letters* **2011**, *11*, 4997-5001.

(93) Yan, C.; Matsuda, W.; Pepperberg, D. R.; Zimmerman, S. C.; Leckband, D. E.: Synthesis and characterization of an electroactive surface that releases gamma-aminobutyric acid (GABA). *Journal of colloid and interface science* **2006**, *296*, 165-177.

(94) Bunimovich, Y. L.; Ge, G. L.; Beverly, K. C.; Ries, R. S.; Hood, L.; Heath, J. R.: Electrochemically programmed, spatially selective biofunctionalization of silicon wires. *Langmuir : the ACS journal of surfaces and colloids* **2004**, *20*, 10630-10638.

(95) Hodneland, C. D.; Mrksich, M.: Biomolecular surfaces that release ligands under electrochemical control. *Journal of the American Chemical Society* **2000**, *122*, 4235-4236.

(96) Yeo, W. S.; Yousaf, M. N.; Mrksich, M.: Dynamic interfaces between cells and surfaces: Electroactive substrates that sequentially release and attach cells. *Journal of the American Chemical Society* **2003**, *125*, 14994-14995.

(97) Lamb, B. M.; Yousaf, M. N.: Redox-Switchable Surface for Controlling Peptide Structure. *Journal of the American Chemical Society* **2011**, *133*, 8870-8873.

(98) Ciampi, S.; James, M.; Le Saux, G.; Gaus, K.; Gooding, J. J.: Electrochemical "Switching" of Si(100) Modular Assemblies. *Journal of the American Chemical Society* **2012**, *134*, 844-847.

(99) An, Q.; Brinkmann, J.; Huskens, J.; Krabbenborg, S.; de Boer, J.; Jonkheijm, P.: A supramolecular system for the electrochemically controlled release of cells. *Angew Chem Int Ed Engl* **2012**, *51*, 12233-7.

(100) Jonas, A. M.; Glinel, K.; Oren, R.; Nysten, B.; Huck, W. T.: Thermo-responsive polymer brushes with tunable collapse temperatures in the physiological range. *Macromolecules* **2007**, *40*, 4403-4405.

(101) Kushida, A.; Yamato, M.; Konno, C.; Kikuchi, A.; Sakurai, Y.; Okano, T.: Decrease in culture temperature releases monolayer endothelial cell sheets together with deposited fibronectin matrix from temperature-responsive culture surfaces. *J. Biomed. Mater. Res.* **1999**, *45*, 355-362.

(102) Ebara, M.; Yamato, M.; Aoyagi, T.; Kikuchi, A.; Sakai, K.; Okano, T.: Temperature-responsive cell culture surfaces enable "on-off" affinity control between cell integrins and RGDS ligands. *Biomacromolecules* **2004**, *5*, 505-510.

(103) Balamurugan, S.; Ista, L. K.; Yan, J.; López, G. P.; Fick, J.; Himmelhaus, M.; Grunze, M.: Reversible protein adsorption and bioadhesion on monolayers terminated with mixtures of oligo (ethylene glycol) and methyl groups. *Journal of the American Chemical Society* **2005**, *127*, 14548-14549.

(104) Zareie, H. M.; Boyer, C.; Bulmus, V.; Nateghi, E.; Davis, T. P.: Temperature-responsive self-assembled monolayers of oligo(ethylene glycol): Control of biomolecular recognition. *ACS Nano* **2008**, *2*, 757-765.

(105) Nakanishi, J.; Nakayama, H.; Yamaguchi, K.; Garcia, A. J.; Horiike, Y.: Dynamic culture substrate that captures a specific extracellular matrix protein in response to light. *Sci. Technol. Adv. Mater.* **2011**, *12*.

(106) Liu, D. B.; Xie, Y. Y.; Shao, H. W.; Jiang, X. Y.: Using Azobenzene-Embedded Self-Assembled Monolayers To Photochemically Control Cell Adhesion Reversibly. *Angew. Chem.-Int. Edit.* **2009**, *48*, 4406-4408.

(107) Auernheimer, J.; Dahmen, C.; Hersel, U.; Bausch, A.; Kessler, H.: Photoswitched cell adhesion on surfaces with RGD peptides. *Journal of the American Chemical Society* **2005**, *127*, 16107-16110.

(108) Gong, Y. H.; Li, C.; Yang, J.; Wang, H. Y.; Zhuo, R. X.; Zhang, X. Z.: Photoresponsive "Smart Template" via Host-Guest Interaction for Reversible Cell Adhesion. *Macromolecules* **2011**, *44*, 7499-7502.

(109) Yeo, W.-S.; Mrksich, M.: Electroactive self-assembled monolayers that permit orthogonal control over the adhesion of cells to patterned substrates. *Langmuir : the ACS journal of surfaces and colloids* **2006**, *22*, 10816-10820.

(110) Lee, C. S.; Baker, S. E.; Marcus, M. S.; Yang, W. S.; Eriksson, M. A.; Hamers, R. J.: Electrically addressable biomolecular functionalization of carbon nanotube and carbon nanofiber electrodes. *Nano letters* **2004**, *4*, 1713-1716.

(111) Curreli, M.; Li, C.; Sun, Y. H.; Lei, B.; Gundersen, M. A.; Thompson, M. E.; Zhou, C. W.: Selective functionalization of In2O3 nanowire mat devices for biosensing applications. *Journal of the American Chemical Society* **2005**, *127*, 6922-6923.

(112) Yang, W. S.; Baker, S. E.; Butler, J. E.; Lee, C. S.; Russell, J. N.; Shang, L.; Sun, B.; Hamers, R. J.: Electrically addressable biomolecular functionalization of conductive nanocrystalline diamond thin films. *Chemistry of Materials* **2005**, *17*, 938-940.

(113) Knezevic, J.; Langer, A.; Hampel, P. A.; Kaiser, W.; Strasser, R.; Rant, U.: Quantitation of affinity, avidity, and binding kinetics of protein analytes with a dynamically switchable biosurface. *Journal of the American Chemical Society* **2012**, *134*, 15225-15228.

(114) Kaiser, W.; Rant, U.: Conformations of end-tethered DNA molecules on gold surfaces: influences of applied electric potential, electrolyte screening, and temperature. *Journal of the American Chemical Society* **2010**, *132*, 7935-7945.

(115) Lahann, J.; Mitragotri, S.; Tran, T.-N.; Kaido, H.; Sundaram, J.; Choi, I. S.; Hoffer, S.; Somorjai, G. A.; Langer, R.: A reversibly switching surface. *Science* **2003**, *299*, 371-374.

(116) Tokuhisa, H.; Liu, J. a.; Omori, K.; Kanesato, M.; Hiratani, K.; Baker, L. A.: Efficient biosensor interfaces based on space-controlled self-assembled monolayers. *Langmuir : the ACS journal of surfaces and colloids* **2008**, *25*, 1633-1637.

(117) Liu, Y.; Mu, L.; Liu, B.; Zhang, S.; Yang, P.; Kong, J.: Controlled protein assembly on a switchable surface. *Chem. Commun.* **2004**, 1194-1195.

(118) Pranzetti, A.; Davis, M.; Yeung, C. L.; Preece, J. A.; Koelsch, P.; Mendes, P. M.: Direct Observation of Reversible Biomolecule Switching Controlled By Electrical Stimulus. *Advanced Materials Interfaces* **2014**, n/a-n/a.

(119) Josephs, E. A.; Ye, T.: A single-molecule view of conformational switching of DNA Tethered to a Gold Electrode. *Journal of the American Chemical Society* **2012**, *134*, 10021-10030.

(120) Liu, Y.; Mu, L.; Liu, B. H.; Zhang, S.; Yang, P. Y.; Kong, J. L.: Controlled protein assembly on a switchable surface. *Chem. Commun.* **2004**, 1194-1195.

(121) Yeung, C. L.; Iqbal, P.; Allan, M.; Lashkor, M.; Preece, J. A.; Mendes, P. M.: Tuning Specific Biomolecular Interactions Using Electro-Switchable Oligopeptide Surfaces. *Advanced Functional Materials* **2010**, *20*, 2657-2663.

(122) Yeung, C. L.; Wang, X.; Lashkor, M.; Cantini, E.; Rawson, F. J.; Iqbal, P.; Preece, J. A.; Ma, J.; Mendes, P. M.: Modulation of Biointeractions by Electrically Switchable Oligopeptide Surfaces: Structural Requirements and Mechanism. *Advanced Materials Interfaces* **2014**, *1*, n/a-n/a.

(123) Ng, C. C. A.; Magenau, A.; Ngalim, S. H.; Ciampi, S.; Chockalingham, M.; Harper, J. B.; Gaus, K.; Gooding, J. J.: Using an Electrical Potential to Reversibly Switch Surfaces between Two States for Dynamically Controlling Cell Adhesion. *Angewandte Chemie (International ed. in English)* **2012**, *51*, 7706-10.

(124) Bolduc, O. R.; Masson, J. F.: Monolayers of 3-mercaptopropyl-amino acid to reduce the nonspecific adsorption of serum proteins on the surface of biosensors. *Langmuir : the ACS journal of surfaces and colloids* **2008**, *24*, 12085-91.

(125) Frey, W.; Meyer, D. E.; Chilkoti, A.: Thermodynamically reversible addressing of a stimuli responsive fusion protein onto a patterned surface template. *Langmuir : the ACS journal of surfaces and colloids* **2003**, *19*, 1641-1653.

(126) Nath, N.; Chilkoti, A.: Fabrication of a reversible protein array directly from cell lysate using a stimuli-responsive polypeptide. *Analytical Chemistry* **2003**, *75*, 709-715.

(127) Hyun, J.; Lee, W. K.; Nath, N.; Chilkoti, A.; Zauscher, S.: Capture and release of proteins on the nanoscale by stimuli-responsive elastin-like polypeptide "switches". *Journal of the American Chemical Society* **2004**, *126*, 7330-7335.

(128) Miller, L. L.; Zhou, Q. X.: Poly(N-methylpyrrolylium) poly(styrenesulfonate) - a conductive, electrically switchable cation exchanger that cathodically binds and anodically releases dopamine. *Macromolecules* **1987**, *20*, 1594-1597.

(129) Cao, Z.; Mi, L.; Mendiola, J.; Ella-Menye, J. R.; Zhang, L.; Xue, H.; Jiang, S.: Reversibly switching the function of a surface between attacking and defending against bacteria. *Angewandte Chemie International Edition* **2012**, *51*, 2602-2605.

(130) Good, R. J.: Contact angle, wetting, and adhesion: a critical review. *Journal of adhesion science and technology* **1992**, *6*, 1269-1302.

(131) Chen, W.; Fadeev, A. Y.; Hsieh, M. C.; Öner, D.; Youngblood, J.; McCarthy, T. J.: Ultrahydrophobic and ultralyophobic surfaces: some comments and examples. *Langmuir : the ACS journal of surfaces and colloids* **1999**, *15*, 3395-3399.

(132) Theeten, J.; Aspnes, D.: Ellipsometry in thin film analysis. *Annual Review of Materials Science* **1981**, *11*, 97-122.

(133) Gonçalves, D.; Irene, E. A.: Fundamentals and applications of spectroscopic ellipsometry. *Química Nova* **2002**, *25*, 794-800.

(134) Wood, R. W.: On a remarkable case of uneven distribution of light in a diffraction grating spectrum. *Philosophical Magazine* **1902**, *4*, 396-402.

(135) Ritchie, R.; Arakawa, E.; Cowan, J.; Hamm, R.: Surface-plasmon resonance effect in grating diffraction. *Physical Review Letters* **1968**, *21*, 1530.

(136) Otto, A.: Excitation of nonradiative surface plasma waves in silver by method of frustrated total reflection. *Zeitschrift Fur Physik* **1968**, *216*, 398-&.

(137) Kretschm.E; Raether, H.: Radiative decay of non radiative surface plasmons excited by light. *Zeitschrift Fur Naturforschung Part a-Astrophysik Physik Und Physikalische Chemie* **1968**, *A 23*, 2135-&.

(138) Harrick, N. J.: *Internal reflection spectroscopy*; Harrick Scientific Corp., 1967.

(139) Stenberg, E.; Persson, B.; Roos, H.; Urbaniczky, C.: Quantitative determination of surface concentration of protein with surface plasmon resonance

using radiolabeled proteins. *Journal of colloid and interface science* **1991**, *143*, 513-526.

(140) Patskovsky, S.; Jacquemart, R.; Meunier, M.; De Crescenzo, G.; Kabashin, A. V.: Phase-sensitive spatially-modulated surface plasmon resonance polarimetry for detection of biomolecular interactions. *Sensors and Actuators B: Chemical* **2008**, *133*, 628-631.

(141) Woodruff, D. P.; Delchar, T. A.: *Modern techniques of surface science*; Cambridge University Press, 1994.

(142) Chusuei, C. C.; Goodman, D. W.: X-Ray photoelectron spectroscopy. *Encyclopedia of Physical Science and Technology* **2002**, *17*, 921-938.

(143) Castner, D. G.; Hinds, K.; Grainger, D. W.: X-ray photoelectron spectroscopy sulfur 2p study of organic thiol and disulfide binding interactions with gold surfaces. *Langmuir : the ACS journal of surfaces and colloids* **1996**, *12*, 5083-5086.

(144) Zareie, H. M.; Boyer, C.; Bulmus, V.; Nateghi, E.; Davis, T. P.: Temperature-Responsive Self-Assembled Monolayers of Oligo(ethylene glycol): Control of Biomolecular Recognition

ACSNano **2008**, *2*, 757-765.

(145) Balamurugan, S.; Ista, L. K.; Yan, J.; Lopez, G. P.; Fick, J.; Himmelhaus, M.; Grunze, M.: Reversible protein adsorption and bioadhesion on monolayers terminated with mixtures of oligo(ethylene glycol) and methyl groups. *J. Am. Chem. Soc.* **2005**, *127*, 14548-14549.

(146) Demirel, G. B.; Dilsiz, N.; Ergun, M. A.; Cakmak, M.; Caykara, T.: Photocontrollable DNA hybridization on reversibly photoresponsive surfaces. *J. Mater. Chem.* **2011**, *21*, 10415-10420.

(147) Mannix, R. J.; Kumar, S.; Cassiola, F.; Montoya-Zavala, M.; Feinstein, E.; Prentiss, M.; Ingber, D. E.: Nanomagnetic actuation of receptor-mediated signal transduction. *Nat. Nanotechnol.* **2008**, *3*, 36-40.

(148) Mu, L.; Liu, Y.; Zhang, S.; Liu, B. H.; Kong, J.: Selective assembly of specifically charged proteins on an electrochemically switched surface. *New J. Chem.* **2005**, *29*, 847-852.

(149) Mao, Y. D.; Luo, C. X.; Ouyang, Q.: Studies of temperature-dependent electronic transduction on DNA hairpin loop sensor. *Nucleic Acids Research* **2003**, *31*, e108.

(150) Immoos, C. E.; Lee, S. J.; Grinstaff, M. W.: Conformationally gated electrochemical gene detection. *ChemBioChem* **2004**, *5*, 1100-1103.

(151) Rant, U.; Arinaga, K.; Scherer, S.; Pringsheim, E.; Fujita, S.; Yokoyama, N.; Tornow, M.; Abstreiter, G.: Switchable DNA interfaces for the highly sensitive detection of label-free DNA targets. *Proc. Natl. Acad. Sci. U. S. A.* **2007**, *104*, 17364-17369.

(152) Xiao, Y.; Lubin, A. A.; Baker, B. R.; Plaxco, K. W.; Heeger, A. J.: Single-step electronic detection of femtomolar DNA by target-induced strand displacement in an electrode-bound duplex. *Proceedings of the National Academy of Sciences of the United States of America* **2006**, *103*, 16677-16680.

(153) George, P. M.; LaVan, D. A.; Burdick, J. A.; Chen, C. Y.; Liang, E.; Langer, R.: Electrically controlled drug delivery from biotin-doped conductive polypyrrole. *Adv. Mater.* **2006**, *18*, 577-+.

(154) Blankespoor, R. L.; Miller, L. L.: Polymerized 3-methoxythiophene - a processable material for the controlled release of anions. *J. Chem. Soc.-Chem. Commun.* **1985**, 90-92.

(155) Pyo, M.; Maeder, G.; Kennedy, R. T.; Reynolds, J. R.: Controlled release of biological molecules from conducting polymer modified electrodes: The potential dependent release of adenosine 5′-triphosphate from poly(pyrrole adenosine 5′-triphosphate) films. *J. Electroanal. Chem.* **1994**, *368*, 329-332.

(156) Pernaut, J. M.; Reynolds, J. R.: Use of conducting electroactive polymers for drug delivery and sensing of bioactive molecules. A redox chemistry approach. *Journal of Physical Chemistry B* **2000**, *104*, 4080-4090.

(157) Huber, D. L.; Manginell, R. P.; Samara, M. A.; Kim, B. I.; Bunker, B. C.: Programmed adsorption and release of proteins in a microfluidic device. *Science* **2003**, *301*, 352-354.

(158) Yamanaka, H.; Yoshizako, K.; Akiyama, Y.; Sota, H.; Hasegawa, Y.; Shinohara, Y.; Kikuchi, A.; Okano, T.: Affinity chromatography with collapsibly tethered ligands. *Analytical Chemistry* **2003**, *75*, 1658-1663.

(159) Yoshizako, K.; Akiyama, Y.; Yamanaka, H.; Shinohara, Y.; Hasegawa, Y.; Carredano, E.; Kikuchi, A.; Okano, T.: Regulation of protein binding toward a

ligand on chromatographic matrixes by masking and forced-releasing effects using thermoresponsive polymer. *Analytical Chemistry* **2002**, *74*, 4160-4166.

(160) Nagase, K.; Kobayashi, J.; Kikuchi, A.; Akiyama, Y.; Kanazawa, H.; Okano, T.: Interfacial property modulation of thermoresponsive polymer brush surfaces and their interaction with biomolecules. *Langmuir : the ACS journal of surfaces and colloids* **2007**, *23*, 9409-9415.

(161) Lutolf, M. P.; Lauer-Fields, J. L.; Schmoekel, H. G.; Metters, A. T.; Weber, F. E.; Fields, G. B.; Hubbell, J. A.: Synthetic matrix metalloproteinase-sensitive hydrogels for the conduction of tissue regeneration: Engineering cell-invasion characteristics. *Proc. Natl. Acad. Sci. U. S. A.* **2003**, *100*, 5413-5418.

(162) Weidner, T.; Bretthauer, F.; Ballav, N.; Motschmann, H.; Orendi, H.; Bruhn, C.; Siemeling, U.; Zharnikov, M.: Correlation between the Molecular Structure and Photoresponse in Aliphatic Self-Assembled Monolayers with Azobenzene Tailgroups. *Langmuir : the ACS journal of surfaces and colloids* **2008**, *24*, 11691-11700.

(163) Pradier, C. M.; Salmain, M.; Zheng, L.; Jaouen, G.: Specific binding of avidin to biotin immobilised on modified gold surfaces - Fourier transform infrared reflection absorption spectroscopy analysis. *Surf. Sci.* **2002**, *502*, 193-202.

(164) Yam, C. M.; Pradier, C. M.; Salmain, M.; Marcus, P.; Jaouen, G.: Binding of biotin to gold surfaces functionalized by self-assembled monolayers of cystamine and cysteamine: Combined FT-IRRAS and XPS characterization. *Journal of colloid and interface science* **2001**, *235*, 183-189.

(165) Hooper, A. E.; Werho, D.; Hopson, T.; Palmer, O.: Evaluation of amine- and amide-terminated self-assembled monolayers as 'Molecular glues' for Au and SiO2 substrates. *Surf. Interface Anal.* **2001**, *31*, 809-814.

(166) Moulder, J. F.; Stickle, W. F.; Sobol, P. E.; Bomben, K. D.: *Handbook of X-ray Photoelectron Spectroscopy*; Perkin-Elmer Corp: Eden Prairie, MN, USA, 1992.

(167) Ulman, A.: Formation and structure of self-assembled monolayers. *Chem. Rev.* **1996**, *96*, 1533-1554.

(168) Zheng, J.; Li, L. Y.; Tsao, H. K.; Sheng, Y. J.; Chen, S. F.; Jiang, S. Y.: Strong repulsive forces between protein and oligo (ethylene glycol) self-assembled monolayers: A molecular simulation study. *Biophysical Journal* **2005**, *89*, 158-166.

(169) Wang, R. L. C.; Kreuzer, H. J.; Grunze, M.: The interaction of oligo(ethylene oxide) with water: a quantum mechanical study. *PCCP Phys. Chem. Chem. Phys.* **2000**, *2*, 3613-3622.

(170) Wang, R. L. C.; Kreuzer, H. J.; Grunze, M.: Molecular conformation and solvation of oligo(ethylene glycol)-terminated self-assembled monolayers and their resistance to protein adsorption. *Journal of Physical Chemistry B* **1997**, *101*, 9767-9773.

(171) Pertsin, A. J.; Grunze, M.; Kreuzer, H. J.; Wang, R. L. C.: The effect of electrostatic fields on an oligo(ethylene glycol) terminated alkanethiol self-assembled monolayer. *PCCP Phys. Chem. Chem. Phys.* **2000**, *2*, 1729-1733.

(172) Li, L.; Zhang, L.; Fan, J.; Greenberg, K.; Desiderio, S.; Rassool, F. V.; Small, D.: Defective non-homologous end joining blocks B-cell development in FLT3/ITD mice. *Blood* **2011**.

(173) Li, L. Y.; Chen, S. F.; Zheng, J.; Ratner, B. D.; Jiang, S. Y.: Protein adsorption on oligo(ethylene glycol)-terminated alkanethiolate self-assembled monolayers: The molecular basis for nonfouling behavior. *Journal of Physical Chemistry B* **2005**, *109*, 2934-2941.

(174) Porter, M. D.; Bright, T. B.; Allara, D. L.; Chidsey, C. E.: Spontaneously organized molecular assemblies. 4. Structural characterization of n-alkyl thiol monolayers on gold by optical ellipsometry, infrared spectroscopy, and electrochemistry. *Journal of the American Chemical Society* **1987**, *109*, 3559-3568.

(175) Masson, J. F.; Battaglia, T. M.; Cramer, J.; Beaudoin, S.; Sierks, M.; Booksh, K. S.: Reduction of nonspecific protein binding on surface plasmon resonance biosensors. *Analytical and Bioanalytical Chemistry* **2006**, *386*, 1951-1959.

(176) Spinke, J.; Liley, M.; Schmitt, F. J.; Guder, H. J.; Angermaier, L.; Knoll, W.: Molecular recognition at self-assembled monolayers - optimization of surface functionalization. *Journal of Chemical Physics* **1993**, *99*, 7012-7019.

(177) Livnah, O.; Bayer, E. A.; Wilchek, M.; Sussman, J. L.: 3-DIMENSIONAL STRUCTURES OF AVIDIN AND THE AVIDIN-BIOTIN COMPLEX. *Proceedings of the National Academy of Sciences of the United States of America* **1993**, *90*, 5076-5080.

(178) Sledz, P.; Kaminski, R.; Chruszcz, M.; Zimmerman, M. D.; Minor, W.; Wozniak, K.: An experimental charge density of HEPES. *Acta Crystallographica Section B: Structural Science* **2010**, *66*, 482-492.

(179) Godsey, M. H.; Minasov, G.; Shuvalova, L.; Brunzelle, J. S.; Vorontsov, I. I.; Collart, F. R.; Anderson, W. F.: The 2.2 Å resolution crystal structure of Bacillus cereus Nif3-family protein YqfO reveals a conserved dimetal-binding motif and a regulatory domain. *Protein Science* **2007**, *16*, 1285-1293.

(180) Pranzetti, A.; Mieszkin, S.; Iqbal, P.; Rawson, F. J.; Callow, M. E.; Callow, J. A.; Koelsch, P.; Preece, J. A.; Mendes, P. M.: An Electrically Reversible Switchable Surface to Control and Study Early Bacterial Adhesion Dynamics in Real-Time. *Adv. Mater.* **2013**, *25*, 2181-2185.

(181) Liu, D.; Xie, Y.; Shao, H.; Jiang, X.: Using Azobenzene-Embedded Self-Assembled Monolayers To Photochemically Control Cell Adhesion Reversibly. *Angew. Chem.-Int. Edit.* **2009**, *48*, 4406-4408.

(182) Fraser, I.; Hughes, D.; Gordon, S.: Divalent cation-independent macrophage adhesion inhibited by monoclonal antibody to murine scavenger receptor. **1993**.

(183) Anderson, J. M.; Rodriguez, A.; Chang, D. T.: Foreign body reaction to biomaterials. In *Seminars in immunology*; Elsevier, 2008; Vol. 20; pp 86-100.

(184) Geissmann, F.; Manz, M. G.; Jung, S.; Sieweke, M. H.; Merad, M.; Ley, K.: Development of monocytes, macrophages, and dendritic cells. *Science* **2010**, *327*, 656-661.

(185) Brown, B. N.; Badylak, S. F.: Expanded applications, shifting paradigms and an improved understanding of host–biomaterial interactions. *Acta Biomater.* **2013**, *9*, 4948-4955.

(186) Wang, H.; Chen, S.; Li, L.; Jiang, S.: Improved Method for the Preparation of Carboxylic Acid and Amine Terminated Self-Assembled Monolayers of Alkanethiolates. *Langmuir : the ACS journal of surfaces and colloids* **2005**, *21*, 2633-2636.

(187) Jung, H. J.; Ahn, K.-D.; Han, D. K.; Ahn, D.-J.: Surface characteristics and fibroblast adhesion behavior of RGD-immobilized biodegradable PLLA films. *Macromolecular Research* **2005**, *13*, 446-452.

(188) Zhang, H.-L.; Zhang, J.; Li, H.-Y.; Liu, Z.-F.; Li, H.-L.: Structural investigation of a new series of azobenzene-containing self-assembled monolayers on gold. *Materials Science and Engineering: C* **1999**, *8–9*, 179-185.

(189) Mrksich, M.: Using self-assembled monolayers to model the extracellular matrix. *Acta Biomater.* **2009**, *5*, 832-841.

(190) Ratner, B. D.; Bryant, S. J.: Biomaterials: where we have been and where we are going. *Annu. Rev. Biomed. Eng.* **2004**, *6*, 41-75.

(191) Toullec, J.-Y.: Crustacean primary cell culture: A technical approach. *Methods Cell Sci* **1999**, *21*, 193-198.

(192) Channon, J.; Leslie, C. C.: A calcium-dependent mechanism for associating a soluble arachidonoyl-hydrolyzing phospholipase A2 with membrane in

the macrophage cell line RAW 264.7. *Journal of Biological Chemistry* **1990**, *265*, 5409-5413.

(193) Mahoney, J. R.; Beutler, B. A.; Letrang, N.; Vine, W.; Ikeda, Y.; Kawakami, M.; Cerami, A.: Lipopolysaccharide-treated RAW 264.7 cells produce mediator that inhbits lipoprotein-lipase in 3T3-L1 cells. *J. Immunol.* **1985**, *134*, 1673-1675.

(194) Wischerhoff, E.; Uhlig, K.; Lankenau, A.; Borner, H. G.; Laschewsky, A.; Duschl, C.; Lutz, J. F.: Controlled cell adhesion on PEG-based switchable surfaces. *Angew Chem Int Ed Engl* **2008**, *47*, 5666-8.

(195) Desai, N. P.; Hubbell, J. A.: Solution technique to incorporate polyethylene oxide and other water-soluble polymers into surfaces of polymeric biomaterials. *Biomaterials* **1991**, *12*, 144-153.

(196) Zhang, M.; Desai, T.; Ferrari, M.: Proteins and cells on PEG immobilized silicon surfaces. *Biomaterials* **1998**, *19*, 953-960.

(197) Faucheux, N.; Schweiss, R.; Lützow, K.; Werner, C.; Groth, T.: Self-assembled monolayers with different terminating groups as model substrates for cell adhesion studies. *Biomaterials* **2004**, *25*, 2721-2730.

(198) Arnold, M.; Cavalcanti-Adam, E. A.; Glass, R.; Blümmel, J.; Eck, W.; Kantlehner, M.; Kessler, H.; Spatz, J. P.: Activation of Integrin Function by Nanopatterned Adhesive Interfaces. *ChemPhysChem* **2004**, *5*, 383-388.

(199) Geiger, B.; Spatz, J. P.; Bershadsky, A. D.: Environmental sensing through focal adhesions. *Nature Reviews Molecular Cell Biology* **2009**, *10*, 21-33.

(200) *Principles of Cellular Engineering: Understanding the Biomolecular Interface*; Academic Press, 2006.

(201) Roberts, C.; Chen, C. S.; Mrksich, M.; Martichonok, V.; Ingber, D. E.; Whitesides, G. M.: Using Mixed Self-Assembled Monolayers Presenting RGD and (EG)3OH Groups To Characterize Long-Term Attachment of Bovine Capillary Endothelial Cells to Surfaces. *Journal of the American Chemical Society* **1998**, *120*, 6548-6555.

(202) Lee, M. H.; Brass, D. A.; Morris, R.; Composto, R. J.; Ducheyne, P.: The effect of non-specific interactions on cellular adhesion using model surfaces. *Biomaterials* **2005**, *26*, 1721-1730.

(203) Le Saux, G.; Magenau, A.; Bocking, T.; Gaus, K.; Gooding, J. J.: The relative importance of topography and RGD ligand density for endothelial cell adhesion. *PLoS One* **2011**, *6*, e21869.

(204) Yeo, W.-S.; Mrksich, M.: Electroactive Substrates that Reveal Aldehyde Groups for Bio-Immobilization. *Adv. Mater.* **2004**, *16*, 1352-1356.

(205) Underwood, P. A.; Steele, J. G.; Dalton, B. A.: Effects of Polystyrene Surface-Chemistry on the Biological-Activity of Solid-Phase Fibronectin and Vitronectin, Analyzed with Monoclonal-Antibodies. *Journal of Cell Science* **1993**, *104*, 793-803.

(206) Pierschbacher, M. D.; Ruoslahti, E.: Influence of stereochemistry of the sequence Arg-Gly-Asp-Xaa on binding specificity in cell adhesion. *Journal of Biological Chemistry* **1987**, *262*, 17294-17298.

(207) McClary, K. B.; Ugarova, T.; Grainger, D. W.: Modulating fibroblast adhesion, spreading, and proliferation using self-assembled monolayer films of alkylthiolates on gold. *J. Biomed. Mater. Res.* **2000**, *50*, 428-439.

(208) Wang, H.; Chen, S. F.; Li, L. Y.; Jiang, S. Y.: Improved method for the preparation of carboxylic acid and amine terminated self-assembled monolayers of alkanethiolates. *Langmuir : the ACS journal of surfaces and colloids* **2005**, *21*, 2633-2636.

Appendix I

Solution ratio (Biotin-4KC:C11HEG)	N area	S area	S/N	No. of C11HEG
1:10 a	0.00689	0.00526	0.763	6.397
1:10 b	0.00678	0.00973	0.635	3.722
1:40 a	0.00268	0.00421	1.570	15.279
1:40 b	0.00391	0.00636	1.030	7.276
1:100 a	0.00383	0.00643	1.678	16.467
1:100 b	0.00330	0.00685	2.075	20.833

Table 6.1 *XPS data of **biotin-4KC:C11HEG** SAMs at different solution ratios.*

Solution ratio (Biotin-4KC:C11HEG)	No. of C11HEG	Average	Error
1:10 a	6	5	1
1:10 b	4		
1:40 a	15	11	6
1:40 b	7		
1:100 a	16	19	4
1:100 b	21		

Table 6.2 *Average **C11HEG** SAMs per **biotin-4KC** at different solution ratios.*

Appendix II

Solution ratio GRGDS-HEGC:C11TEG)	S	N	S/N	No. of C11TEG
1:40 a	0.00603	0.00789	0.764	6.647
1:40 b	0.00869	0.01192	0.729	6.296
1:40 c	0.00540	0.01085	0.497	3.977

Table 6.3 *XPS data of **GRGDS-HEGC:C11TEG** SAMs at different solution ratios.*

Solution ratio GRGDS-HEGC:C11TEG)	No. of C11TEG	Average	Error
1:40 a	7	6	1
1:40 b	6		
1:40 c	4		

Table 6.4 *Average **C11TEG** SAMs per **GRGDS-HEGC** at different solution ratios.*

Appendix III

	Response Units of Complex media		
SAMs	**DMEM**	**DMEM-FBS**	**DMEM-FBS-HEPES**
Biotin-4KC	376.2	1639.8	1541.9
C3TEG	98.7	1005.1	854.6
C11TEG	39.3	344.7	180.3
C11HEG	4	3.5	183.3

Table 6.5 *Showing the response unitrs or different complex media on the following pure SAMs:* ***Biotin-4KC****,* ***C3TEG****,* ***C11TEG*** *and* ***C11HEG****.*

Appendix IV

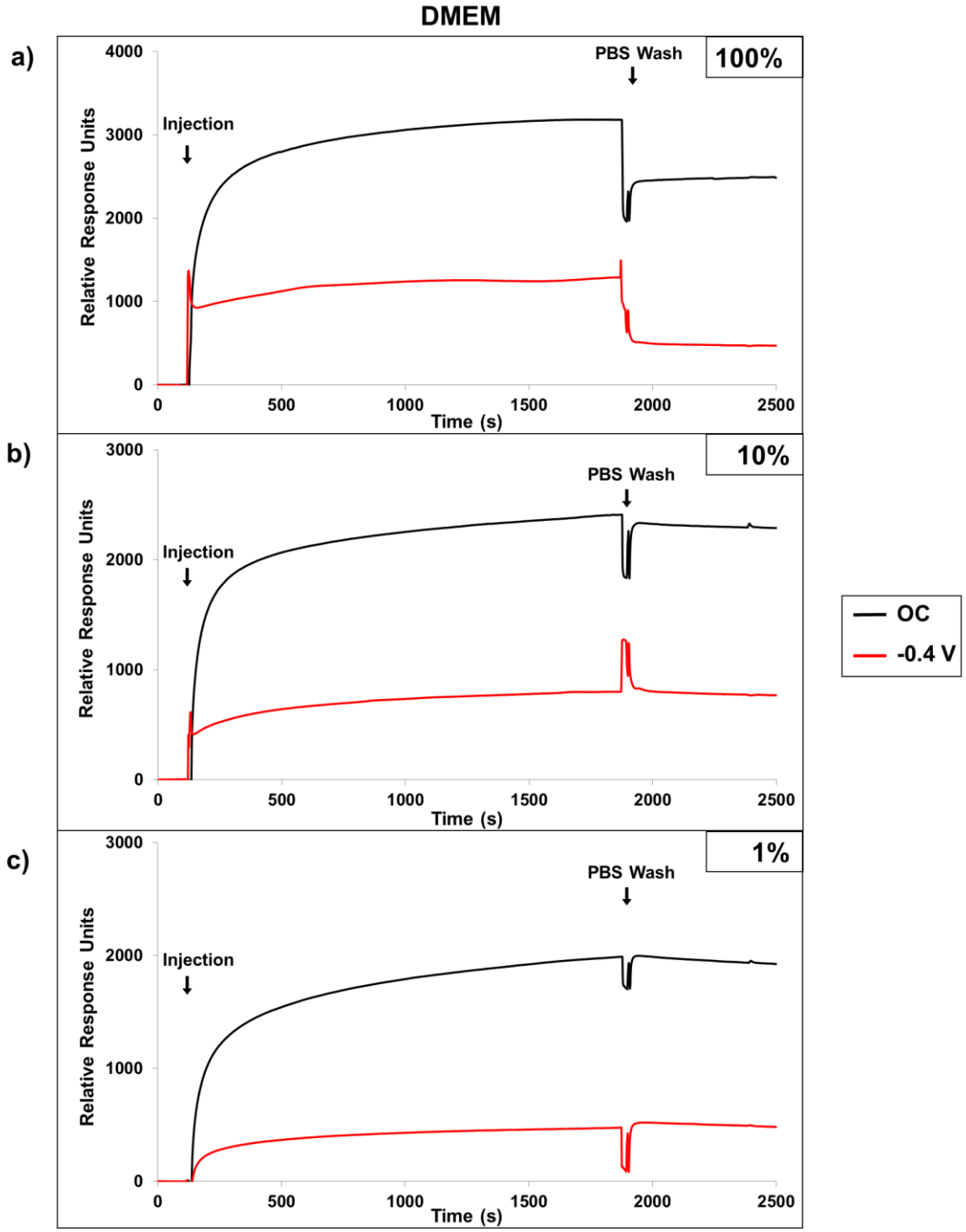

Figure 6.1 *Representative SPR sensorgram traces for the OC (black trace) and -0.4 V applied potential (red trace) interactions of dilutions of DMEM with* ***biotin-4KC:C11TEG*** *at a) 1%, b) 10% and c) 100%.*

Appendix V

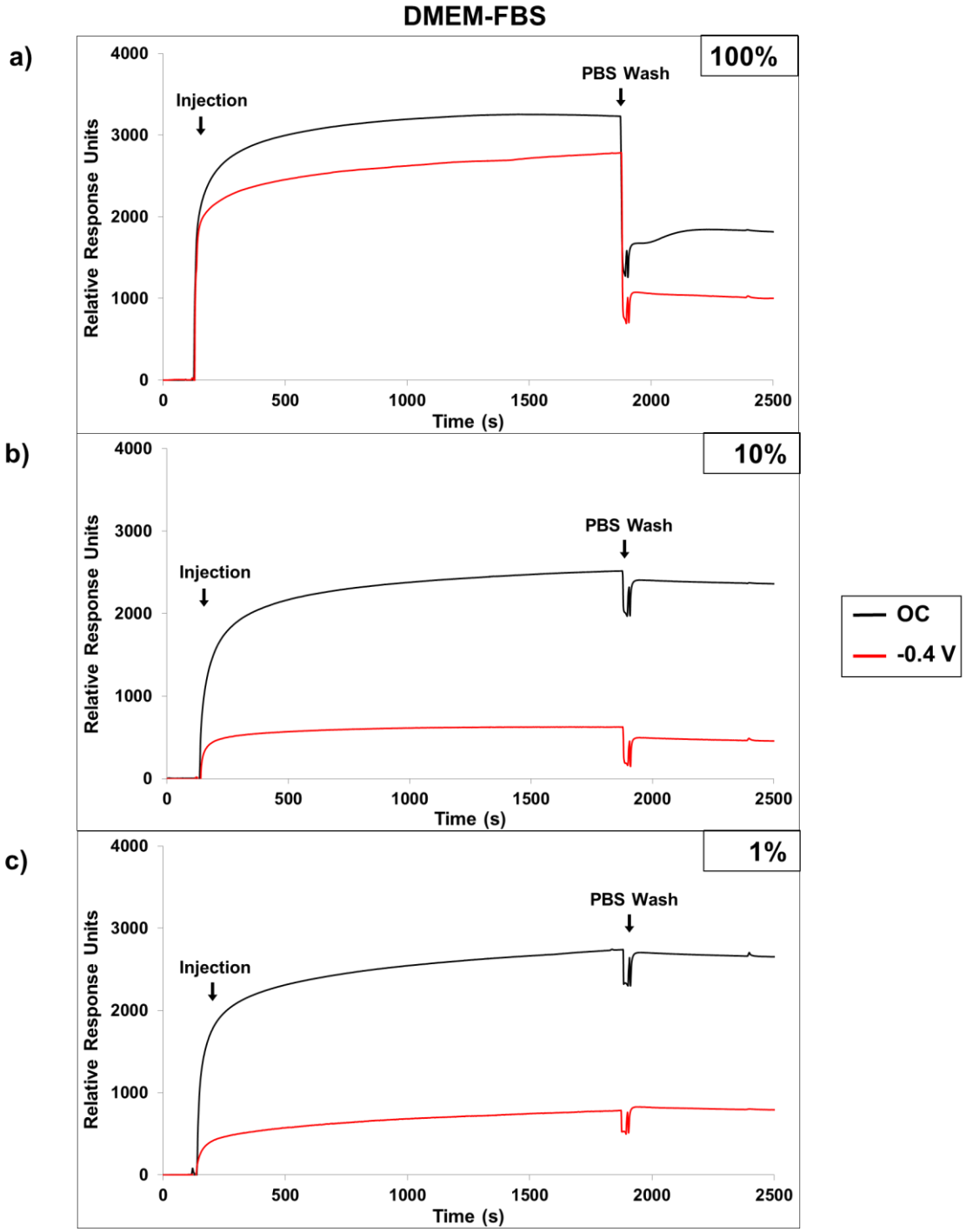

Figure 6.2 *Representative SPR sensorgram traces for the OC (black trace) and -0.4 V applied potential (red trace) interactions of dilutions of DMEM-FBS with* ***biotin-4KC:C11TEG*** *at a) 1%, b) 10% and c) 100%*

Appendix VI

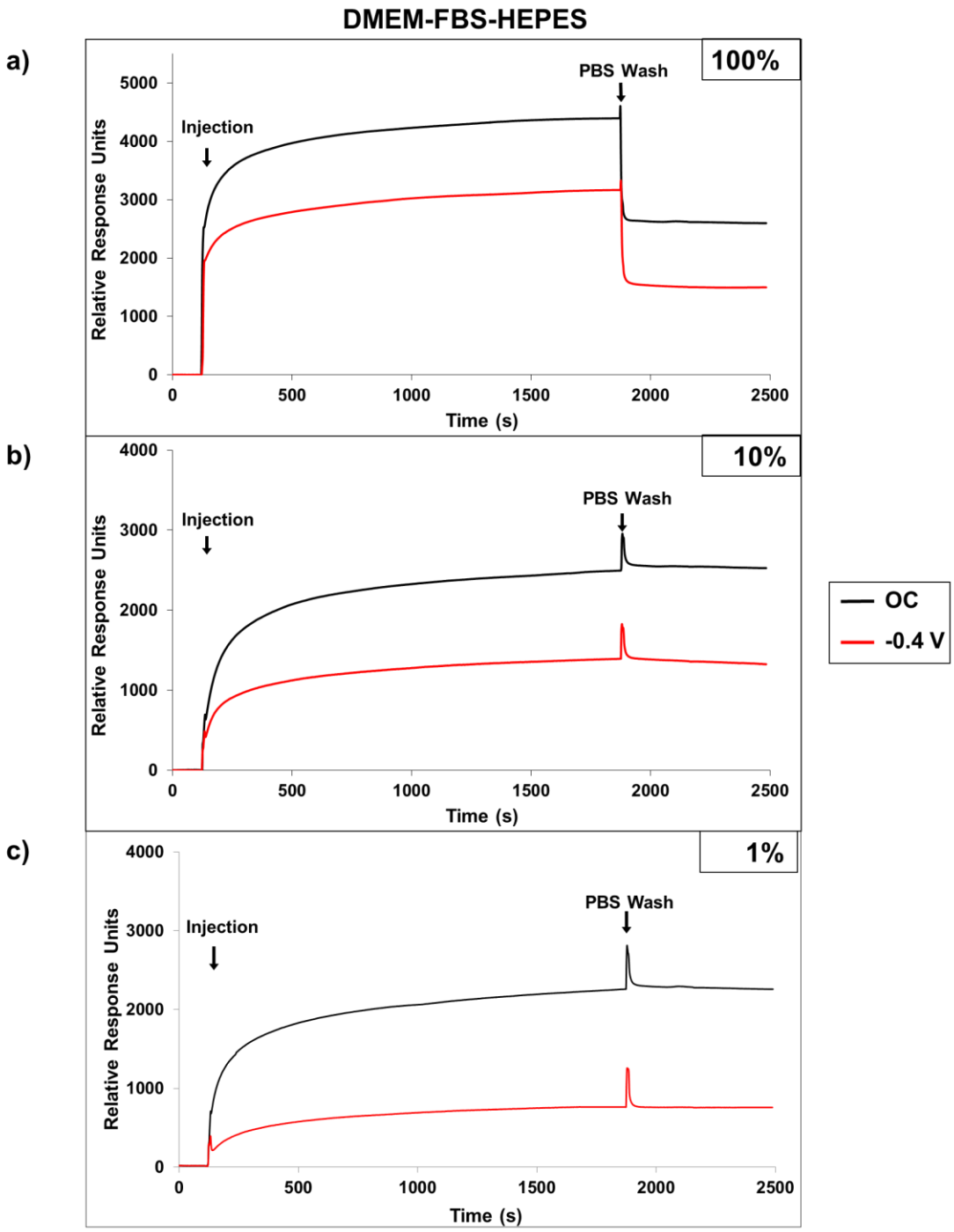

Figure 6.3 *Representative SPR sensorgram traces for the OC (black trace) and -0.4 V applied potential (red trace) interactions of dilutions of DMEM-HEPES-FBS with* ***biotin-4KC:C11TEG*** *at a) 1%, b) 10% and c) 100%*

Appendix VII

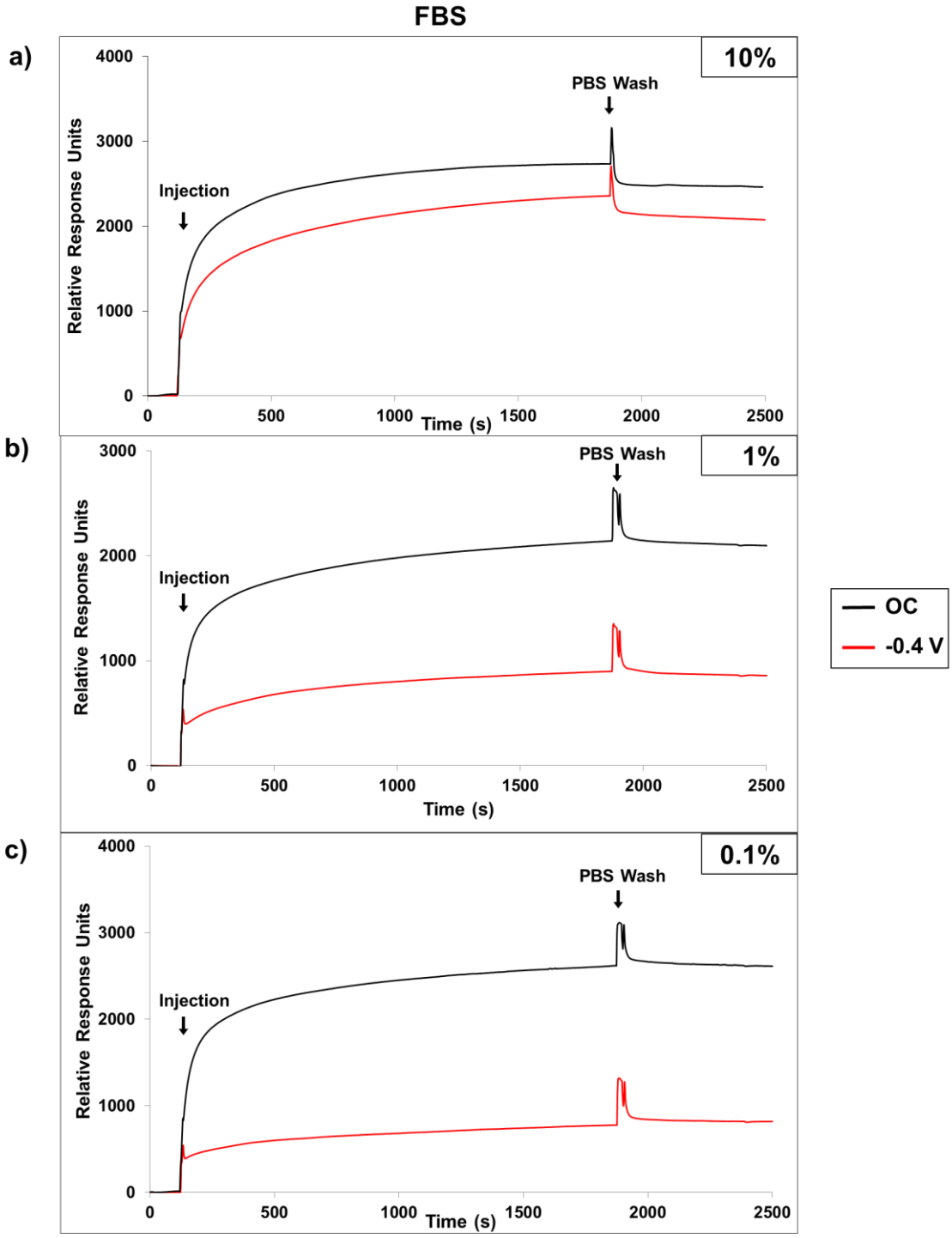

Figure 6.4 *Representative SPR sensorgram traces for the OC (black trace) and -0.4 V applied potential (red trace) interactions of dilutions of FBS with* ***biotin-4KC:C11TEG*** *at a) 1%, b) 10% and c) 100%.*

Appendix VIII

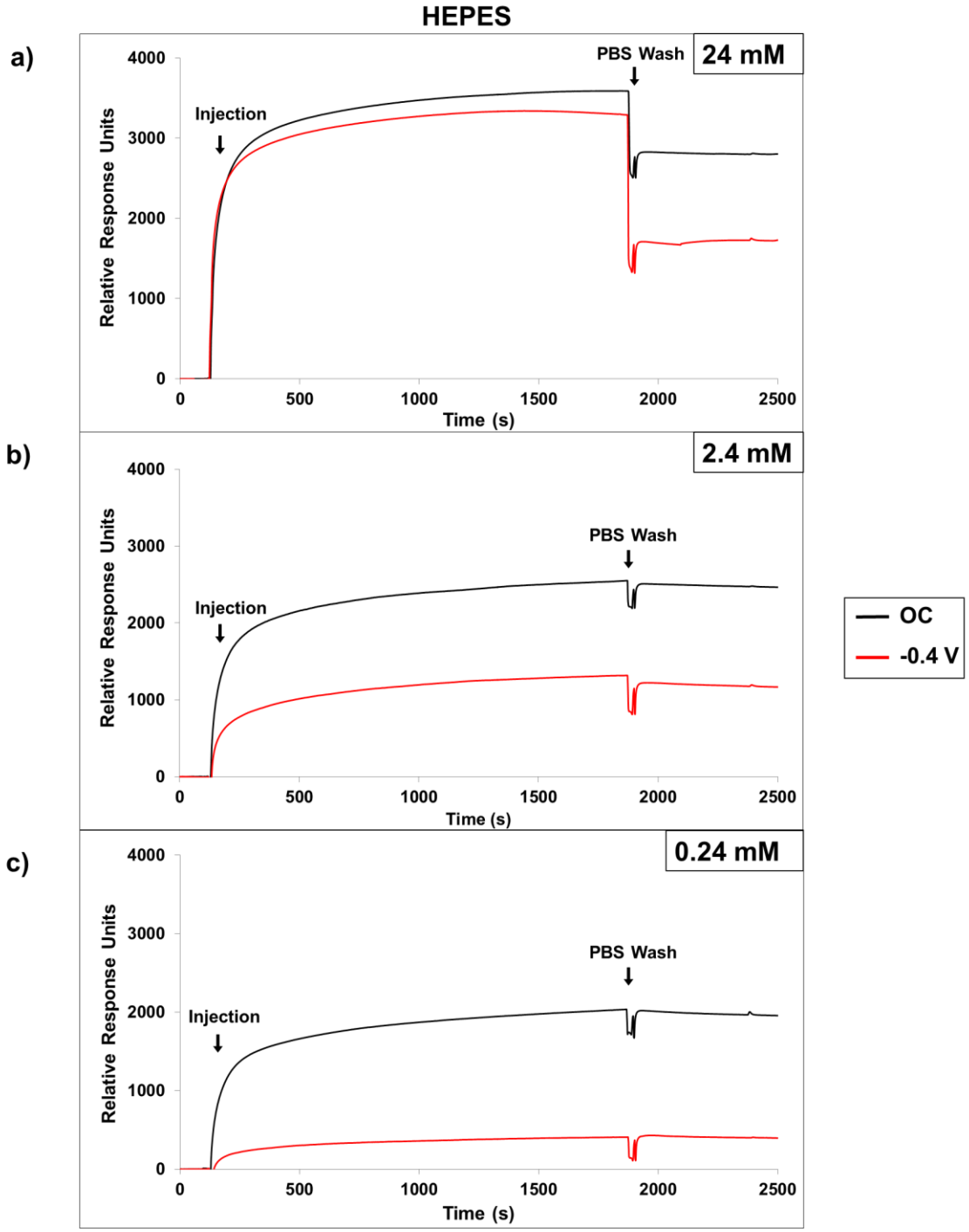

Figure 6.5 *Representative SPR sensorgram traces for the OC (black trace) and -0.4 V applied potential (red trace) interactions of dilutions of HEPES with* ***biotin-4KC:C11TEG*** *at a) 1%, b) 10% and c) 100%.*